

Equilibrium Constants by NMR and emf . . . . .	Blixt, J., and Glaser, J.	2
Block Copolymers on Surfaces . . . . .	Blum, F. D.	4
Mode-Switched Radiofrequency Coils . . . . .	Barker, P. B., Shungu, D. C., and Schoeniger, J.	7
Position Available . . . . .	Hughes, D. A.	8
Lactate Edited Self-Diffusion Coefficient Measurements . . . . .	Sotak, C. H.	9
Fast Phase Sensitive COSY . . . . .	Turner, C. J.	15
SELRESOLV: Selective Measurements of Long Range C,H-Coupling Constants . . . . .	Ochs, M., and Berger, S.	16
Real or Artifact? . . . . .	Thoma, W. J.	18
H,D Exchange in Technetium-99 Complexes . . . . .	Ovenall, D., and Albanese, J.	21
Position Available . . . . .	Hasson, N.	22
3D NMR: Displaying the Results from Pulse Sequence Simulations . . . . .	Butler, L. G.	23
Models for Porphyrin Ring-Current Shifts . . . . .	Cross, K. J.	27
Methods for Solvent Suppression and Baseplane Flattening of NOESY and ROESY Spectra . . . . .	Ni, F.	28
Position Available . . . . .	Stilbs, P.	30
Neighbors . . . . .	Kline, A. D., Vandygriff, J., and Occolowitz, J.	33
Al NMR of Zeolites . . . . .	Ray, G. J.	34
Solid Phase <sup>13</sup> C NMR of a Dibenzo-15-Crown-5 Ether and Its NaNCS Complex . . . . .	Buchanan, G. W.	36
NMR Imaging of the Cockroach . . . . .	Williams, S. C. R.	39
NMR of Fluorinated $\beta$ -Diketones . . . . .	Lindon, J. C., and Farrant, R. D.	40
The Third Dimension <i>a la</i> JEOL GSX Spectrometers . . . . .	Byrd, R. A.	41
Planning Relaxation Time Measurements of Quadrupolar Nuclei in Solids . . . . .	Woessner, D. E.	45
Position Available . . . . .	Randall, E.	46
Overlapping COSY Cross Peaks . . . . .	Freeman, R.	48

*Continued on page 68*

A monthly collection of informal private letters from Laboratories of NMR. Information contained herein is solely for the use of the reader. Quotation is *not* permitted, except by direct arrangement with the author of the letter, and the material quoted *must* be referred to as a "Private Communication". Reference to the TAMU NMR Newsletter by name in the open literature is strictly forbidden.

These restrictions apply equally to both the actual Newsletter participant-recipients and to all others who are allowed open access to the Newsletter issues. Strict adherence to this policy is considered essential to the successful continuation of the Newsletter as an informal medium of exchange of NMR information.



TABLE 1 DEUTERATED SOLVENTS

Cat. No.	Description	Formula	Min. Purity (%)	Density (g/ml)	MP (°C)	BP (°C)	$n_D^{20} \times 10^6 @ (°C)$
D-11	Acetone-d <sub>6</sub>	CD <sub>3</sub> COCD <sub>3</sub>	99.8%	1.17	-17	56	0.551 (32)
D-120	Acetone-d <sub>6</sub>	CD <sub>3</sub> COCD <sub>3</sub>	99.8%	1.17	-17	56	0.551 (32)
D-13	Acetone-d <sub>6</sub>	CD <sub>3</sub> COCD <sub>3</sub>	99.8%	1.17	-17	56	0.551 (32)
D-121	Acetone-d <sub>6</sub> + 1% TMS	CD <sub>3</sub> COCD <sub>3</sub>	99.8%	1.17	-17	56	0.551 (32)
D-129	Cost-conscious quality NMR solvents offered by Wilmad, such as CDCl <sub>3</sub> , are frequently priced lower than more traditional sources. Included in this offering are the most common solvents, like Acetone-d <sub>6</sub> , Benzene-d <sub>6</sub> , D <sub>2</sub> O, and DMSO-d <sub>6</sub> , as well as some of the most unusual solvents for specialty applications, like 1,1,2,2-Tetrachloroethane-d <sub>2</sub> , Octane-d <sub>8</sub> , and Trifluoroacetic Acid-d.						0.543 (20)
D-14	Chloroform-d	CDCl <sub>3</sub>	99.8%	1.50	-64	62	0.611
D-21	Chloroform-d	CDCl <sub>3</sub>	99.8%	1.50	-64	62	0.611
D-122	Chloroform-d	CDCl <sub>3</sub>	99.8%	1.50	-64	62	0.611
D-130	Chloroform-d	CDCl <sub>3</sub>	99.8%	1.50	-64	62	0.611
D-28	Chloroform-d	CDCl <sub>3</sub>	99.8%	1.50	-64	62	0.740 (20)
D-31	Chloroform-d + 1% TMS	CDCl <sub>3</sub>	99.8%	1.50	-64	62	0.740 (20)

VARIAN  
BOX/500 SHEETS

Cat. No.	Size	Instrument Model	Type
WCV-100 (S-100A)	11" X 26"	HA-100, HA-100, HA-100D	Gridded-Two Color
WCV-60 (S-60C)	11" X 26"	HA-60, HA-60, HA-60D	Gridded-Two Color
WCV-XL (S-XL)	11" X 26"	HA-XL, HA-XL, HA-XLD	Gridded-Two Color
WCV-XLFT (S-XLFT)	11" X 26"	HA-XLFT, HA-XLFT, HA-XLFTD	Gridded-Two Color
WCV-XL 200	11" X 26"	XL-200, XL-300, XL-400	Gridded-Two Color
WCV-20 (CFT-20)	11" X 16 3/4"	CFT-20, FT-80, FT-80A	Gridded-Two Color
WCV-11 (CFT-11)	11" X 17"	All Models	Blank

We provide the largest variety of paper and pens for NMR recorders or plotters available anywhere. Included in these listing are the newest spectrometers from Varian, Bruker, (and IBM), General Electric and JEOL, as well as the latest models, such as the Hewlett Packard 7475A, 7550A, and Thinkjet 2225A, Zeta 8 or 8A, and Western Graphtec 4730 plotters and printers.

Searching for the Unusual Requirement?  
WILMAD HAS YOUR ANSWER!

The most comprehensive offering of "widgets, gadgets and specials" for NMR spectroscopy, including:

**Spatula for 5mm NMR Tubes**

**Three types of Valve NMR Tubes**

(including the new J. Young Valve Tube)

**Solvent Jet NMR Tube Cleaners**

**pH Electrode for 5mm NMR Tubes**

**Taperlok® NMR Tubes**

**A multitude of Coaxial Inserts**

**Alumina NMR Tube for Si-29 Studies**

**Ultra-thin wall NMR Tubes**

**Throwaway "THRIFT" and "ECONOMY" NMR Tubes**

Serving the Spectroscopic Aftermarket



**WILMAD GLASS COMPANY**

Route 40 and Oak Road • Buena, NJ 08310 U.S.A.

609-697-3000 • TWX 510-687-8911

FAX 609-697-0536

## TEXAS A&amp;M NMR NEWSLETTER

NO. 383, AUGUST 1990

## AUTHOR INDEX

Ackerman, J. I. . . . .	67	Dichl, P. . . . .	62	Miknis, F. . . . .	65	Shehan, P. . . . .	53
Adam, B. . . . .	53	Farrant, R. D. . . . .	40	Netzcl, D. A. . . . .	65	Shungu, D. C. . . . .	7
Albanese, J. . . . .	21	Freeman, R. . . . .	48	Ni, F. . . . .	28	Sotak, C. H. . . . .	9
Barker, P. B. . . . .	7	Garrido, I. . . . .	67	O'Byrne, E. M. . . . .	59	Stilbs, P. . . . .	30
Berger, S. . . . .	16	Glaser, J. . . . .	2	Occolowitz, J. . . . .	33	Thoma, W. J. . . . .	18
Blixt, J. . . . .	2	Gupta, R. K. . . . .	59	Ochs, M. . . . .	16	Turner, C. J. . . . .	15
Blum, F. D. . . . .	4	Hasson, N. . . . .	22	Ovenall, D. . . . .	21	Vandygriff, J. . . . .	33
Buchanan, G. W. . . . .	36	Hughes, D. A. . . . .	8	Paul, P. K. . . . .	59	Vega, S. . . . .	55
Butler, L. G. . . . .	23	Jelicks, L. A. . . . .	59	Randall, E. . . . .	46	Wellard, M. . . . .	53
Byrd, R. A. . . . .	41	Jokisaari, J. . . . .	62	Ray, G. J. . . . .	34	Williams, S. C. R. . . . .	39
Craik, D. . . . .	53	Kline, A. D. . . . .	33	Schoeniger, J. . . . .	7	Woessner, D. E. . . . .	45
Cross, K. J. . . . .	27	Lindon, J. C. . . . .	40	Shapiro, B. L. . . . .	68	Zax, D. B. . . . .	55

## TEXAS A&amp;M NMR NEWSLETTER

NO. 383, AUGUST 1990

## ADVERTISER INDEX

American Microwave Technology, Inc. . . . .	37	JEOL . . . . .	outside back cover
Bio-Rad, Sadtler Division . . . . .	47	Nalorac Cryogenics Corporation . . . . .	25
Bruker Instruments, Inc. . . . .	31	Otsuka Electronics (U.S.A.) Inc. . . . .	5
Chemagnetics, Inc. . . . .	63	Oxford Instruments Ltd. . . . .	57
Doty Scientific, Inc. . . . .	19	Programmed Test Sources, Inc. . . . .	61
Fremont Magnetic Resonance . . . . .	43	Varian . . . . .	51
GE NMR Instruments . . . . .	11, inside back cover	Wilmad Glass Company, Inc. . . . .	inside front cover

## SPONSORS OF THE TAMU NMR NEWSLETTER

Abbott Laboratories  
 Analogic Corporation  
 The British Petroleum Co., Ltd. (England)  
 Bruker Instruments, Inc.  
 Burroughs Wellcome Co.  
 Cryomagnet Systems, Inc.  
 The Dow Chemical Company  
 Eastman Kodak Company  
 E. I. du Pont de Nemours & Company  
 GE NMR Instruments  
 JEOL (U.S.A.) Inc., Analytical Instruments Division  
 The Lilly Research Laboratories, Eli Lilly & Company  
 Merck Sharp & Dohme/Isotopes  
 Millipore Corporation, Waters Chromatography Division

The Monsanto Company  
 New Methods Research, Inc.  
 NMR Technologies Inc.  
 Norell, Inc.  
 The Procter & Gamble Company, Miami Valley Labs  
 Programmed Test Sources, Inc.  
 Shell Development Company  
 Siemens Medical Systems, Inc.  
 Spectroscopy Imaging Systems Corporation  
 Spectral Data Services, Inc.  
 Tecmag  
 Unilever Research  
 Union Carbide Corporation  
 Varian, Analytical Instrument Division

*The Newsletter's fiscal viability depends very heavily on the funds provided by our Advertisers and Sponsors. Please do whatever you can to let them know that their support is noted and appreciated.*

## FORTHCOMING NMR MEETINGS

Bat-Sheva Workshop on New Developments and Applications in NMR and ESR Spectroscopy, October 14-24, 1990, Israel; Contact: Dr. D. Goldfarb, The Weizmann Institute of Science, Rehovot, Israel. See Newsletter 377, 10.

Eastern Analytical Symposium, Garden State Convention Center, Somerset, NJ; NMR Symposia and Poster Sessions on Nov. 13 and 14, 1990; Contact D. C. Dalgarno or C. A. Evans, Schering-Plough Research, 60 Orange St., Bloomfield, NJ 07003; (201) 429-3957; FAX: (201) 429-3916.

Advanced Tomographic Imaging Methods for the Analysis of Materials, Symposium at the Fall Meeting of the Materials Research Society, Boston, Mass., Nov. 26 - Dec. 1, 1990; See Newsletter 378, 57.

Additional listings of meetings, etc., are invited.

## All Newsletter Correspondence

Should Be Addressed To:

Dr. Bernard L. Shapiro  
 TAMU NMR Newsletter  
 966 Elsinore Court  
 Palo Alto, CA 94303, U.S.A.

(415) 493-5971

## DEADLINE DATES\*

No. 385 (October) -----14 September 1990

No. 386 (November) -----12 October 1990

No. 387 (December) -----9 November 1990

No. 388 (January) -----7 December 1990

\*Please note that these deadline dates have been moved a bit forward from those previously in effect.



KUNGL TEKNISKA HÖGSKOLAN  
ROYAL INSTITUTE OF TECHNOLOGY

*Dept. of Inorganic Chemistry*  
*Dr. Julius Glaser*

Handläggare, direktvalsr

Stockholm, June 21, 1990

(received 6/27/90)

Prof. B.L. Shapiro  
TAMU NMR Newsletter  
966 Elsinore Court  
Palo Alto  
California 94303, USA

## "Equilibrium Constants by NMR and emf"

*Dear Prof. Shapiro,*

During the last 40-50 years, the solution chemists have determined a large number of equilibrium constants. The latter have contributed to a better and more quantitative understanding of solution chemistry, which in its turn led to several industrial and environmental applications.

Several methods have been used for determining the constants: solubility studies, potentiometry, spectrophotometry, and you name it. Now, in the era of multinuclear NMR, a new tool has been added to the chemist's arsenal. With NMR, we can 'see' several things of which the chemists in the old times could only dream, e.g. microscopic equilibrium constants, structures of species in dilute solution, fast kinetics, etc.

Particularly, the combination of NMR and potentiometry seems to be the method of choice for determining accurate equilibrium constants. A simple example is given here. For weak acids (in this case HCN),  $^{13}\text{C}$  NMR and a glass electrode will do. In the case of the fast exchange regime (on the NMR timescale) between the protonated and unprotonated species (here HCN and  $\text{CN}^-$ ),  $^{13}\text{C}$  NMR spectra can look as in Figure 1. From these spectra, we obtain the dissociation constant,  $K_a$ :

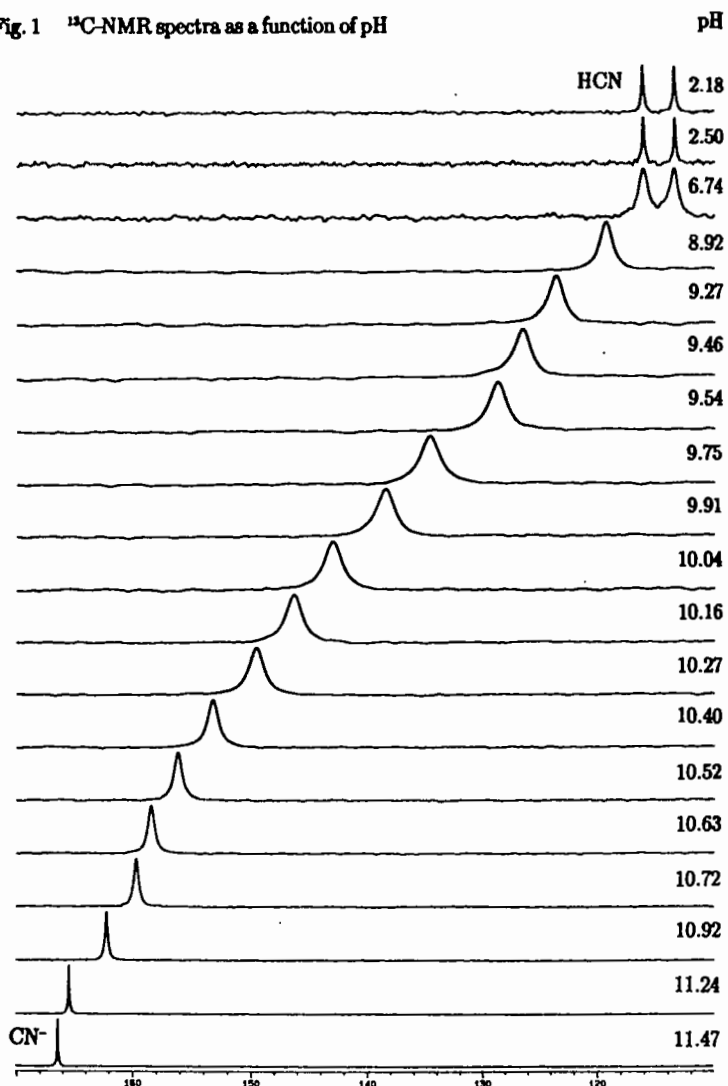
$$\text{p}K_a = \text{pH} + \log[(\delta_{\text{CN}} - \delta_{\text{exp}})/(\delta_{\text{exp}} - \delta_{\text{HCN}})] \quad (1)$$

where  $\delta_{\text{exp}}$ ,  $\delta_{\text{CN}}$  and  $\delta_{\text{HCN}}$  are experimental  $^{13}\text{C}$  chemical shifts and the individual chemical shifts for  $\text{CN}^-$  and HCN, respectively. The pH values in each experimental point can be measured by glass electrode. This method yields equilibrium constants with accuracy within 2-3 hundredths of a logarithmic unit, i.e. at least as good as potentiometry (emf), which has for a long time been (and still is) considered as the most accurate method.

The combination of NMR and emf has some disadvantages; for example, you need an NMR spectrometer. On the other hand, when you have one, you don't have to worry about nasty things like the total concentration of cyanide (HCN is volatile!) or (non-paramagnetic) impurities coming from the ionic media, which can sometimes spoil the emf data. Moreover, analyzing the data in Figure 1 we can also obtain kinetic information on the proton exchange between HCN,  $\text{CN}^-$  and  $\text{H}_2\text{O}$ .

An attentive reader will see a peculiarity in this figure: the doublet ( $J_{\text{C-H}} = 271 \text{ Hz}$ ) originating from the HCN molecule gossips about the long lifetime of the proton, which is really remarkable for an inorganic acid in aqueous solution.

Fig. 1  $^{13}\text{C}$ -NMR spectra as a function of pH



Sincerely,

*Johan Blixt*

Johan Blixt

*Julius Glaser*

Julius Glaser





UNIVERSITY OF MISSOURI-ROLLA

June 13, 1990 (received 6/23/90)

Dr. Bernard L. Shapiro  
TAMU NMR Newsletter  
966 Elsinore Court  
Palo Alto, CA 94303

College of Arts and Sciences

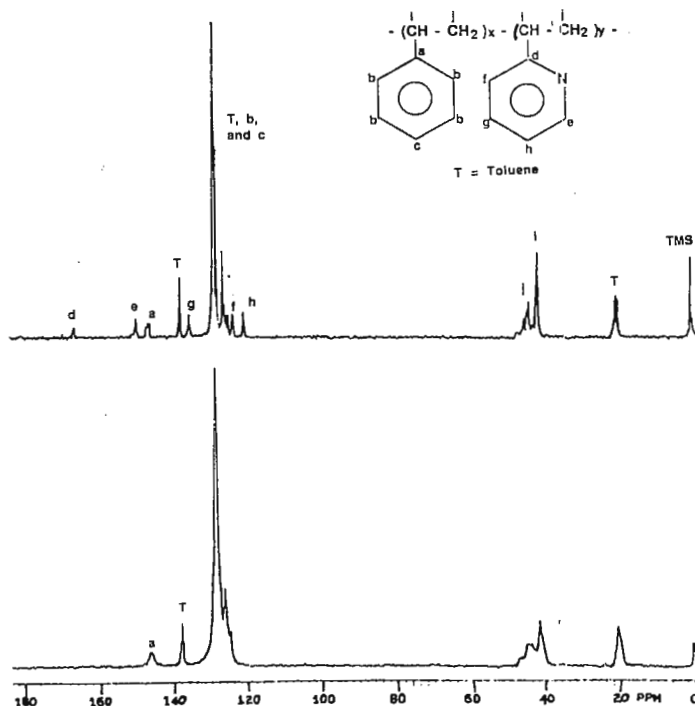
Department of Chemistry

142 Schrenk Hall  
Rolla, MO 65401-0249  
Telephone (314) 341-4420  
FAX (314) 341-6033

## Block Copolymers on Surfaces

Dear Barry:

We have been working on the dynamics of block copolymers on solid surfaces. To do this we specifically label part of the molecule with deuterium and then observe either deuterium NMR line shapes or relaxation times to determine the dynamics of these molecules. We have done considerable amount of work with block copolymers made from styrene and 2-vinylpyridine. These materials adsorb on the surface via the vinylpyridine groups and the styrenes extend away from the surface. Depending upon the solvent quality the styrene segments may either be highly extended or fairly compact at the interface. Shown in the figure below are carbon-13 spectra of the PVP-STY in toluene and adsorbed on the surface of silica-swollen with toluene. It can be seen from these figures that all of the carbon-13 resonances are clearly distinguishable in the solution spectra. However, on the surface only the styrene segments appear. This is because the polymers bond via the vinylpyridine and these are too broad to be seen in the high resolution spectra. From our deuterium NMR relaxation studies, we have estimated that the styrene segments are swollen to about 4 times their normal radius of gyration in solution. The paper is currently in press in *Macromolecules* and in addition, a paper reviewing the state of magnetic resonance of polymers adsorbed on surfaces is available in *Colloids and Surfaces* **45**, 361-376 (1990).



Sincerely,

Frank D. Blum  
Associate Professor of Chemistry  
and Senior Investigator  
Materials Research Center

# Where Research and Technology Meet...



## VIVOSPEC™ Magnetic Resonance Imaging Spectrometer

The *New* VIVOSPEC Imaging Spectrometer developed, designed, and engineered by users for the widest range of applications in medical, in vivo, and industrial research.

**The VIVOSPEC System- Innovative In User Accessibility And Flexibility.**

- New VIVOMOUSE™ Control
- Real Time Display and Control

- Reliable by Design
- Comfort Shim™ Software
- Self-Shielded Gradients
- DEC VAX Station 3200 Computer
- Magnet Sizes and Field Strengths to Fit Your Needs
- Versatile Multinuclear Probe and Positioning Systems
- Multi-Slice Multi-Echo Imaging
- Concurrent Multinuclear Imaging and Spectroscopy
- Consoles, Subsystems, and Components
- Complementary Monitoring

Otsuka Electronics is dedicated to innovation and leadership in this rapidly developing technological era with a commitment to excellence in supplying the most advanced, flexible and accessible magnetic resonance systems.

FIND OUT MORE ABOUT THE FLEXIBILITY AND CAPABILITY OF THE VIVOSPEC IMAGING SPECTROMETER... Flexibility To Start Meeting YOUR Needs Today. Fill out the attached reply card or.

**Call Now! (215) 789-7474.**



**OTSUKA ELECTRONICS (U.S.A.) INC.**

Raymond Drive • Havertown, Pennsylvania 19083 USA • (215) 789-7474 • FAX (215) 789-8081

# VIVOSPEC: SYSTEM SPECIFICATIONS

## RF UNIT

Frequency	5 - 300 MHz
Synthesizer	PTS-500, Computer Controlled
Frequency Step	0.1 Hz
Phase Control	0 - 360 Degrees
Phase, Discrete Steps	0, 90, 180, 270 Degrees
Phase, Variable Steps	0.1 Degree Resolution
Output Power	Computer Controlled: 12 Bit DAC
Power Control	0 - 100 %
Linearity of Power Control	±1%
RF Amplifier Power Output	1000W
Preamplifier	Broadband
Noise Figure	< 2dB

## COMPUTER SYSTEM

Computer	DEC VAX Station 3200, 24 MByte RAM Standard, Up To 64 MByte Optional, 350 MByte Hard Drive, 44 MByte Removable Cartridge Drive, 600 MByte Optical Drive
Control	VIVOMOUSE™ Control Device With Assignable Knob
Display	19 Inch 256 Grey Scale Level Display, 1024 X 864 Resolution
Hard Copy Output Device	Hewlett Packard Laser Jet II Printer

## SOFTWARE

VMS Ver. 5 Operating System, Graphic Work Station  
Software, Shell Environment For Easy Operating System  
Access, IDL Software For Curve Fitting And Data Analysis

## PULSE PROGRAMMER AND DIGITAL INTERFACE

Pulse Programmer	2K X 128 Bit Word Memory, 5 - 16 Bit Loop Counters, 32 Bit Timer, 100 nsec Resolution
Digital Interface	Controls 2 Synthesizers: Frequency, Amplitude, And Phase For 2 RF Channels, 4 Gradient Channels, All With 12 Bit Resolution. 14 Bit A/D At 100 KHz, Audio Filter 51.2 KHz In 200 Hz Steps. Local Memory Buffer 64 KByte. External Gating Input.

## GRADIENTS

Gradient Coils	2 Gauss/cm Minimum
Rise Time (10 - 90 %)	1 msec Maximum (Uncompensated)
Power Supply	TECHRON Model 7570

## HETERONUCLEAR DECOUPLER

Frequency	5 - 300 MHz
Synthesizer	PTS-500, Computer Controlled
Frequency Step	0.1 Hz
Phase Control	0 - 360 Degrees
Phase, Discrete Steps	0, 90, 180, 270 Degrees
Phase, Variable Steps	0.1 Degree Resolution
Output Power	Computer Controlled: 12 Bit DAC
Power Control	0 - 100 %
Linearity of Power Control	±1%
RF Amplifier Power Output	100W CW

## STANDARD MAGNET CONFIGURATIONS

Field (T)/Bore (cm)	2/31	2/30.5	2.4/40	4.7/20	4.7/31	4.7/40	7/20
Bore With RT Shims And Gradients (cm)	26.5	26	33	15	26.5	31	15
Helium Evaporation (ml/hr)	50	50	50	50	55	60	50
Nitrogen Evaporation (ml/hr)	400	400	400	400	450	500	400
Half Length (mm)	350	275	570	396	460	735	575
5 Gauss Line — Radial From Center (m)	3.4	3.2	4.7	3.7	5.3	6.4	5.1
— Axial From Center (m)	4.4	4.0	5.9	4.7	6.7	8.1	6.4

Other Magnet Sizes And Field Strengths Available On Special Order

Specifications subject to change



**OTSUKA ELECTRONICS (U.S.A.) INC.**

### NORTH AMERICA

**OTSUKA ELECTRONICS (U.S.A.), INC.**  
1 Raymond Drive  
Havertown, Pennsylvania 19083 USA  
(215) 789-7474  
FAX (215) 789-8081

### EUROPE

**OTSUKA ELECTRONICS (EUROPE) LTD.**  
P.O. Box 11  
Abingdon, OXON OX14 1RW  
ENGLAND  
0235-554454

### FAR EAST

**OTSUKA ELECTRONICS CO., LTD.**  
HEAD OFFICE  
3-26-3  
Shodai-Tajika  
Hirakata, Osaka 573  
JAPAN  
0720-55-8550

### OTSUKA ELECTRONICS CO., LTD.

TOKYO OFFICE  
2F. Hashikan-LK Bldg.  
1-6 Azuma-Cho  
Hachioji, Tokyo 192  
JAPAN  
0426-44-4951



**THE JOHNS HOPKINS UNIVERSITY**  
**SCHOOL OF MEDICINE**  
*and*  
**THE JOHNS HOPKINS HOSPITAL**

DEPARTMENT OF RADIOLOGY  
 AND  
 RADIOLOGICAL SCIENCE

Mailing Address:  
 THE JOHNS HOPKINS HOSPITAL  
 Baltimore, Md. 21205

Professor B.L. Shapiro,  
 TAMU NMR Newsletter,  
 966 Elsinore Court,  
 Palo Alto, CA 94303

July 12th 1990  
 (received 7/20/90)

Mode-Switched Radiofrequency Coils

Dear Professor Shapiro,

A few years ago, there was appreciable interest in spatial localization methods using  $B_1$  field gradients (Rotating Frame Imaging (RFI), Fourier Series Imaging, "Depth" Pulses etc.).  $B_1$  gradients can be turned on and off very rapidly, do not generate eddy currents which perturb the homogeneity of the magnetic field, and they can be selectively applied to a single nucleus in a heteronuclear spin system. Most experiments that are performed using  $B_0$  field gradients (imaging, localized spectroscopy, diffusion measurements, coherence transfer pathway selection) have analogues which use  $B_1$  gradients. However,  $B_1$  gradients techniques have not found widespread use mainly because of the difficulty of producing good  $B_1$  field gradient coils.

In order to address the problem of building a  $B_1$  gradient coil, we have recently been working on the concept of "Mode-Switching". Many of the radiofrequency coils used in NMR resonate at more than one frequency. Examples include the Helmholtz and Birdcage coils. Mode-switching is defined as the ability within a pulse sequence to change the coil mode which resonates at the NMR frequency. For a simple Helmholtz coil, there are two modes which correspond to co- and counter-rotating current flow in each loop - the co-rotating mode produces a homogeneous field while the counter-rotating mode produces a gradient field. The two modes resonate at slightly different frequencies depending on the mutual coupling of the two loops. If the coil is initially tuned so that the co-rotating mode is on-resonance, the counter-rotating mode can be brought on-resonance by switching in additional capacitance (figure 1). Mode-switching allows a single radiofrequency coil to be used to generate both  $B_1$  field gradients and homogeneous  $B_1$  fields. A prototype mode-switched coil (1 turn, radius=1.7cm, separation=3.0cm) was built for  $^{31}\text{P}$  in a 4.7 Tesla magnet (81 MHz). Mode-switching was verified by recording the magnetization profile of a cylindrical sample along the coil axis using a  $B_0$  gradient recalled echo imaging sequence. Figure 2A shows the magnetization profile for the mode-switched coil in homogeneous transmit/receive mode, 2B shows the profile in gradient transmit/homogeneous receive mode. The calculated magnetization profiles are shown in 2C and 2D respectively,

with best wishes,

*Peter Barker.*

Peter B. Barker.,

*Dikoma C. Shungu*

Dikoma C. Shungu,

Joseph Schoeniger

Figure 1

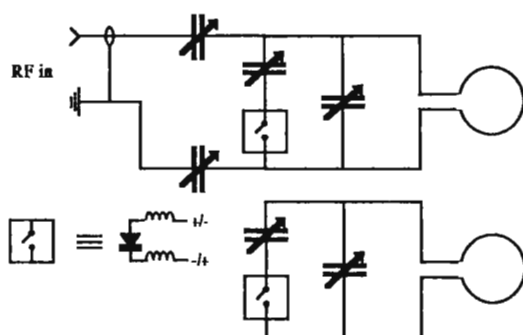
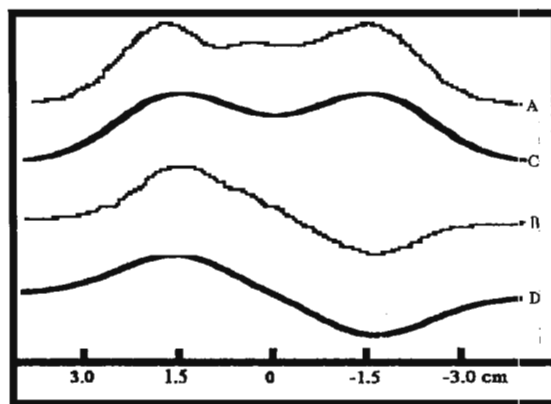


Figure 2



## POSITION AVAILABLE

**CHEMAGNETICS, INC.**, a rapidly growing **NMR** company is seeking an **APPLICATIONS CHEMIST**. Primary responsibilities will include demonstration of the company's products to prospective customers, maintaining a current knowledge of **NMR** literature and assisting in the identification of new developments in the field which have commercial significance. Some travel required to customer sites and to represent the company at technical meetings. Experience in solids **NMR** and good verbal and written communication skills essential. Position reports to the Director of Sales and Marketing. Send confidential resume and salary history to:

**CHEMAGNETICS, INC.**  
**2555 MIDPOINT DRIVE**  
**FORT COLLINS, COLORADO 80525**



Biomedical Engineering Department

100 Institute Road  
 Worcester, MA 01609-2280  
 (508) 831-5447  
 FAX (508) 831-5483

July 6, 1990  
 (received 7/8/90)

Dr. Bernard L. Shapiro  
 TAMU NMR Newsletter  
 966 Elsinore Court  
 Palo Alto, California 94303

### Lactate Edited Self-Diffusion Coefficient Measurements

Dear Dr. Shapiro,

Knowledge of the self-diffusion coefficient of biological metabolites would provide important information concerning compartmentation and mobility and could potentially be used to characterize the disease state of a tissue or organ. Unfortunately, the direct measurement of the diffusion coefficient of protonated metabolites, such as lactate, by the conventional Stejskal-Tanner technique (1) is frequently impossible due to the presence of interfering resonances (such as lipid). Therefore, the lactate diffusion measurement must be implemented in concert with a suitable spectral editing technique.

The STimulated Echo Zero Quantum Coherence (STEZQC) and STEZQC-2D spectral editing techniques have recently been suggested for obtaining *in vivo* lactic acid spectra from a localized volume (2,3). The volume localized STE sequence (unshaded part of Figure 1) creates ZQ (and higher order) coherences in coupled spin systems following the first two 90° pulses. The ZQ's evolve during the interval,  $t_1$ , between the second and third 90° pulses, and manifest themselves as an amplitude modulation of the corresponding single quantum (SQ) signal generated following the third 90° pulse. The observed ZQ modulation frequency is equal to the chemical shift difference (in Hz) between the coupled spins. The observed SQ signals from noncoupled spins are not modulated.

In the STEZQC-2D experiment, a series of STE spectra are collected in which the ZQ evolution period,  $t_1$ , is incremented. Subsequent two-dimensional Fourier transformation yields a plot of chemical shift versus ZQ modulation frequency. Peaks due to lactate appear at  $\pm 250$  Hz (the chemical shift difference between the coupled methyl and methine resonances at 2.0T). Peaks due to noncoupled spins appear at zero frequency. Peaks arising from partially coupled lipid resonances can be distinguished from lactate based upon differences in their respective ZQ frequencies.

In addition to the classical Stejskal-Tanner spin-echo technique, diffusion measurements can also be performed using the STE pulse sequence (4). A pair of pulsed-field gradients (the shaded gradient pulses in Figure 1) are introduced into the respective TE/2 periods and a series of STE spectra are collected in which the diffusion gradient pulse separation,  $\Delta$ , is successively increased, for example, by incrementing the  $t_1$  interval between the second and third 90° pulses. This incarnation of the diffusion measurement is identical to the implementation of the STEZQC-2D experiment and allows the two methods to be executed simultaneously.

Information about the lactate diffusion coefficient is encoded in the linewidth of the corresponding peak in the ZQ frequency dimension. In addition to the diffusion information, however, the linewidth also contains contributions due to the intrinsic relaxation attenuation of the signal in the ZQ domain. Since this information is not known in advance, it must be elucidated by comparison to a second experiment in which the diffusion gradients are either absent or of a different strength. The self-diffusion coefficient,  $D$ , can then be calculated from the expression (5)

$$D(\text{cm}^2/\text{sec}) = \pi[\Delta\nu_{1/2}(2) - \Delta\nu_{1/2}(1)] / \gamma^2(2/\pi)^2 \delta^2 [G(2)^2 - G(1)^2] \quad [1]$$

where  $\Delta\nu_{1/2}(1)$  and  $\Delta\nu_{1/2}(2)$  are the FWHH of the ZQ lines from the first and second experiments, respectively,  $\delta$  is the diffusion gradient duration,  $G(1)$  and  $G(2)$  are the gradient amplitudes for the first and second experiments, respectively, and the factor of  $(2/\pi)^2$  was added to take into account that half-sine shaped, diffusion-sensitive gradients are being used in the pulse sequence in Figure 1.

A volume localized, STEZQC-2D diffusion measurement was performed on a 20 mm, spherical polyethylene phantom containing peanut oil and 100 mM N-acetylalanine (in D<sub>2</sub>O), which has an AX<sub>3</sub> spin system similar to lactic acid. Data were acquired using a GE 2.0T/45 cm CSI-II imaging spectrometer, equipped with 20 gauss/cm self-shielded gradients, operating at 85.56 MHz for protons. Spectra were obtained from a 1-cc volume at the interface of the two phases (Figure 2) using a 4.5-cm-diameter "birdcage" imaging coil. The two requisite experiments were acquired in an interleaved fashion to minimize the effects of instrumental instabilities over the course of the measurement. In the first experiment,  $G(1)$  was set to 0 gauss/cm and  $t_1$  was incremented from 8 to 774.5 ms, in 1.5 ms steps (resulting in a concomitant increase in  $\Delta$  from 26 to 792.5 ms). The repetition time was 2.8 s,  $\delta$  was 10 ms, TE was 136 ms (1/J for the AX<sub>3</sub> spin system), and two averages were acquired for each  $t_1$  increment with



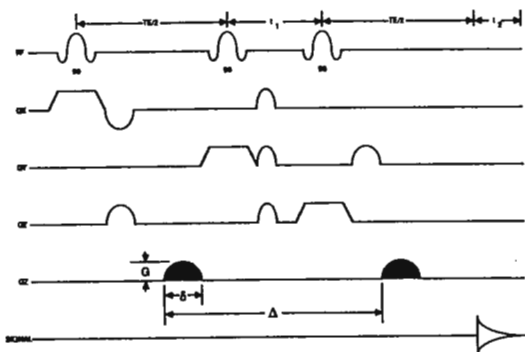


Figure 1. Volume localized, diffusion sensitive Stimulated echo (STE) pulse sequence.

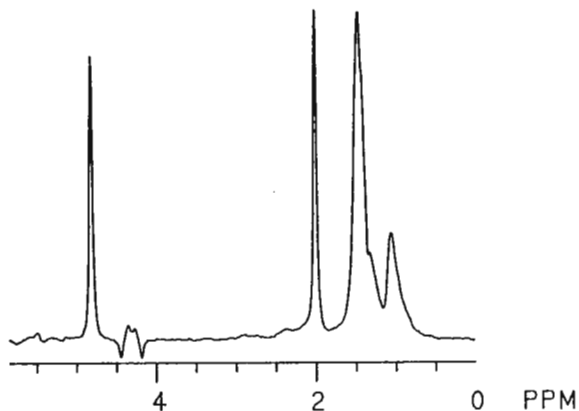


Figure 2. STE spectrum from a 1 cc volume within a phantom containing 100 mM N-acetyl alanine (in D<sub>2</sub>O) and peanut oil.

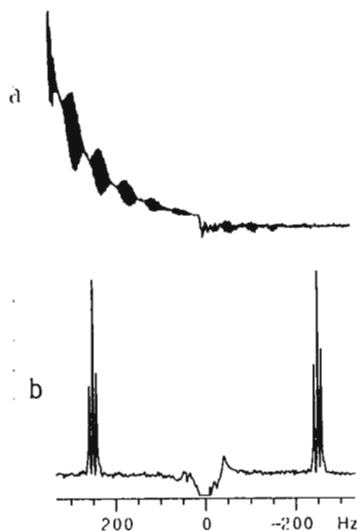


Figure 3. (a) ZQ time domain signal (real and imaginary data) extracted from 2D dataset (at 1.3 ppm) acquired with  $G=0$  gauss/cm. (b) Expansion of Fourier transform of (a).

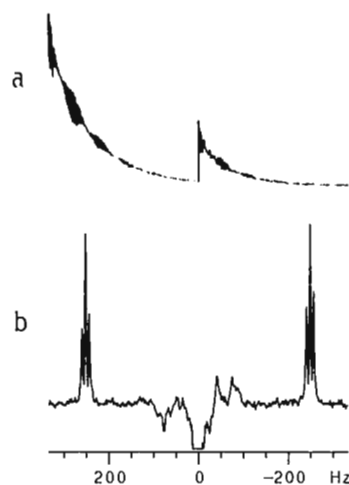


Figure 4. (a) ZQ time domain signal (real and imaginary data) extracted from 2D dataset (at 1.3 ppm) acquired with  $G=5$  gauss/cm. (b) Expansion of Fourier transform of (a).

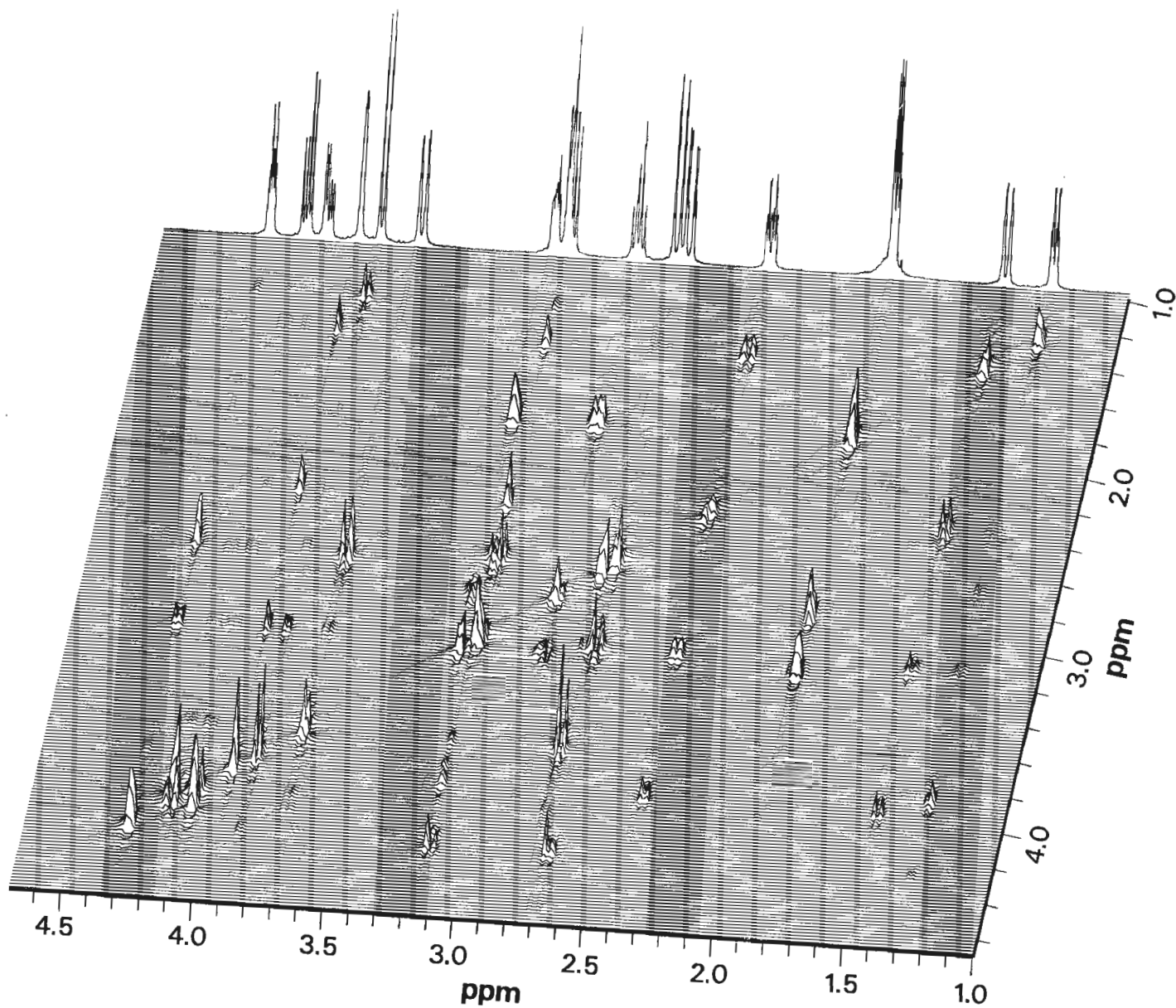
phase cycling to remove the dc offset from the FID. The parameters for the second experiment were identical to the first except that  $G(2)$  was set to 5 gauss/cm. Both 2D datasets were Fourier transformed in the first dimension and then transposed. The time domain signals at 1.31 ppm (the chemical shift of the coupled  $-CH_3$  group in the AX<sub>3</sub> system) were then extracted from each dataset (Figures 3a and 4a) and Fourier transformed (Figures 3b and 4b). The linewidth for each spectrum was measured by fitting the central peak of the triplets at  $\pm 250$  Hz with a Lorentzian function. The linewidths averaged 1.94 Hz and 3.11 Hz for the first and second experiments, respectively. From these data, the diffusion constant was calculated from equation [1] to be  $5.1 \times 10^{-6}$  cm<sup>2</sup>/s (at 22°C), which is in good agreement with the average value of  $4.8 (\pm 0.1) \times 10^{-6}$  cm<sup>2</sup>/s ( $N=4$ ) (at 18°C) we have measured for this compound using the Stejskal-Tanner spin-echo method.

Sincerely,

*Chris Sotak*

Chris Sotak

1. E. O. Stejskal and J. E. Tanner, *J. Chem. Phys.* **42**, 288 (1965).
2. C. H. Sotak and D. M. Freeman, *J. Magn. Reson.* **77**, 382 (1988).
3. C. H. Sotak, *Magn. Reson. Med.* **7**, 364 (1988).
4. J. E. Tanner, *J. Chem. Phys.* **52**, 2523 (1970).
5. C. H. Sotak and S. C. Moore, *J. Magn. Reson.*, submitted.



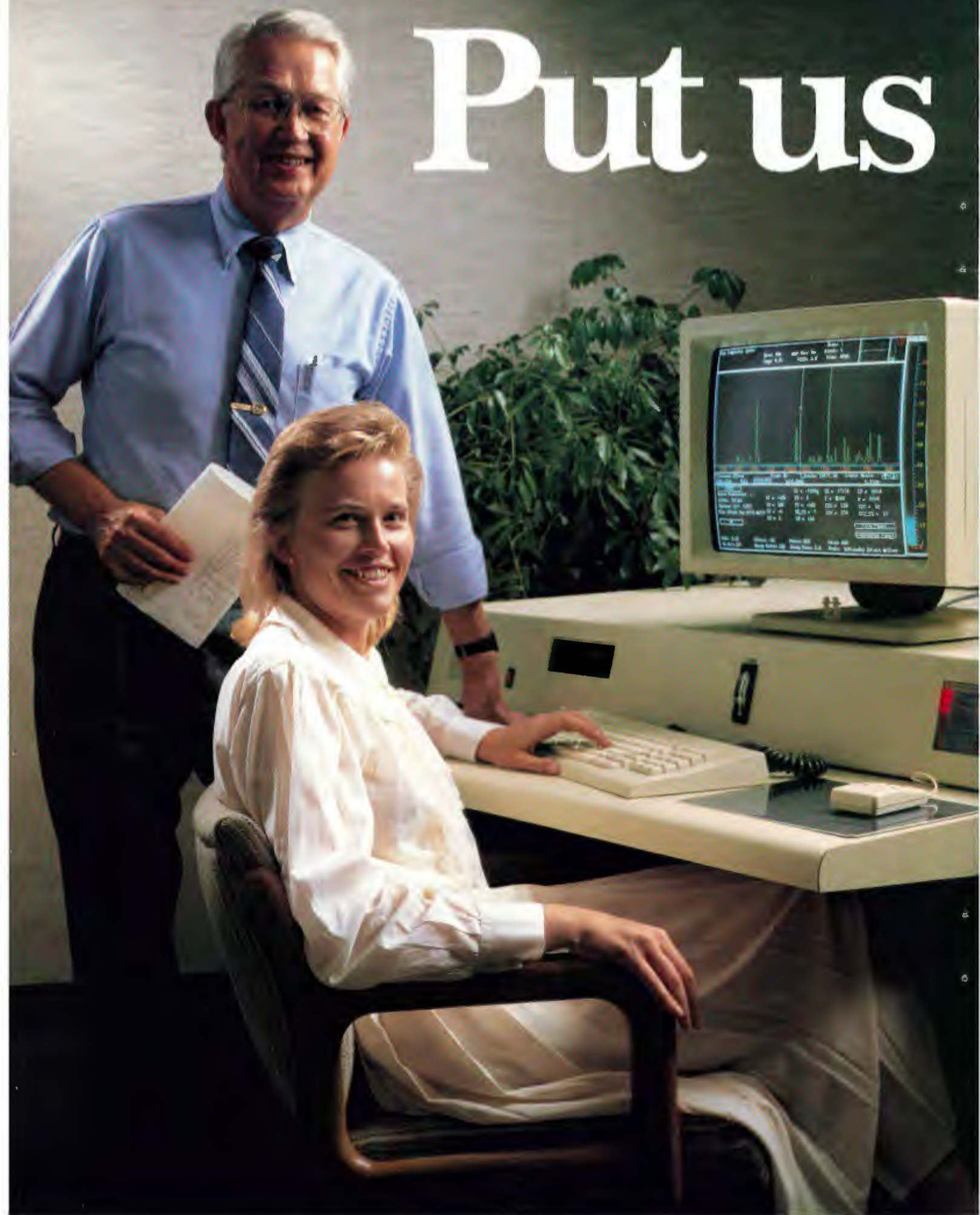
**HOHAHA of Strychnine on an Omega 600**



***GE NMR Instruments***



# Put us



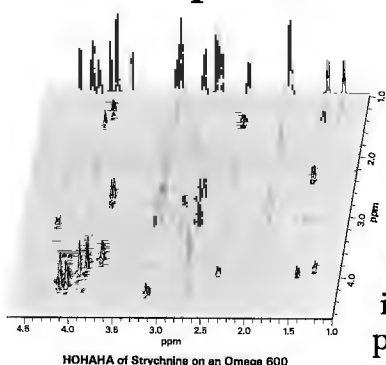


# to the test.

**T**here's only one way to be certain you're getting the best NMR system—test it yourself. Challenge its capabilities with your samples. Compare its results against your requirements.

See for yourself how GE spectrometer and CSI imaging systems measure up.

## In RF performance



For outstanding RF stability in phase-sensitive work, inverse transfers and INADEQUATE experiments:

■ Amplitude stability of .043% in 90° pulse test of single acquisition in doped

water, repeated 10 times. Amplitude stability of .17% with 1 microsec. pulse.

■ Average deviation in 13° test of 0.5% in amplitude, representing stability of 0.07° in phase.

■ High-performance 200 kHz ADC with up to 32 MByte of 64 bit on-board memory for direct acquisition of experiments into memory.

## In gradient control

The GE Acustar™ and Microstar™ shielded gradient systems improve image quality and localization by

eliminating eddy current effects for submillisecond settling times and better signal-to-noise performance. They also expand applications into oil core analysis, chemical toxicity testing, and monitoring of microscopic processes and reactions.

## In data processing

GE opens NMR data processing and system operation to users at every level of expertise.

Mouse-directed panel menus let beginners use the system immediately. And programming designed by GE specifically for NMR applications lets experienced users attempt the most complex experiments.

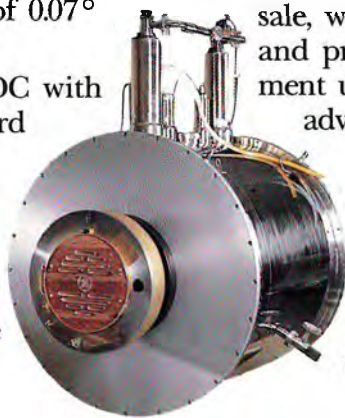
## In customer service and support

At GE, we're with you before and after the sale, with convenient financing packages and prompt service—as well as equipment upgrades, software updates and advanced applications.

To arrange a demonstration or for more information, write us today at 255 Fourier Ave., Fremont, CA 94539.

Or call 800-543-5934.

You'll be pleased with the results.



**GE NMR Instruments**

# Alpha HDR

## The New Standard in Digitizer Performance

Dynamic range vs. spectral width; spectral width vs. digital resolution. Trade-offs have been required due to NMR system hardware limitations. With the Omega™ Data system's Alpha HDR digitizer, no trade-offs are necessary. As shown in Figure 2 with a 16-bit dynamic range, 200 KHz spectral width, 64-bit complex acquisition word size, and up to 32 MBytes (4 MWords complex) of on-board acquisition memory available, the spectrometer is no longer the limiting factor when designing the most demanding experiments. Other outstanding features of the Alpha HDR include variable dwell periods, phase shifts of each sampled data point as small as 0.05 degrees, and segmentation of the digitizer memory into as many as 64K blocks. These features further distinguish the GN-series spectrometer equipped with the Omega Data System as the leader in NMR technology.

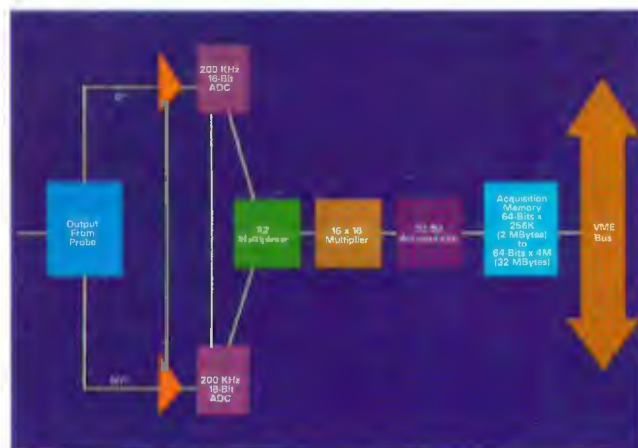


Fig. 1  
The Alpha HDR digitizer.

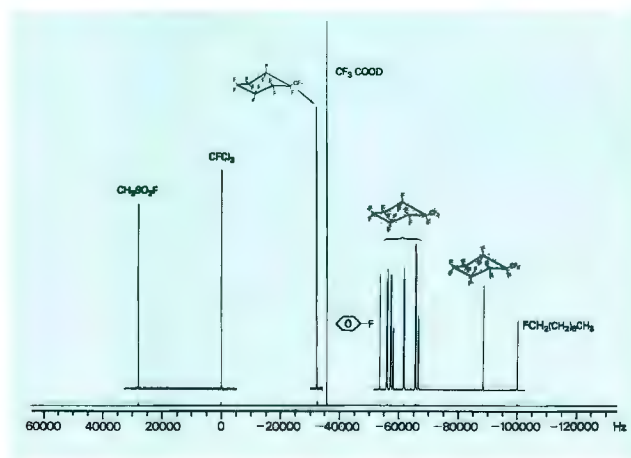


Fig. 2  
200 KHz spectral width <sup>19</sup>F spectrum acquired on a GN-500 Omega System. Note the extremely flat baseline obtained with the Alpha HDR.



### GE NMR Instruments

255 FOURIER AVENUE, FREMONT, CA 94539  
(415) 683-4408, TELEX 910 381 7025 GE NMR FRMT  
PRAUNHEIMER LANOSTRASSE 50, D-6 FRANKFURT 90  
WEST GERMANY 4969 760 7431, TELEX 041 2002 GEG

*Columbia University in the City of New York*

C. J. Turner  
Department of Chemistry  
Havemeyer Hall  
New York NY 10027  
Friday, July 6, 1990  
Phone 212-854-4601

(received 7/18/90)

Dear Barry:

Fast Phase Sensitive COSY

Its always nice to try and make experiments go faster. The major problem with trying to speed up the acquisition of 2-D data is interference between adjacent transients. We could describe the basic PSCOSY phase cycle as 0 2 if the phase of the second pulse is never altered and the phase of the first pulse is identical to that of the receiver, in the first hypercomplex data set. Thus the interference terms generated two adjacent transients can be referred to 0 2 and 2 0.

Unfortunately phase cycles are non-commutative and therefore these two interference terms 0 2 and 2 0 do not cancel. However, we can cancel the interference by inverting the phase of the first pulse in alternate repetitions of the COSY sequence, a process very much akin to that of axial peak suppression. Furthermore, we can see that these four terms: 0 0, 0 2, 2 0, and 2 2 comprise all the possible permutations of two 0's and two 2's and thus suggest that in order to cancel interference between three adjacent transients we need all the possible permutations of three 0's and three 2's, i.e. : 0 0 0, 0 0 2, 0 2 0, 0 2 2, 2 0 0, 2 0 2, 2 2 0, and 2 2 2. We overlap these interference terms in order to minimize the length of the cycle. Obviously the cycle will have to contain the three step procedures 0 0 0 and 2 2 2, since this is the only way such interference terms can be generated. So far the cycle would have six steps. However, these two three step procedures (0 0 0 and 2 2 2) need to be separated from each other. In order to avoid redundancy, we shall have to invert the phase after the first three steps leading to 0 0 0 2. Equally, we need to invert the phase of the step before 2 2 2, therefore we also need 0 2 2 2. If we simply place these two four step procedures next to each other we get: 0 0 0 2 0 2 2 2, which turns out to be the shortest way to cancel interference between three adjacent transients. It is easier to see why this works if we break this eight step cycle down into its overlapping three step terms, thus:

0 0 0 2 0 2 2 2

is made up of:

0 0 0  
0 0 2  
0 2 0  
2 0 2  
0 2 2  
2 2 2  
2 2 0  
2 0 0

This also demonstrates the necessity to use a multiple of the number of steps in the cycle, since some of these interference terms are generated by overlap from the end of one sequence to the beginning of the next. Strictly speaking we should refer to this cycle as  $(00020222)_n$ .

Not only will this cycle cancel artifacts generated by interference between three transients but also those generated by interference between two transients, since the relevant two step interference terms are: 0 0, 0 0, 0 2, 2 0, 0 2, 2 2, 2 2, and 2 0.

Best Wishes

Chris



## PHILIPPS-UNIVERSITÄT MARBURG

FACHBEREICH CHEMIE

Prof. Dr. S. Berger



FB CHEMIE · HANS-MEERWEIN-STR. · D-3550 MARBURG

BITNET: BERGER@DMRHRZ11

MARBURG, DEN 29.6.90

TELEFON (06421) 28-1 (received 7/2/90)

DURCHWAHL: (06421) 28 5520

TELEX 482372

Prof. Dr. B. L. Shapiro  
TAMU-NMR Newsletter  
966 Elsinore Court  
Palo Alto, Cal. 94303  
USA

**SELRESOLV: Selective Measurements of Long Range C,H-Coupling Constants**

Dear Professor Shapiro,

we would like to communicate a new variety of our selective pulse sequences<sup>1,2</sup>. Sometimes one needs to know a long range C,H-spin coupling constant accurately. Usually one measures the gated decoupled carbon spectrum which, however, has to be analyzed carefully, because several protons exhibit spin coupling to the carbon atom in question and furthermore, very often the spin system is of higher order. Our sequence SELRESOLV tackles this problem by proton spectroscopy and belongs therefore to the class of inverse experiments, where first of all the signals of carbon-12 bound protons have to be suppressed. In addition, the proton proton multipletts must be separated from proton carbon couplings. We achieved this by a standard 2D J-resolved scheme. To obtain the information of only one carbon atom we used at the start of the sequence one selective half gaussian pulse. There are several other proposals in the literature to solve the same problem<sup>3-5</sup>, but we feel our method has the advantage that the desired coupling constant can be directly read from the 2D-spectrum. The example given on the opposite page is 2-hydroxynaphthalene, carbon atom 2 was selected and its long range coupling to hydrogen 4 was observed.

Sincerely yours

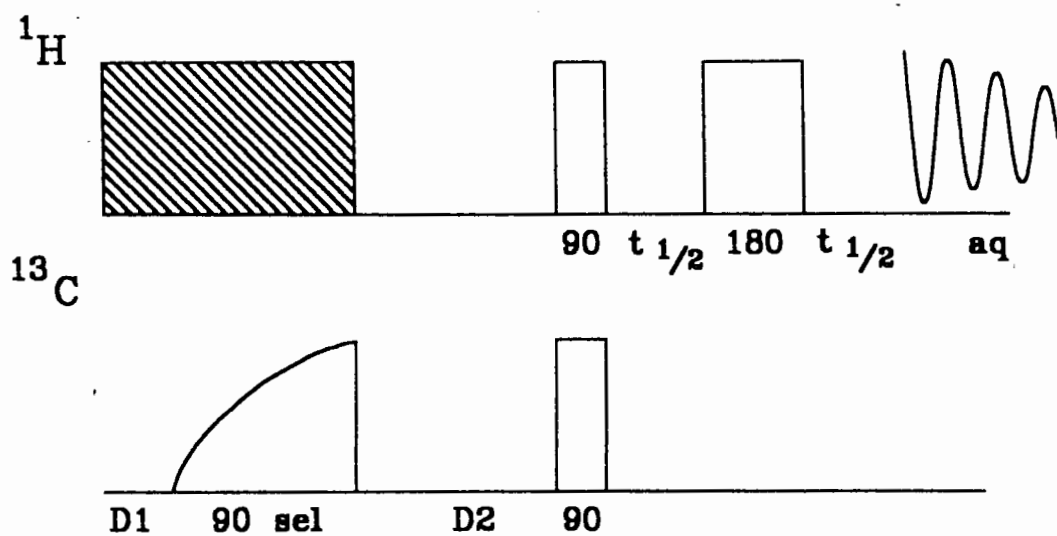
Handwritten signature of Matthias Ochs.

Matthias Ochs

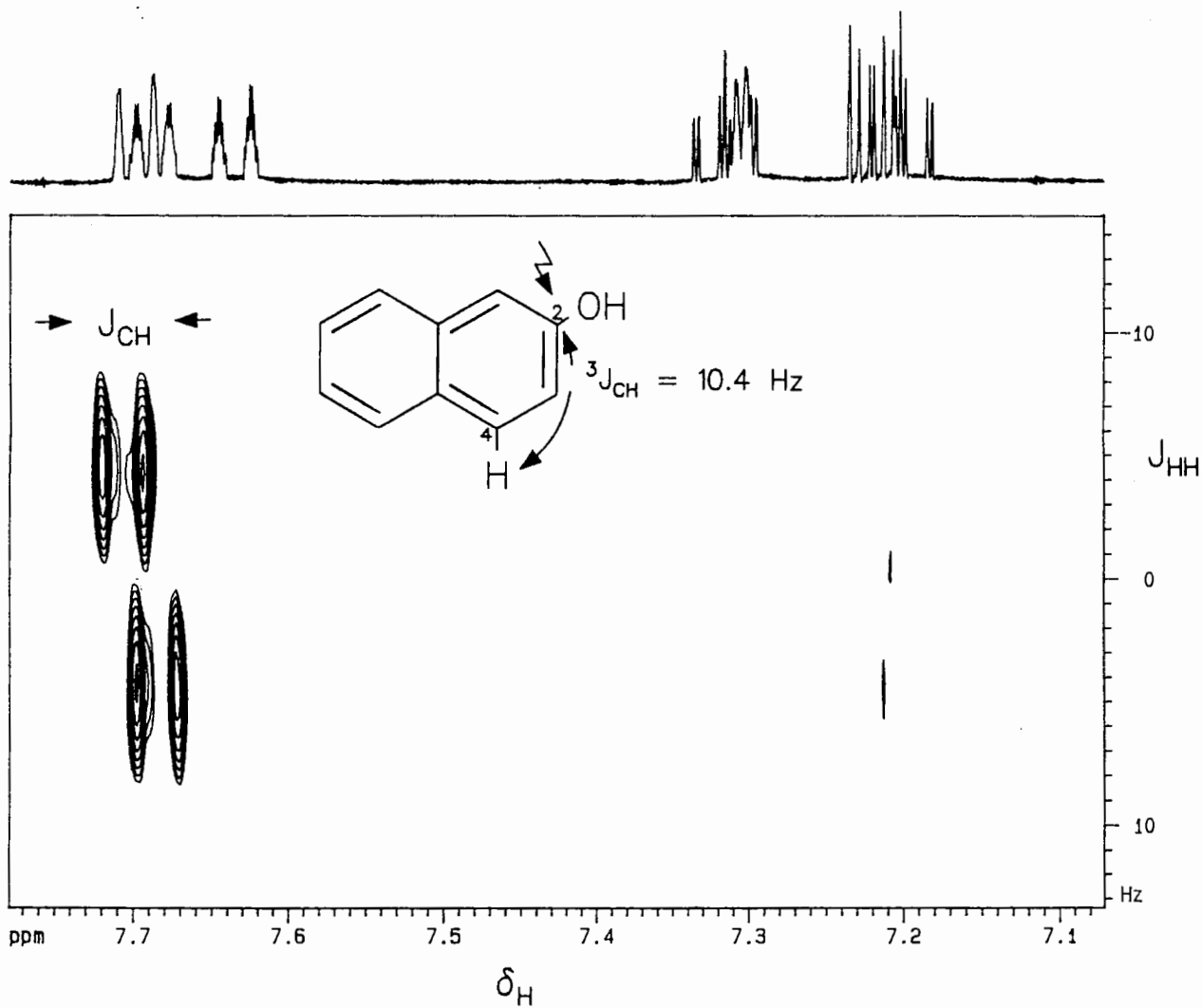
Handwritten signature of Stefan Berger.

Stefan Berger

- 1) S. Berger, Angewandte Chemie Int. Ed. **27**, 1196 (1988).
- 2) S. Berger, J. Magn. Reson. **81**, 561 (1989).
- 3) A. Bax, R. Freeman, J. Am. Chem. Soc. **104**, 1099 (1982).
- 4) T. K. Pratum, P. K. Hammen, N. H. Anderson, J. Magn. Reson. **78**, 376 (1988).
- 5) Bermel, W., Wagner, K., Griesinger, C., J. Magn. Reson. **83** 223 (1989).



D1 = presaturation, D2 =  $1/2J(\text{CH})$ , sel = selective pulse





# OREGON HEALTH SCIENCES UNIVERSITY

3181 S.W. Sam Jackson Park Road, Portland, OR 97201-3098  
Mail Code UHN 72, (503) 494-4498, FAX (503) 494-4621

*School of Medicine  
Department of Diagnostic Radiology*

Dr. B. L. Shapiro  
Texas A&M Newsletter  
966 Elsinore Court  
Palo Alto, CA 94303

June 12, 1990  
(received 6/20/90)

RE: Real or Artifact?

Dear Dr. Shapiro:

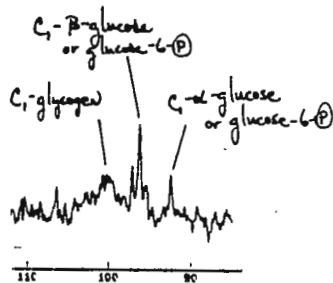
During the frantic days of my departure from the University of Iowa, I collected some data that I can neither fully interpret, nor reproduce for lack of access to the proper spectrometer. The confusing data were observed when  $^{13}\text{C}$ -labeled fructose (either  $\text{C}_1$  or  $\text{C}_6$  labeled) was presented to isolated perfused rat liver. The natural abundance  $^{13}\text{C}$  spectra appear to be proton decoupled, as do the resonances from metabolites that appear in the difference spectra. Four of the nine livers overall, and all three of the livers receiving  $[6-^{13}\text{C}]$ -fructose display a "triplet" (figure) centered where we expect proton decoupled  $[1-^{13}\text{C}]$ -glucose +  $[1-^{13}\text{C}]$ -glucose-6-phosphate to resonant as a singlet (96.8 ppm referenced to  $\text{C}_6$ -glucose at 61.4 ppm). Only one of nine perchloric acid extracts prepared from the livers showed a "triplet" in the region in question. The chemical shifts for the new peaks are 97.6 and 96.0 ppm respectively.

What is the origin of the peaks, improper decoupling or fructose metabolism? In our desire to minimize tissue heating by keeping the decoupler power low, were we observing some "spin tickling" phenomenon? The "doublet" (the two additional peaks) of the in vivo spectra has a coupling constant 1/2 that of proton coupled  $[1-^{13}\text{C}]$  glucose in the extracts. If the doublet is due to insufficient decoupling, why are there two discreet sets of peaks?

Two metabolites involved in glycogen synthesis that have resonances in this region are glucose-1-phosphate and UDP-glucose. Since both of these contain a phosphorylated hemiacetal linkage, the extraction conditions may have been too harsh for their survival, or the liver may have been clamped after the levels were decreased. Fructose does not cause an insulin effect, therefore it was not included in the perfusion media. If we were able to observe UDP-glucose and glucose-1-P we could enhance our understanding of glycogen turnover under physiological conditions, such as diabetes where insulin is about.

The data was acquired on a Brüker MSL 300, 89mm bore magnet. While I did not "scope" the decoupler output for this experiment, the machine was extremely clean for all the parameters we examined for other experiments. If anyone can account for the observation by proton-carbon interactions or improper decoupler instrumentation, I would be most interested in their ideas.

Sincerely,



William J. Thoma, PhD  
Assistant Professor

*Schools:  
Schools of Dentistry, Medicine, Nursing*

*Clinical Facilities:  
University Hospital,  
Doernbecher Children's Hospital,  
Child Development and Rehabilitation Center,  
University Clinics*

*Special Research Divisions:  
Biomedical Information Communication Center,  
Center for Research on Occupational and  
Environmental Toxicology,  
Vollum Institute for  
Advanced Biomedical Research*

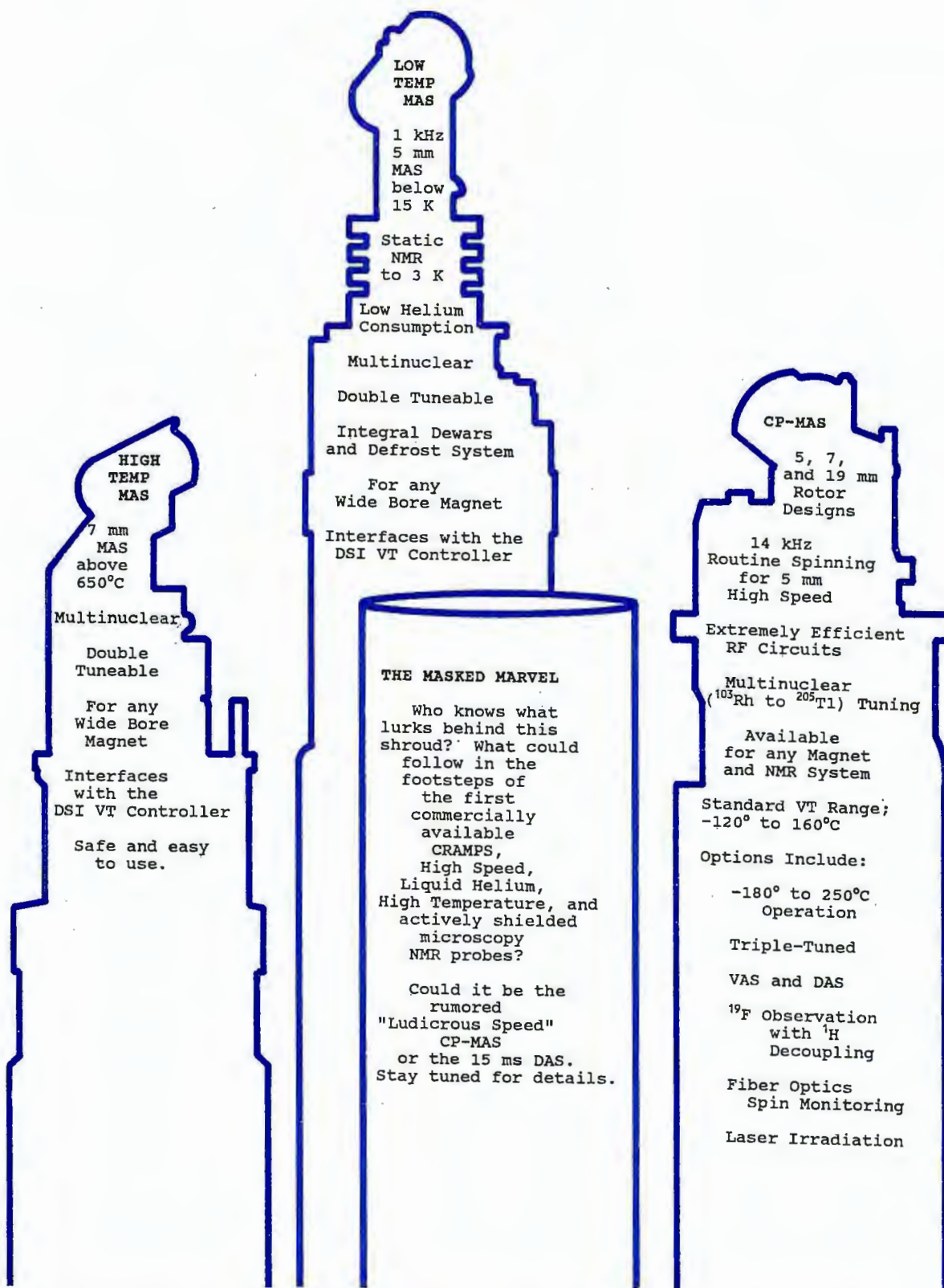




# Doty Scientific







DOTY SCIENTIFIC, INC., 600 CLEMSON RD., COLUMBIA, SC 29223 USA

Main (803) 788-6497 Sales (803) 699-3806 Fax (803) 736-5495



E. I. DU PONT DE NEMOURS & COMPANY  
INCORPORATED

P.O. Box 80328  
WILMINGTON, DELAWARE 19880-0328

1990 June 28  
)deviecer 09/50/70(

CENTRAL RESEARCH & DEVELOPMENT DEPARTMENT  
EXPERIMENTAL STATION

Dr. Bernard L. Shapiro  
TAMU NMR Newsletter  
966 Elsinore Court  
Palo Alto, CA 94303

Dear Barry,

During a recent study of technetium-99 complexes, we wanted to determine if the hydrogen directly bonded to the technetium in the compound  $(\text{Tc}(\text{PMe}_3)_4(\text{NHSCNH}_2)\text{H})^+(\text{PF}_6)^-$  could be readily replaced by deuterium. The spectrometer being used was a 1981 vintage Bruker WM-400. It has been upgraded from time to time but still has the original magnet which drifts downfield at about one ppm per day. This presents no problems unless one wants to look at weak deuterium samples requiring long data collection times. It is also difficult to shim such samples, since the use of a deuterated solvent for shimming would create a dynamic range problem, and the deuterium FID of the solute is too weak to be of use in shimming.

Since we were using protiated solvents, clearly what we needed was a proton lock and this was surprisingly easy to implement using a balanced mixer as a bidirectional frequency converter (1). A broadband probe tuned to the deuterium NMR frequency of 61.4 MHz was used. The lock cable was connected to one of the outer ports of a high level balanced mixer (Mini-Circuits model ZFM-2H) and the other outer port of the mixer was connected to the proton decoupling coil of the probe. About 1 volt of RF at 338.7225 MHz from a PTS-500 synthesizer was fed to the center port of the mixer. The deuterium lock pulses at 61.4 MHz are upconverted in the mixer to proton lock pulses at 400.13 MHz and excite the protons in the solvent via the proton decoupling coil. The resulting proton lock signal is downconverted in the same mixer back to 61.4 MHz. Despite losses in the mixer, the spectrometer can be easily locked up and shimmed using the protons in the solvent.

The lower spectrum in the figure shows the hydride resonance of the technetium hydride compound in solution in  $\text{CD}_2\text{Cl}_2$  at 33° C. using the normal deuterium lock, while the upper spectrum shows the deuteride resonance of the technetium deuteride run in  $\text{CH}_2\text{Cl}_2$  with a proton lock. The deuteride was prepared from the hydride by treatment with Methanol- $\text{d}_4$ . Both spectra are triplets of triplets resulting from couplings to P-31 in the four phosphine ligands. Since, in corresponding compounds, P-D splittings are smaller than P-H splittings by the ratio of the NMR frequencies, the peaks in the two spectra are superimposable when the spectra are plotted on the same chemical shift scale.

Please credit this contribution to the account of Don Bly.

Reference 1. Fred Brown. W6HPH, An Introduction to the Bilateral Converter, QST Magazine, December 1981, p. 34.

Derick Ovenall

and

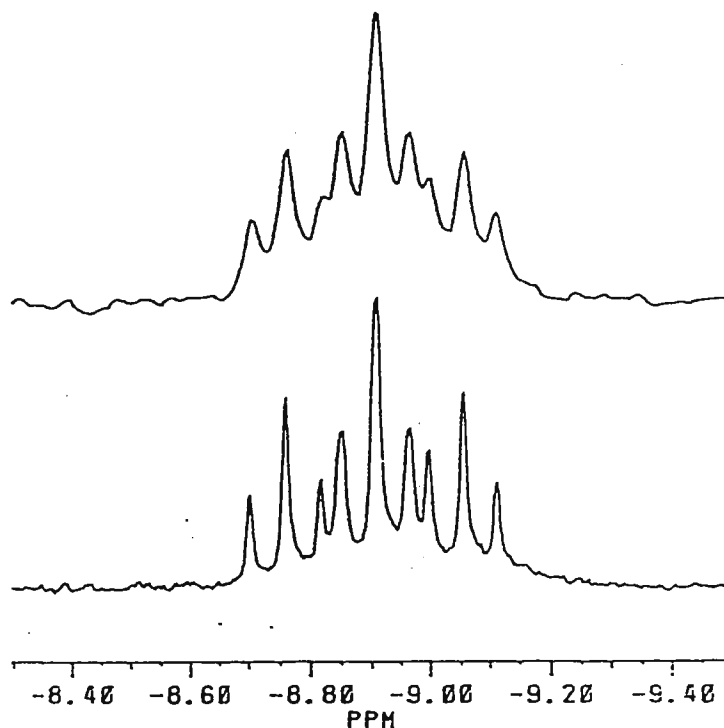
Joseph Albanese

*Derick Ovenall*

*Joseph Albanese*

383-22 Top spectrum: Deuterium NMR of Technetium Deuteride in  $\text{CH}_2\text{Cl}_2$  using proton lock.

Bottom spectrum: Proton NMR of Technetium Hydride in  $\text{CD}_2\text{Cl}_2$  using deuterium lock.



POSTDOCTORAL SCIENTIST

## IN VIVO NMR/IMAGING

SmithKline Beecham Pharmaceuticals, a worldwide leader in pharmaceutical research, has a challenging opportunity in its Biological Nuclear Magnetic Resonance Research Group. This is a postdoctoral scientist position in NMR imaging and in vivo NMR spectroscopy. The successful candidate will be working in the area of development of in vivo NMR techniques and its application to pharmacological research.

The NMR group is equipped with two 500 MHz spectrometers and a 400 MHz spectrometer with micro-imaging and solids accessories. A Sun 4, a Sparcstation and a Microvax, connected to the spectrometers via standard networking, are used for off line data processing and image analysis. In addition we have access to a clinical 1.5 T instrument. Candidates should have a Ph.D. in physics, chemistry or biology with a strong background in NMR and an interest in in vivo NMR.

Our state-of-the-art research facilities are located in suburban Philadelphia, near Valley Forge, PA. We offer a competitive compensation/benefits package as well as the opportunity for growth in a scientifically intense environment structured on creativity, teamwork and commitment. Please send your C.V. to

Nancy Hasson, Employment Administrator, #H0145, SmithKline Beecham Pharmaceuticals, P.O. Box 1539, King of Prussia, PA 19406-0939. We are an Equal Opportunity Employer, M/F/H/V.



**SmithKline Beecham**  
Pharmaceuticals





Department of Chemistry  
LOUISIANA STATE UNIVERSITY AND AGRICULTURAL AND MECHANICAL COLLEGE  
BATON ROUGE • LOUISIANA • 70803-1804

Dr. B. L. Shapiro, Editor  
TAMU NMR Newsletter  
966 Elsinore Court  
Palo Alto, CA 94393

504/388-3361  
FAX 504/388-3458  
BUTLER@CHVAX.LSU.EDU  
June 21, 1990  
(received 6/28/90)

### 3D NMR: Displaying the Results from Pulse Sequence Simulations.

Dear Dr. Shapiro:

In some situations, it is so easy to simulate a pulse sequence that the simulation is done before one has a "feel" for the effects of the pulse sequence. Recalling the pedagogical nature of Bloch diagrams, it is beneficial to display calculated spin magnetizations in a similar manner. However, for spin systems with the potential for dipolar or quadrupolar order, the length as well as the orientation of the spin magnetization is variable. To indicate both length and orientation of a vector on a 2D display, be it on paper or a computer screen, some three dimensional visual cueing is required. Herein, the possibilities of stereo diagrams are explored.

As an introduction to stereo diagrams, the evolution of the deuterium spin magnetization for a solution state spin echo pulse sequence,  $90_x - \tau_1 - 180_y - \tau_2 - \text{ACQ}$ , with  $e^2 q_{zz} Q/h = 0$  kHz, is shown in Figure 1. As the off-resonance condition increases, finite pulse length effects reduce the refocussing efficiency of the spin echo pulse sequence. Since the quadrupole coupling constant is zero, there can be no quadrupolar order, thus the length of the spin magnetization vector will be constant, in the absence of relaxation effects, and equal to the equilibrium magnetization,  $M_0$ . The radius of the sphere is set equal to  $M_0$ . "X" marks the spot on the trace where signal acquisition is to begin.

To view the stereo diagram with naked-eye stereopsis, the instructions of J. C. Speakman are offered here (*Chem. Brit.* 14, 107 1978):

"look at the diagram from your normal reading distance, with spectacles if these be worn ordinarily; be careful to keep the horizontal line relating the pair parallel to a line connecting your eyes. To foster the illusion, at first, it may help to hold a piece of card (say, 20 cm  $\times$  8 cm) as an extension of the nose, so that the right eye sees only the right-hand picture, and 'vice versa'. Be sure the diagram is well illuminated and free from unilateral shadows cast by the card. When stereopsis has been attained, the card may be withdrawn. Some people have to overcome a psychological reluctance; to submit to a 'willing suspension of disbelief'.

The stereo diagram is composed of two nearly identical images. The image on the left is rotated  $-4^\circ$ , relative to the right-hand image, about the page or screen y axis. The separation between the centers of the two images is important; the optimal distance for a normal stereo viewer is about that of the human eye spacing, 65 mm. A slightly closer spacing, 50 mm, may be easier for beginning naked eye stereopsis. With a  $-4^\circ$  rotation and no further image manipulation, the effective viewing distance is infinity.

The sabbatical hospitality of the Naval Research Laboratory and useful discussions with J. B. Miller, D. C. Cory, J. Walton, and A. N. Garraway are gratefully acknowledged.

Sincerely

Les Butler  
Associate Professor of Inorganic Chemistry

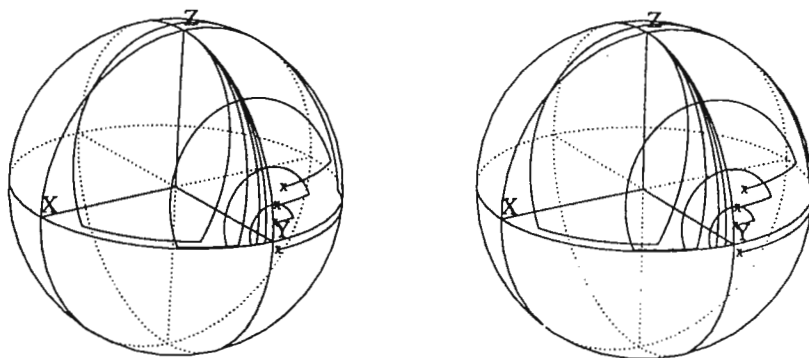


Fig. 1 Calculated trajectories of the deuterium spin magnetization for a solution state spin echo pulse sequence,  $90_x - \tau_1 - 180_y - \tau_2 - \text{ACQ}$ . Relevant parameters are:  $\nu(^2\text{H}) = 30.7 \text{ MHz}$ ,  $\tau_{90} = 3 \mu\text{s}$ ,  $\tau_1 = 3 \mu\text{s}$ ,  $\tau_2 = 4.5 \mu\text{s}$ , sampling interval =  $0.05 \mu\text{s}$ ,  $e^2 q_{zz} Q/h = 0 \text{ kHz}$ , and  $T = 300 \text{ K}$ . The off-resonance conditions are: 5, 10, 20, and 40 kHz.

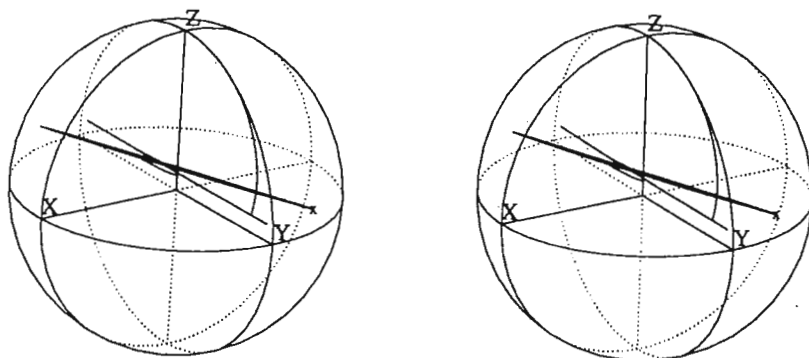


Fig. 2 Calculated trajectories of the deuterium spin magnetization for a solid state spin echo pulse sequence,  $90_x - \tau_1 - 90_y - \tau_2 - \text{ACQ}$ . Relevant parameters are:  $\nu(^2\text{H}) = 30.7 \text{ MHz}$ ,  $\tau_{90} = 3 \mu\text{s}$ ,  $\tau_1 = 25 \mu\text{s}$ ,  $\tau_2 = 26.5 \mu\text{s}$ , sampling interval =  $0.05 \mu\text{s}$ ,  $e^2 q_{zz} Q/h = 170 \text{ kHz}$ ,  $\eta = 0$ ,  $\theta = 90^\circ$ , and  $T = 300 \text{ K}$ .

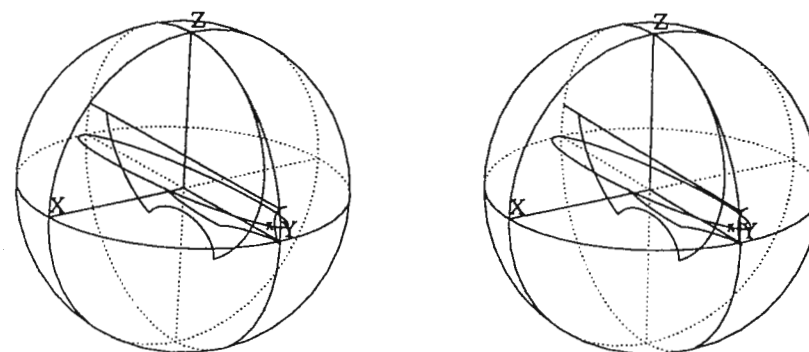


Fig. 3 Calculated trajectories of the deuterium spin magnetization for a solid state spin echo pulse sequence I,  $135_x - 90_x - 45_x - \tau_1 - 135_y - 90_y - 45_y - \tau_2 - \text{ACQ}$ . Relevant parameters are:  $\nu(^2\text{H}) = 30.7 \text{ MHz}$ ,  $\tau_{90} = 3 \mu\text{s}$ ,  $\tau_1 = 25 \mu\text{s}$ ,  $\tau_2 = 28.55 \mu\text{s}$ , sampling interval =  $0.05 \mu\text{s}$ ,  $e^2 q_{zz} Q/h = 170 \text{ kHz}$ ,  $\eta = 0$ ,  $\theta = 90^\circ$ , and  $T = 300 \text{ K}$ .

# Z•SPEC Four Nuclei Probe

## FEATURES:

$^1\text{H}$ ,  $^{19}\text{F}$ ,  $^{31}\text{P}$  and  $^{13}\text{C}$  observe capability without retuning the probe. The four spectra shown on the back were obtained using this probe. The only thing the NMR operator does is change the observe frequency of the spectrometer. The probe contains no internal switches and thus cannot wear out from repeated observe nuclei changes.

## APPLICATIONS:

The Z•SPEC Four Nuclei Probe is a great addition to any NMR lab requiring high efficiency of sample throughput. Laboratories with automatic sample changers or open access environments benefit from the increase in experimental flexibility.

## TECHNICAL:

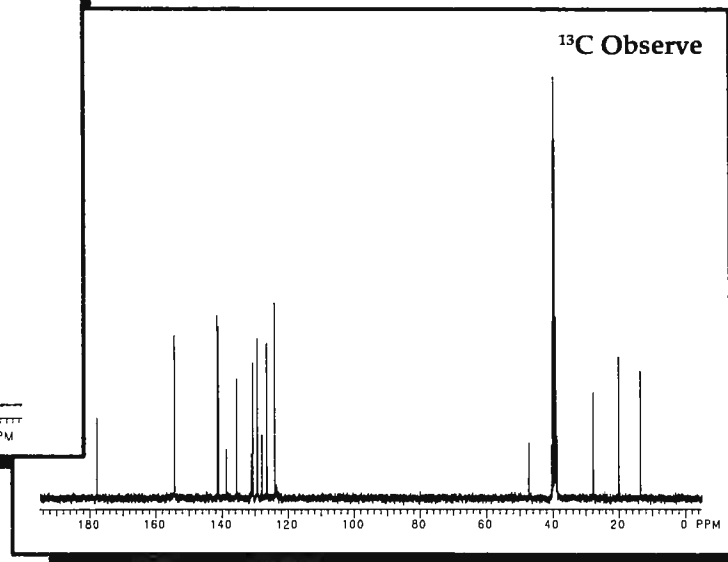
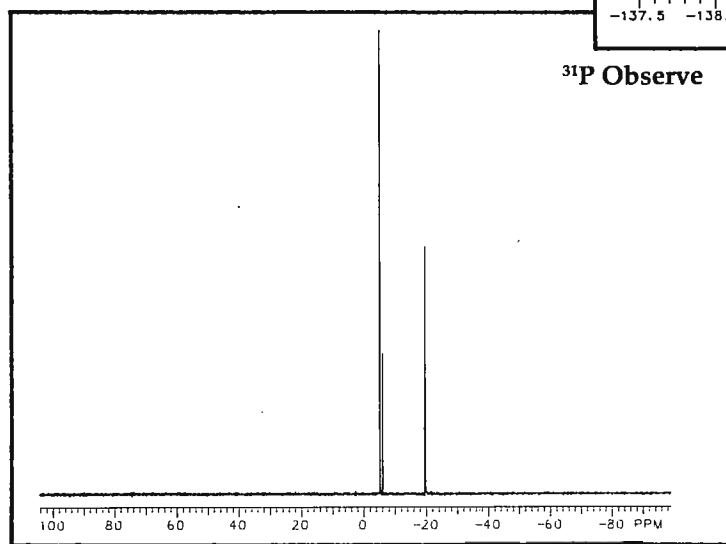
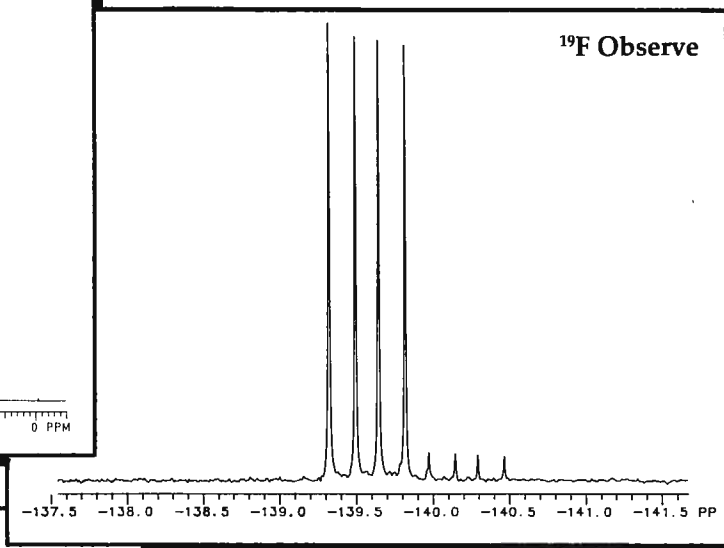
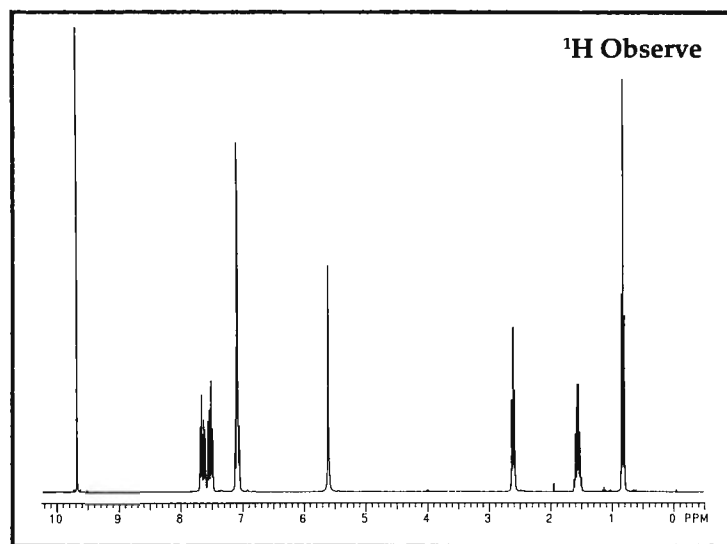
The Z•SPEC Four Nuclei Probe interfaces directly to any Varian 200, 300 or 400 MHz NMR Spectrometer. The probe is capable of observing any of the four nuclei without retuning the observe frequency or changing 1/4 wavelength cables.

For more information, please contact Toby Zens, Manager of the Z•SPEC Products Group.



**NALORAC CRYOGENICS CORPORATION**  
837 Arnold Drive, Suite 600, Martinez, CA 94553  
Tel: (415) 229-3501 • FAX (415) 229-1651

# Z·SPEC Four Nuclei Probe Spectra\*



\* Spectra obtained with spectrometer operating in an automatic and unattended mode.

**NCC**

NALORAC CRYOGENICS CORPORATION  
837 Arnold Drive, Suite 600, Martinez, CA 94553  
Tel: (415) 229-3501 • FAX (415) 229-1651





# THE UNIVERSITY OF NEW SOUTH WALES

P.O. BOX 1 • KENSINGTON • NEW SOUTH WALES • AUSTRALIA • 2033

TELEX AA26054 • TELEGRAPH: UNITECH, SYDNEY • TELEPHONE 697-2222

FAX 61-2-662-2835

DIRECT LINE 697-4720

UNIVERSITY NMR FACILITY  
Dr. K.J. Cross  
PROJECT SCIENTIST

Fri, 6 Jul 1990  
(received 7/14/90)

Dr. Bernard L. Shapiro  
TAMU NMR Newsletter  
966 Elsinore Court  
Palo Alto, CA 94303

Dear Dr. Shapiro,

## Models for Porphyrin Ring-Current Shifts

I have recently been reconsidering models for ring-current shifts experienced by atoms in close proximity to porphyrin ring-systems. In an earlier paper (1) a variety of ring-current models were calibrated using data from X-ray and NMR studies of a variety of heme proteins. The models used were relatively complex to calculate, but gave results in reasonable agreement with experiment.

Of the four models considered, three gave chemical shifts for the  $\alpha$ -CH proton of Met 80 of cytochrome *c* in agreement with the experimental value of -1.42 ppm. The fourth model, a 5-loop Johnson-Bovey model gave a much smaller predicted shift of -0.57 ppm. The decision as to which model was giving the correct result was further complicated by evidence, from the ring-current shifts, that the Met 80 residue was in a slightly different position in the solution studies as compared to the X-ray study.

The model that I have been investigating also predicts a small ring-current shift for this atom. On further investigation, the polar angle  $\theta$  for this atom was found to be very close to  $54.7^\circ$ , the angle at which a dipolar type contribution to the ring-current shift goes to zero. Given that the atom is more than 5 Å from the porphyrin ring, where the ring-current field should be approaching a dipolar field (the higher order multipole contributions to the ring-current field tend rapidly to zero as the distance increases from the aromatic ring), a large ring-current shift is not expected for this resonance.

The large ring-current shift in fact observed for the  $\alpha$ -CH proton, despite the small dipole contribution, can be reconciled by assuming that the  $\alpha$ -CH proton has moved from the X-ray determined location relative to the porphyrin. It is highly likely that the entire Met 80 residue of cytochrome *c* occupies a slightly different orientation in the solution structure as compared to the X-ray determined structure. The 8-loop Johnson-Bovey and both the Haigh-Mallion models appear to be unreliable at angles close to  $54.7^\circ$ .

We are currently investigating the ring-current shifts caused by aromatic side-chains in a series of sea anemone polypeptides. The structures of which have been determined by NMR.

Sincerely,

*Keith Cross*  
Keith Cross

(1) K.J. Cross and P.E. Wright, J. Magn. Reson. **64**, 220-231(1985)

Please credit this contribution to Dr. Ray Norton's account.



Conseil national  
de recherches Canada

National Research  
Council Canada

Institut de recherche  
en biotechnologie

Biotechnology Research  
Institute

Référence      File

6100, avenue Royalmount, Montréal, Québec, Canada H4P 2R2

Tel.: (514) 496-6100

July 1, 1990

Dr. B.L. Shapiro, Editor  
TAMU Newsletter  
966 Elsinore Court  
Palo Alto, CA 94303

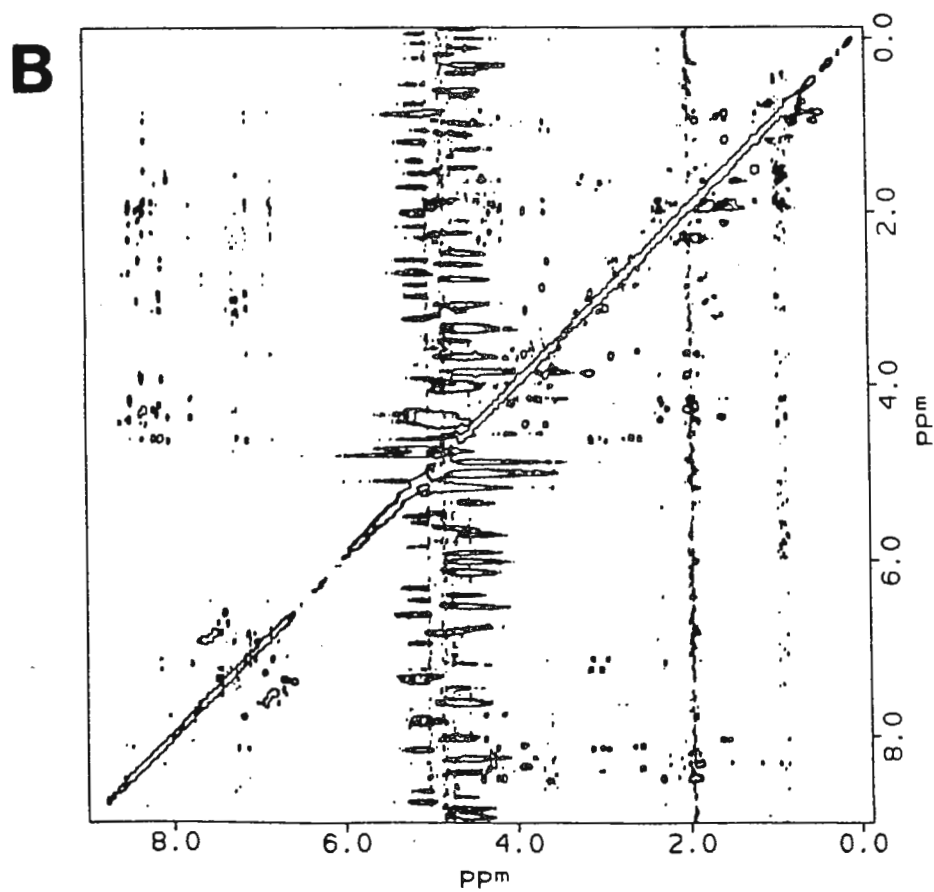
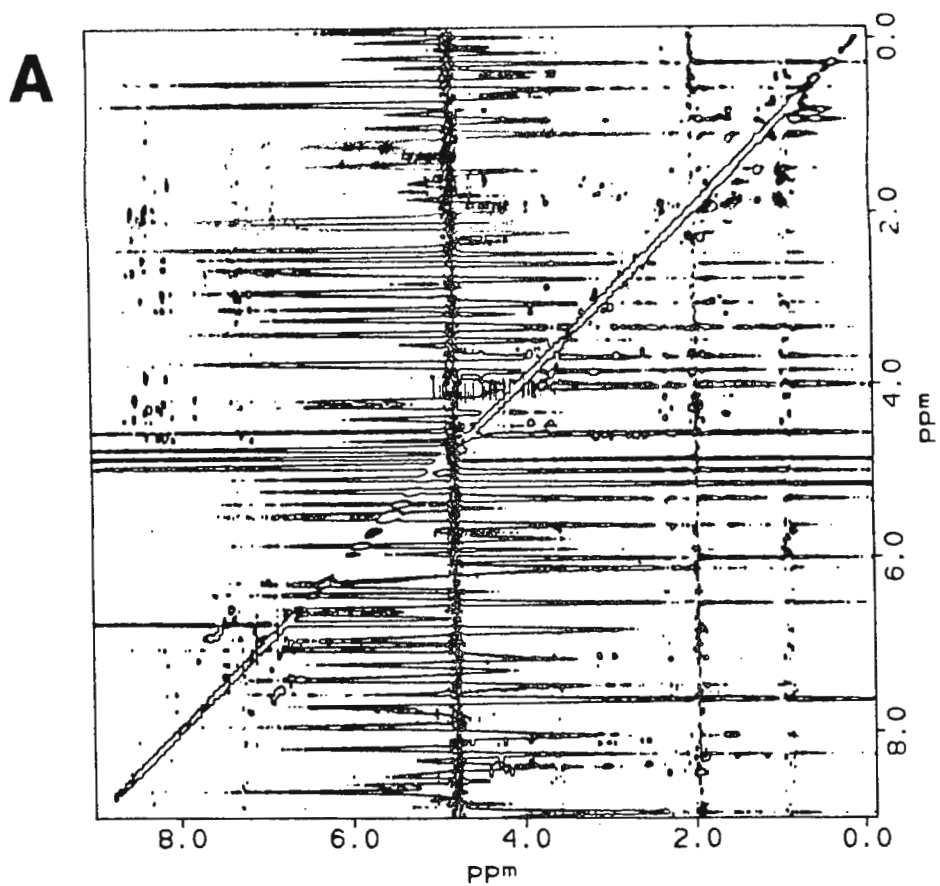
Linear-Prediction Methods for Solvent Suppression and Baseplane  
Flattening of NOESY and ROESY Spectra

Dear Dr. Shapiro,

Cross-relaxation spectra, such as NOESY and ROESY, are of prime importance in the elucidation of the structure and dynamical properties of macromolecules of biological interest. In practice, the interpretation of NOESY and ROESY data is often complicated by the presence of large solvent resonance and baseplane distortions, especially for samples with very low concentration of the material under study (Figure A, the peptide was 3 mM in H<sub>2</sub>O in the presence 0.2 mM thrombin).

Advances in digital signal processing have offered very effective means for the enhancement of spectral quality. Bax and co-workers recently demonstrated that very good solvent suppression can be achieved by a subtraction procedure involving the reconstruction of the large water resonance from the original FIDs acquired with the carrier centered on the solvent (Marion, Ikura and Bax, *JMR* 84, 425, 1989). They also showed that linear prediction (LP) methods can be used to correct the first few data points in the FID, thus reducing the baseline roll caused by these data points (Marion and Bax, *JMR* 83, 205, 1989). We have implemented these methods for use with Dennis Hare's FTNMR program to process spectra (Figure B) acquired on a Brüker AM-500 spectrometer. In this letter, we wish to point out a few enhancements with our implementation.

For phase-sensitive NOESY and ROESY, we always acquire the FID's using TPPI with sine-modulation along  $t_1$  (Otting, Widmer, Wagner and Wüthrich, *JMR* 66, 187, 1986). This eliminates the need for correcting the first data point in  $t_1$  since this point is always zero. The FID matrix can be Fourier transformed and phased along the  $t_1$  dimension using FTNMR. The  $t_2$ -interferograms are used for LP processing since they in general contain much less signals than the full FID. In principle, we need a backward LP to reconstruct the first few data points along  $t_2$ . The commonly used BURG algorithm is designed, however, for the calculation of the forward prediction coefficients. In practice, one does not have to write



a different program for this. Since the BURG algorithm is symmetric in time (Ni and Scheraga, *JMR* 70, 506, 1986), we simply take the first few hundred (e.g. 200) data points and reverse the order before applying the LP extension. After LP, the 200 data points are again reversed and patched to the rest of the FID for Fourier transformation and phasing along the  $t_2$  direction. A special data shuffling is required for the SMX file thus obtained before the spectrum can be displayed and plotted by FTNMR.

LP can also be incorporated to improve solvent suppression by convolution of the time-domain data. In the original procedure (Marion, Ikura and Bax, *JMR* 84, 425, 1989), the solvent signal was reconstructed from the FID via a smoothing operation using a sine-bell shaped or a Gaussian-shaped window function. The first and the last  $M/2$  ( $M$  is the width of the window) data points were then calculated by linear extrapolation of the available solvent signal. We, however, used LP to calculate these missing points in the reconstructed solvent signal. The full solvent FID is then subtracted from the original FID.

Figure B shows the effect of the LP-based solvent suppression and baseplane flattening on the quality of a transferred NOESY spectrum of a 21-residue peptide complexed to thrombin. Both Figure A and B were processed and plotted using identical parameters apart from the LP processing used in obtaining the spectrum in Figure B. The Fortran program was written as a supplementary (USR) command of the FTNMR program. This program and a few FTNMR macros are available upon request by sending an E-mail address to <FENGNI@BRIMV.NRC.CA>. I do not have time to supply these programs using tapes.

Yours sincerely,



Feng Ni, Ph.D  
Protein Engineering

#### Re: POSTDOC POSITION AVAILABLE

I have an immediate opening for a postdoc in the field of NMR studies on adsorption at the liquid-solid interface. The stipend is prolongable to two years in total. Our equipment includes one Bruker MSL-200 (with ethernet, diffusion- and micro-imaging attachments) and one multinuclear JEOL FX-100, equipped for FT-self-diffusion measurements. We also have access to Bruker high-resolution 400 and 200 MHz spectrometers and extensive VAX computing facilities, including Workstation-based NMR1/NMR2/IMAGE/MEM from NMRI, as well as Ethernet transfer between the Bruker spectrometers and the Local Area VAXcluster.

Interested persons please contact Peter Stilbs at the address given below.

Address: Prof. Peter Stilbs  
The Royal Institute of Technology  
Dept. of Physical Chemistry  
S-100 44 STOCKHOLM, Sweden

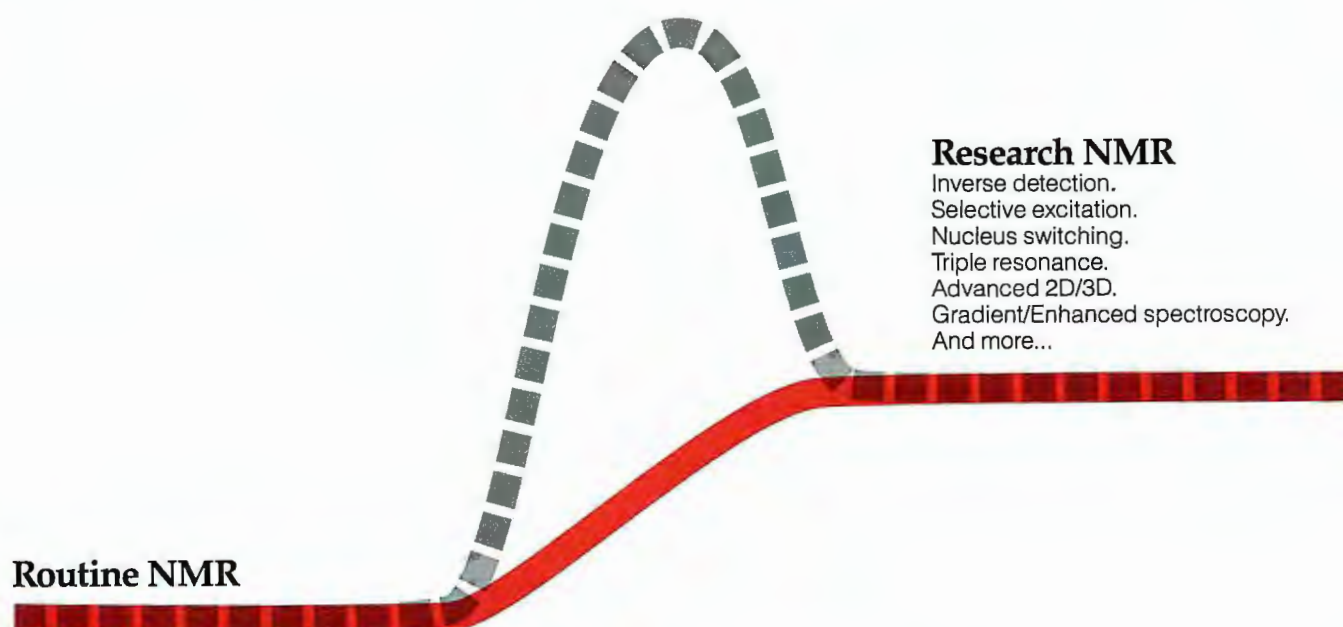
Telephone:  
Nat. 08-7908201  
Int. +46 8-7908201  
Secr. 08-7908594

Telefax:  
Nat 08-7908207  
Int +46 8-7908207  
Cable: Technology

Electronic mail:  
stilbs@sekth.bitnet  
peter@physchem.kth.se



# The AMX overcomes the barrier to cutting edge NMR by delivering unprecedented research flexibility without compromising ease of use.



The AMX is a truly innovative, next-generation instrument. Its unparalleled electronic features include a 451 MHz IF frequency, ultra-precise pulse shape control and an optimized, multi-stage transmitter design. These combine with the powerful UNIX-based X32 computer and unmatched probe and shim designs to produce the most powerful NMR system ever built.

At the same time, Bruker's menu-driven, windows based software, computer switchable probes, automatic sample changer and automated 1D and 2D processing capability totally eliminate the activation barrier to cutting edge

## Bruker AMX Series.



NMR. The unique Router automatically configures the AMX in microseconds to perform the most advanced NMR experiments, and the extensive library of pretested experiments and the clear, concise pulse programming language ensure that you will not waste time and energy on spectrometer set-up.

Don't let your NMR research creativity be hindered by barriers. For details, write:

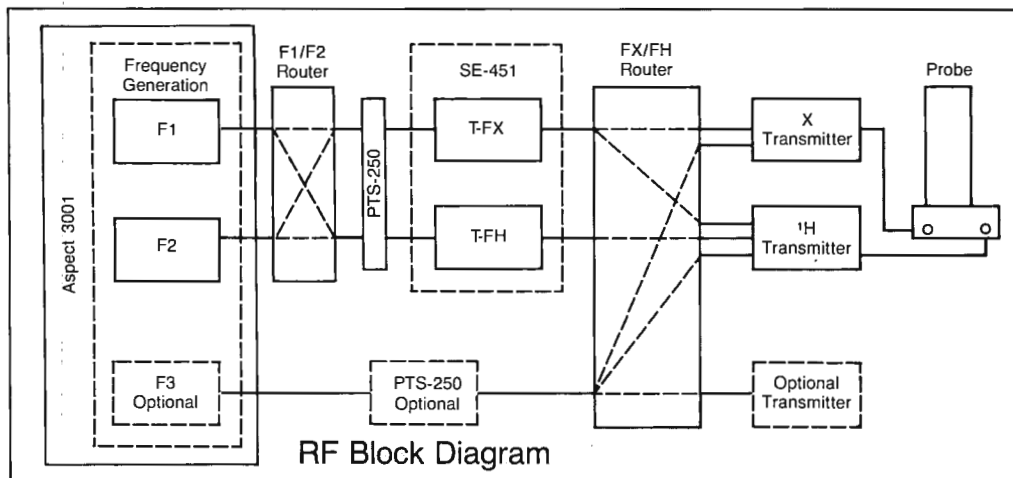
*Bruker Instruments, Inc.  
Manning Park, Billerica, MA 01821*

*In Europe: Bruker Analytische  
Messtechnik GmbH, Silberstreifen,  
D-7512 Rheinstetten 4, W. Germany*

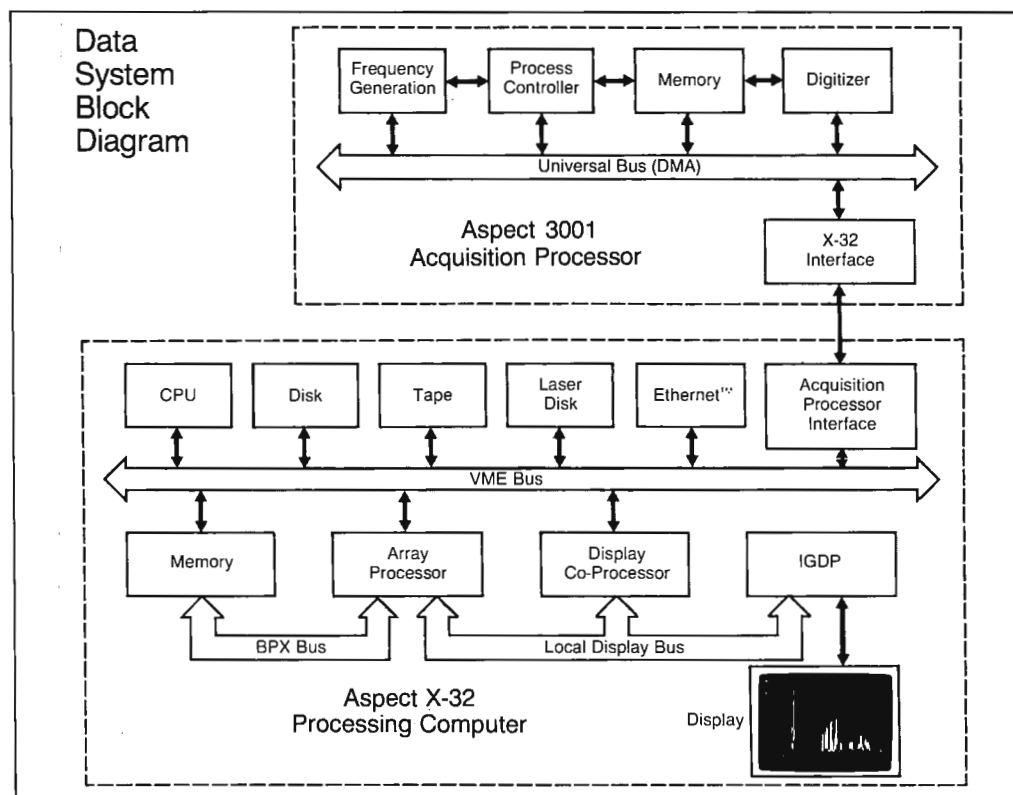
*Comprehensive Support for Innovative Systems*



# AMX Series Block Diagrams



**Multi-channel RF design.** The unique full routing system uses PIN diodes to allow microsecond switching of the frequency paths and RF transmitters.



**Digital Section.** Integration of 32-Bit Aspect X-32 UNIX computer into console together with proven Aspect 3001 acquisition processor. The X-32 is equipped with unique 3-bus structure for optimum NMR data transfer, processing and display.

For more information about the AMX simply call or write:



**Australia:** BRUKER (Australia) Pty. LTD., Earlwood, New South Wales, Tel. 02-5589747  
**Belgium:** BRUKER SPECTROSPIN S.A./N.V., Brussels, Tel. (02) 648 53 99  
**Canada:** BRUKER SPECTROSPIN (Canada) LTD., Milton, Ontario, Tel. (416) 876-4641  
**England:** BRUKER SPECTROSPIN LTD., Coventry, Tel. (0203) 855200  
**France:** SADIS BRUKER SPECTROSPIN SA, Wissembourg, Tel. (088) 88 7368  
**India:** BRUKER INDIA SCIENTIFIC Pvt. LTD., Andheri (West), Bombay, Tel. 22 62 72 32  
**Italy:** BRUKER SPECTROSPIN SRL, Milano, Tel. (02) 23 50 09  
**Japan:** BRUKER JAPAN CO. LTD., Ibaraki-ken, Tel. 0298-52-1234  
**Netherlands:** BRUKER SPECTROSPIN NV, Wormer, Tel. (75) 28 52 51  
**Scandinavia:** BRUKER SPECTROSPIN AB, Täby, Sweden, Tel. (0046) 8 758 03 35  
**Spain:** BRUKER ESPANOLA S.A., Madrid, Tel. 341-259-20-71  
**Switzerland:** SPECTROSPIN AG, Fällanden, Tel. 1-82 59 111  
**W. Germany:** BRUKER ANALYTISCHE MESSTECHNIK GMBH, Rheinstetten, Tel. 0721-5161-0  
 BRUKER ANALYTISCHE MESSTECHNIK GMBH, Karlsruhe, Tel. 0721-5967-0  
 BRUKER-FRANZEN ANALYTIK GMBH, Bremen, Tel. 0421-2205-0  
**USA:** BRUKER INSTRUMENTS, INC., Billerica, MA 01821, 508-667-9580  
 Regional Offices in Chicago, IL, (708) 971-4300/Wilmington, DE, (302) 478-8110  
 Houston, TX, (713) 292-2447/San Jose, CA, (408) 434-1190


**Lilly Research Laboratories**

A Division of Eli Lilly and Company

Professor BL Shapiro  
TAMU Newsletter  
966 Elsinore Ct.  
Palo Alto, CA 94303

Lilly Corporate Center  
Indianapolis, Indiana 46285  
(317) 276-2000

June 1, 1990  
(received 6/29/90)

## Neighbors

Dear Barry,

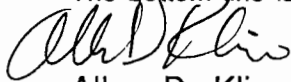
We at Lilly Research Laboratories certainly recognize the importance of a multi-disciplined approach to solving chemical and biological problems. That has created a camaraderie between those of us practicing the various spectroscopic techniques here in Physical Chemistry. This collaboration is enhanced by the close proximity of all of our laboratories.

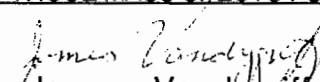
That camaraderie, however, was recently tested when the Mass Spectroscopy lab proposed to place their new double-focus instrument in the adjacent lab to the NMR spectrometers. But what was an obvious infraction to the NMR spectroscopists, was not so obvious to the Mass spectroscopists, nor to management. To prove the validity of our claims and to keep our AM-500 from being magnetically assaulted, we executed the following experiment.

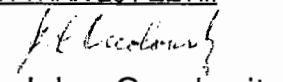
To simulate the presence of the Mass spectrometer, a loaner magnet was setup 26 feet from the NMR magnet and was powered by one of our existing Mass spectrometers. The magnet was ramped from 0 to 50 Amps requiring 56 s for the ramp up and less than 5 s for the ramp down. With the NMR spectrometer in the unlocked mode, we collected a series of 128 1D spectra on a chloroform sample. Each spectrum was stored to disk after a single scan giving a repetition rate of 4.2 s. Four times during this experiment, a loaner magnet was ramped through its cycle. The NMR data were transformed and phased as standard 1D spectra but were contour plotted as a 2D spectrum. For an unperturbed signal the contour plot should have smooth horizontal ridges which extend from beginning to the end of the experiment. The figure below, however, shows the contour plot we actually obtained. The times when the ramping was started are marked on the plot with arrows. The Mass Spect magnet induced a 0.5 Hz shift on the position of the chloroform line and had some effect on its lineshape.

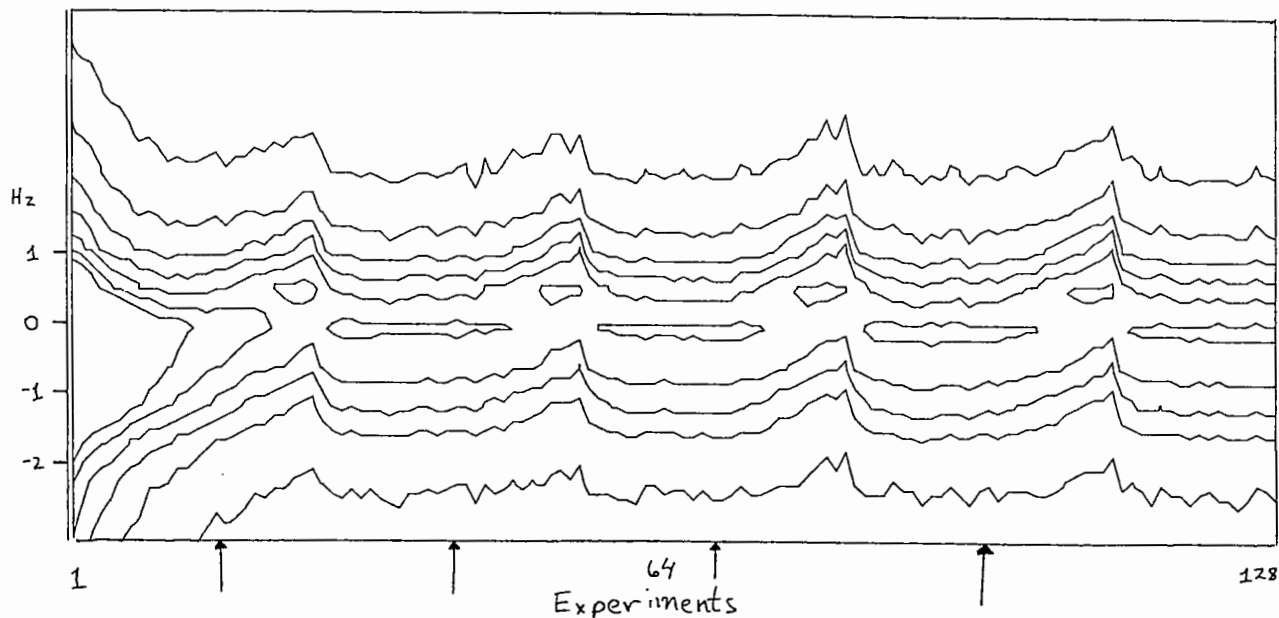
The bottom line is:

KEEP THOSE MASS SPECTS FURTHER BACK THAN 26 FEET!!!

  
Allen D. Kline

  
James Vandygriff

  
John Occolowitz



**Amoco Corporation**

Amoco Research Center  
Post Office Box 3011  
Naperville, Illinois 60566  
708-420-5111

July 12, 1990 (received 7/16/90)

Prof. B. L. Shapiro  
TAMU NMR Newsletter  
966 Elsinor Court  
Palo Alto, CA 94303

**Al NMR of Zeolites**

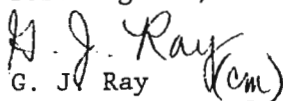
The analysis of zeolites using aluminum NMR is not straightforward. Recently, there have been several reports<sup>1</sup> of a peak at 30 ppm that has been attributed to either an aluminum species in a strained tetrahedral or pentacoordinate environment. By obtaining aluminum spectra at two fields (9.4 and 14.1 T), that both types of species can be found in steam dealuminated Y zeolites.

We studied a series of commercial Union Carbide zeolites, LZ-Y62, LZ-Y82, and LZ-Y20, by aluminum NMR. The LZ-Y62 sample is the ammonium form of an as synthesized Y zeolite, which is steamed to remove aluminum from the framework. The dealuminated sample is exchanged to the ammonium form, LZ-Y82, which is steam dealuminated a second time to form LZ-Y20.

Figure 1 shows the computed lineshapes for a spin 5/2 nucleus calculated for quadrupole couplings of 1, 2, 6, and 8 MHz at the aluminum resonance frequencies of 104 and 156 MHz. The chemical shift was assumed to be 60 ppm. For small couplings (<1 MHz), the peak shape and position is essentially independent of resonance frequency while for larger couplings the peak shifts to lower frequency and assumes the characteristic "doublet" shape. Since both the shape and shift are dependant on resonance frequency, changing magnetic fields can determine whether an apparent "peak" is actually only a component of a complex lineshape.

Figure 2 shows the aluminum spectra of the LZ-Y series. For LZ-Y62 only a single peak believed to be due to framework aluminum is observed. Both LZ-Y82 and -Y20 have several broad peaks characteristic of nonframework aluminum. The peak(s) near 0 ppm are attributable to octahedrally bound aluminum species. Both samples also have considerable intensity in the 30 ppm region of the 104 MHz spectra. At 156 MHz, the spectrum of the LZ-Y20 sample is essentially unchanged, but the LZ-Y82 sample shows that the intensity of seen near 30 ppm in the 104 MHz spectrum has shifted to about 50 ppm. This is consistent with the 30 ppm intensity being the low frequency feature of the quadrupole "doublet". Its shift toward 60 ppm at higher field enables us to assign the aluminum to a tetrahedral species which is presumable experiencing strain because it has left the lattice. The absence of a field dependance for LZ-Y20 indicates that the aluminum responsible for the intensity at 30 ppm has a small quadrupolar coupling. In naturally occurring aluminosilicate minerals, aluminum species having a 30 ppm shift were found to be pentacoordinate<sup>2</sup>, but they also generally had quadrupole couplings of 5 MHz. Therefore, assignment of the 30 ppm peak to a pentacoordinate aluminum is somewhat tenuous. Regardless of the assignment of the 30 ppm peak in LZ-Y20 we have shown that two different nonframework species are present in steamed Y zeolites.

Best regards,

  
G. J. Ray  
Mail Station B-5  
708/420-5217.



- 1) A. Samoson, et al, Chem. Phys. Lett., 1987, 134, 589.
- 2) V. Bosacek and D. Freude, Innovation in Zeolite Materials Science, Elsevier Science Publishers, 1987, p231.
- 3) J. P. Gilson, et al, J. Chem. Soc., Chem Commun., 1987, 91

Acknowledgement: The 156 MHz spectra were obtained by Dr. James Frye at the Colorado State University Regional NMR Center, funded by NSF Grant No. CHE 78-18581.

Figure 1. Computer Simulations of Quadrupolar Lineshapes for 1, 2, 6 and 8 MHz<sub>z</sub> Quadrupolar Couplings at 104 and 156 MHz<sub>z</sub>

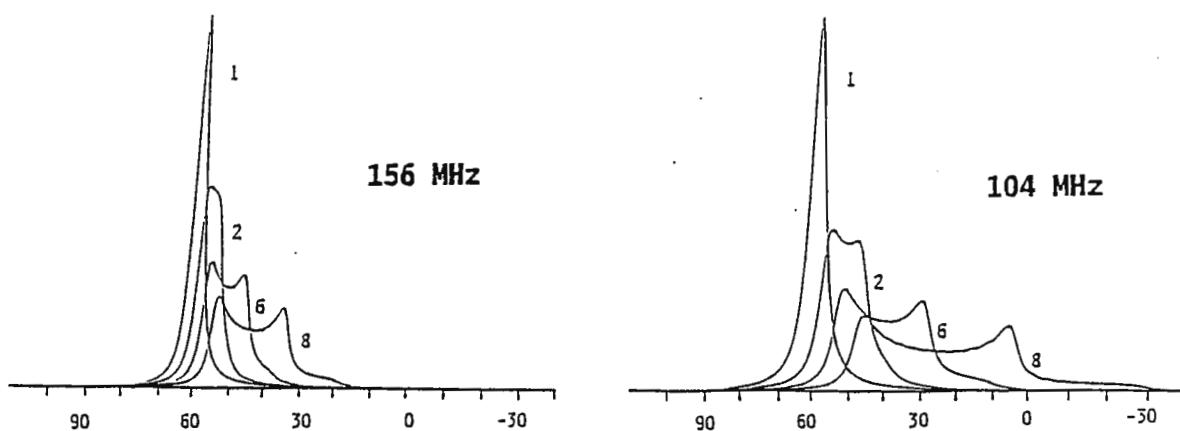
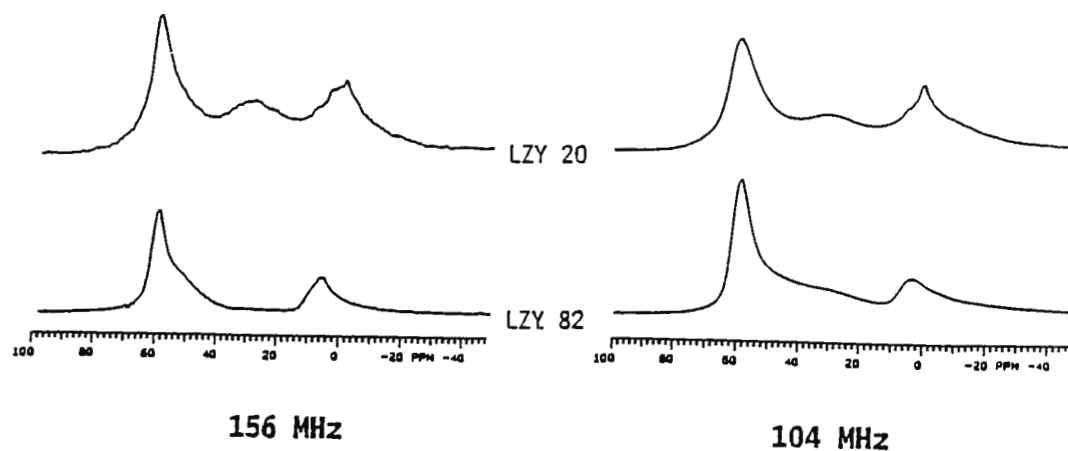


Figure 2. <sup>27</sup>Al NMR Spectra of LZY82 and LZY20 at 104 and 156 MHz<sub>z</sub>





Carleton University  
Ottawa, Canada K1S 5B6

Dr. B.L. Shapiro  
TAMU NMR Newsletter  
966 Elsinore Court  
Palo Alto Cal. 94303

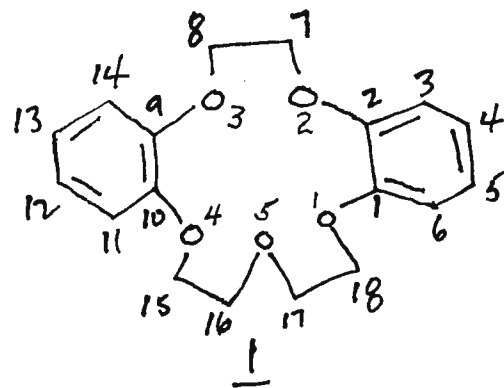
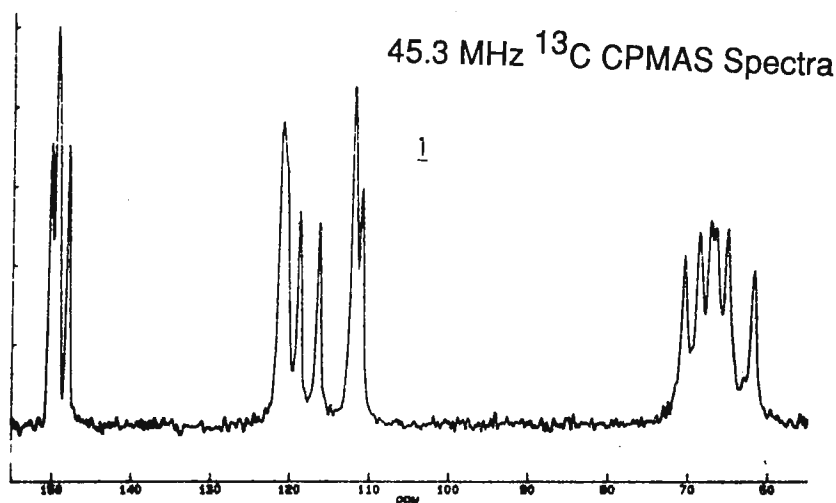
June 18, 1990  
(received 6/25/90)

Title " Solid Phase  $^{13}\text{C}$  NMR of Dibenzo-15-crown-5 ether (1) and its NaNCS Complex (2)"

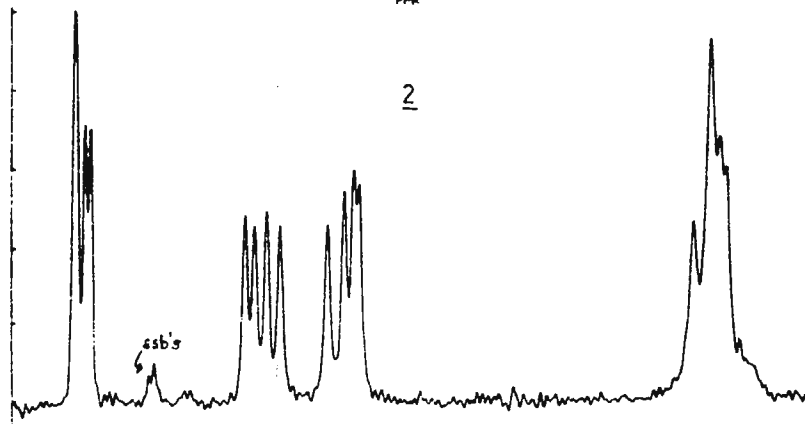
Recently we have obtained single crystal X-ray structures for 1 and 2, which indicate that both are totally devoid of any elements of symmetry. This is reflected in the multiplicity of resonances in the  $^{13}\text{C}$  CPMAS spectra below. Based on torsional angle analysis, the C18 site is deemed to be the most shielded  $\text{CH}_2$  resonance of 1, occurring at 61.88 ppm. In 1, the C18-C17-O5-C16 torsion angle is  $66.5^\circ$ . For 2, this angle expands to  $171.0^\circ$ , which would be expected to deshield C18. From the spectrum of 2, it is evident that the most shielded resonance is at 65.0 ppm, so it appears that the magnitude of the C18 deshielding is at least 3.12 ppm. Of course we look forward to having access to routine solid phase CCCC 2D capability in the near future so that unambiguous assignments will be possible.

Best regards,

G.W. Buchanan, Professor of Chemistry.



2 = 1.NaNCS



# Instant Upgrade of RF Amplifier Performance in Your NMR/MRI System

Install an AMT Series 3000 solid-state pulse power amplifier—6–500MHz at up to 1000 W—into your system. Instant upgrade!

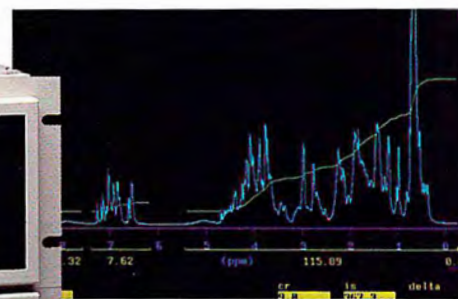
Here's just one example: AMT's RF power envelope detection system guarantees full protection. That means you can operate at low-level CW with full-power peaks on demand.

Pre-saturation water suppression? Cross polarization in solids? No problem—*now!*

## Additional Key Features:

- Broadband Frequency Ranges—6–220MHz, 200–500MHz
- Key Power for Liquids & Solids—50, 150, 300, 1000 Watts
- Excellent Linearity—( $\pm 1.0$ dB)
- Low Pulse Droop—typically less than 5%
- Fast Low Noise Blanking—within 20dB of KTB in  $2\mu$ S

For full information call your NMR/MRI system manufacturer or call Lowell Beezley at AMT: (714) 680-4936.



## Models Available:

3205	6–220MHz	300W
3200	6–220MHz	1000W
3137	200–500MHz	50W
3135	200–500MHz	150W
3134	200–500MHz	300W



an MMD company

1127 S. Placentia Avenue, Fullerton, CA 92631 (714) 680-4936 FAX: 714-871-2453

**Model 3200 Series**  
**6 - 220 MHz, Pulsed,**  
**SOLID STATE, RF Power**  
**Amplifier Systems**

<u>Electrical Specifications:</u>	<u>Models:</u>	<u>3200</u>	<u>3205</u>
Frequency Range	6 - 220 MHz		
Pulse Power (min.) into 50 ohms	1000W	300W	
CW Power (max.) into 50 ohms	100W	30W	
Linearity ( $\pm 1$ dB to 200MHz)	0-800W	0-250W	
(To 220MHz)	0-600W	0-200W	
Gain (typ.)	65dB	60dB	
Gain Flatness	$\pm 4$ dB	$\pm 3$ dB	
Input/Output Impedance	50 ohms		
Input VSWR	< 2:1		
Pulse Width	20mS		
Duty Cycle	Up to 10%		
Amplitude Rise/Fall Time	200nS typ.	150nS typ.	
Amplitude Droop	5% to 10mS typ; 7% max		
Phase Change/Power Output	10 <sup>0</sup> to rated power typ.		
Phase Error Overpulse	4 <sup>0</sup> to 10mS duration typ.		
Noise Figure	11dB typ.	8dB typ.	
Output Noise (blanked)	< 20dB over thermal		
Blanking Delay	< 5uS on, 2uS off, TTL signal		
Protection	1. VSWR- will withstand infinite VSWR at rated power		
	2. Input overdrive- up to +10dBm		
	3. Over duty cycle/pulse width		
	4. Over temperature		
<u>Supplemental Characteristics:</u>			
Connectors (on rear panel)	1. Input- BNC (F)		
	2. Output- Type N (F)		
	3. Blanking- BNC (F)		
	4. Interface- 25pin D(F), EMI filtered		
Indicators, Front Panel	1. Peak power meter	5. CW Mode	
	2. Over temperature	6. Overdrive	
	3. Over duty cycle		
	4. Over pulse width		
System Monitors	1. Thermal		
	2. DC power supply fault		
	3. Over duty cycle		
	4. Over pulse width		
Front Panel Controls	1. A.C. power	3. Duty cycle	
	2. Pulse width		
Cooling	Internal forced air		
Operating Temperature	+10 to 40 <sup>0</sup> C		
A.C. Line Voltage	120/240 VAC, $\pm 10\%$ , 50-60Hz		
	(3200, 220/240V only)		
A.C. Power Requirements	2000 watts	700 watts	
Package	Rack Mount		
Size (HWD, inches)	12.25x19x24	5.25x19x24	





# Queen Mary College

## University of London

Department of Chemistry

Mile End Road, London E1 4NS · Tel: 01-980 4811 · Telex: 893750

Head of Department:  
Professor J.H.P. Utley  
BSc, PhD, DSc, CChem, FRSC

Dr. Bernard L. Shapiro,  
TAMU NMR Newsletter,  
966, Elsinore Court,  
Palo Alto, CA 94303,  
U.S.A.

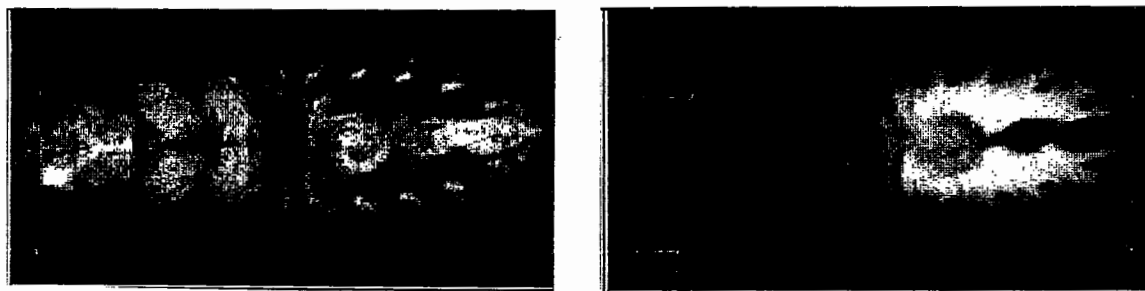
10th July 1990  
(received 7/18/90)

### NMR IMAGING OF THE COCKROACH

Dear Dr. Shapiro,

We have recently been encouraging biologists in a neighbouring department to conjure up new ideas and applications for NMR imaging and spectroscopy. One lucrative response has been the use of NMR imaging in entomology. The figure below shows chemical shift selective NMR images from a coronal slice through a live "Hissing Madagascan Cockroach". This unsavoury creature measured 5 x 1 x 0.5 cm and hissed fervently when lifted off a juicy leaf and placed in a large, porous jar for our study. After the initial fracas, the insect settled in the darkness of our 30 cm bore, 4.7T superconducting magnet. The chemical shift selective NMR images were acquired on a standard SISCO -200 spectrometer by applying a 6ms gaussian-shaped pulse to selectively excite either the water or fat resonance and then refocussing only a 1mm slice by irradiating the subject with a 5 ms sinc-shaped, 180 degree pulse in the presence of a magnetic field gradient of 2 G/cm. The total imaging time for this study was less than 1 hour.

As can be seen from the results, water is found mainly in the thorax and gut whereas fat was only found in the abdominal region. These fat-only and water-only NMR images yields both biochemical informaton and improved delineation relative to the standard spin echo technique. The distribution of fat and water may also be of interest to synthetic chemists working on lipophilic pesticides.



**Figures 1a & 1b.** Two chemical shift selective images of the same, coronal 1mm slice of a cockroach, **1a** is the water-only image and **1b** is the fat-only image. TE = 30 ms, TR = 1s, 512 x 512 data matrix, 4 signal averages per phase encode step. Note the proliferation of fat resonances in the abdominal region.

Ed Randall sends his regards, please credit this contribution to the account of Dr. Geoff Hawkes of the same address.

Regards,

Steve C.R. Williams (extn. 3733).



# The Wellcome Foundation Ltd

## The Wellcome Research Laboratories

Langley Court, South Eden Park Road  
Beckenham, Kent BR3 3BS

telegrams and cables  
WELLAB BECKENHAM  
telex WELLAB 23937 G  
fax 081-650 9862  
telephone 081-658 2211

DEPARTMENT FAX NO: 081-663 3788

BMNC/90/8

Dr. B.L. Shapiro,  
TAMU NMR Newsletter,  
966 Elsinore Court,  
PALO ALTO, CA 94303,  
USA.

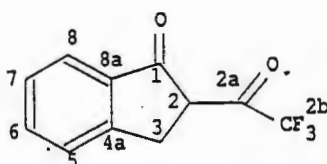
28 June, 1990

(received 7/2/90)

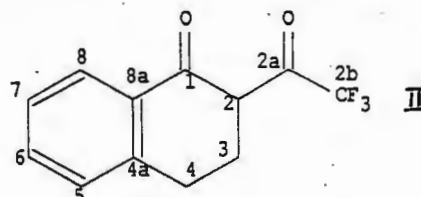
Dear Dr. Shapiro,

### NMR of fluorinated $\beta$ -diketones

As a result of collaboration with Dr. Salman Salman of the University of Baghdad, we have had occasion to study the equilibria in two related molecules shown below



I



II

Using  $^1\text{H}$ ,  $^{13}\text{C}$  and  $^{19}\text{F}$  NMR and especially fully coupled  $^{13}\text{C}$  with the benefit of long range  $^1\text{H}$ - $^{13}\text{C}$  J correlation experiments we have sorted out the various keto, enol and hydrate forms. I won't go into details of how we did it as the material will be published soon. In  $\text{CDCl}_3$ , I is 100% enol but as a mixture of endo and exocyclic enols in fast exchange, with the exocyclic form favoured. In  $\text{DMF-d}_7$ , there is only 40% enol but 60% hydrate with the enols and hydrate in slow exchange. For II in  $\text{CDCl}_3$ , again there is 100% enol, this time approximately equal proportions of exocyclic and endocyclic. However in  $\text{DMF-d}_7$ , no hydrate is formed but there is now 6% of the keto form in slow exchange. The results agree well with M.O. calculations using the AM1 hamiltonian. The oxygen-oxygen internuclear distances in the hydrogen bonds have been estimated from the OH proton chemical shifts, using as a calibration solid state CRAMPS data on model compounds, and these agree with the theoretical calculations. Full details will appear in a paper due to appear in Magnetic Resonance in Chemistry.

Best wishes,

Yours sincerely,

J.C. LINDON      R.D. FARRANT  
Department of Physical Sciences

JCL/ag

Food and Drug Administration  
Bethesda MD 20892July 3, 1990  
(received 7/5/90)Dr. B. L. Shapiro  
TAMU NMR Newsletter  
966 Elsinore Court  
Palo Alto, CA 94303**The Third Dimension a la JEOL GSX Spectrometers**

Dear Barry;

After lapsing into the oblivion of colored sheets and missing issues of TAMU, I would like to re-join the fold with some information regarding the flexibility of the JEOL GSX-500 spectrometer which we have had operating for a little less than 2 years.

The system has a fully broadbanded X-decoupling channel, and with some careful nudging, can even do three channel experiments, e.g.  $^1\text{H}$ , X, Y. The normal two channel, 2D inverse experiments are straightforward and performed with very good sensitivity.

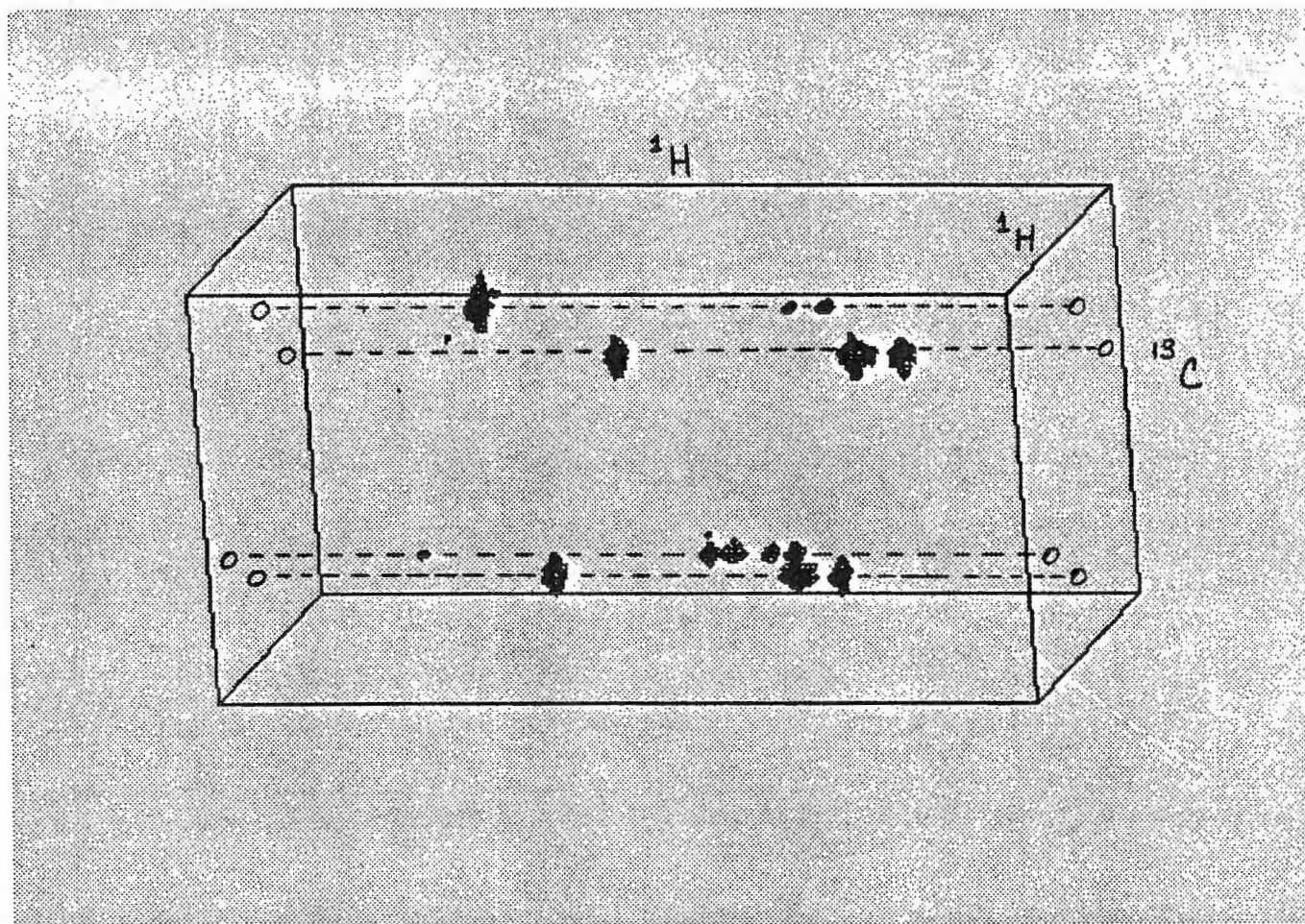
There are some features which we have found needed enhancement, which I will describe in later letters, since at this point I would just like to illustrate the feasibility of performing three-dimensional experiments on this spectrometer. The figure shows a HMQC-TOCSY 3D experiment performed as a test sample on  $^{13}\text{C}$ -labelled glucose. It is a mixture of C1 and C2 labelled glucose with both alpha and beta anomers apparent.

This experiment was performed without any modifications of the spectrometer; in fact, it was run in Sept. 89! The data acquisition was buffered in-memory to minimize delays between  $t_1$  points, and the experiment was performed as hypercomplex in both the indirect dimensions ( $F_1$  &  $F_2$ ). The raw data file was  $256_c \times 128_c \times 32_c$  and the final processed data matrix is  $256_c \times 128_c \times 128_r$ . The data was processed using the program FELIX (Hare Research, Inc.) on a Silicon Graphics 4D25G workstation. The processing is very smooth and the entire transformation is performed in less than 2 hrs, even on my workstation with only 8 MB of memory. I have found the conceptualization of N-dimensional processing in FELIX to be extremely powerful, and the extension to processing a 4D experiment, as Bax showed at the ENC, would be very straightforward!

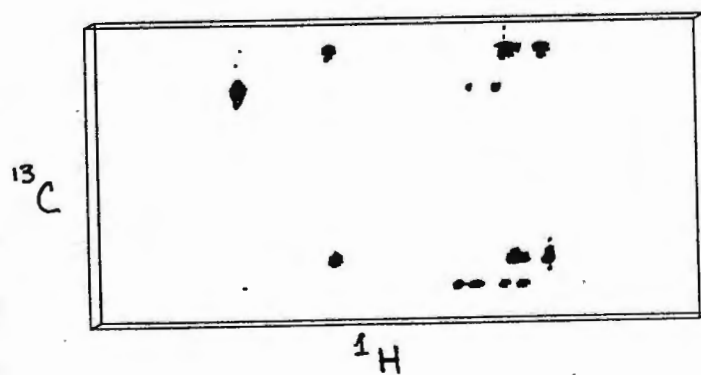
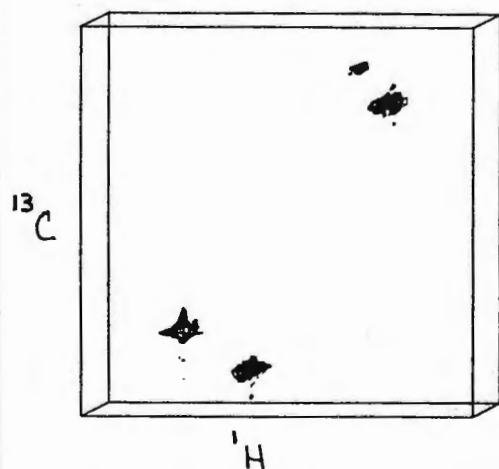
This spectrum illustrates the facility for such experiments and extension to other 3D sequences is simply writing the pulse sequences. We are quite excited about these applications in our research programs, and we hope to present more results soon.

Best regards,

R. Andrew Byrd  
Biophysics Laboratory, FDA  
8800 Rockville Pike  
Bethesda, MD 20892



**HMQC-TOCSY 3D (256 X 128 X 128)**  
 Hypercomplex in both indirect dimension (F1 & F2)  
 In-memory Buffered Acquisition (256<sub>C</sub> x 128<sub>C</sub> x 32<sub>C</sub>)



NB: the presentations do not have the same axes orientation!





*Fremont Magnetic Resonance*

3315 Seldon Court  
Fremont CA 94539  
(415)623-0722  
(415)623-0851 FAX

## QE Probe

$^{31}\text{P}$  /  $^{13}\text{C}$  /  $^1\text{H}$

One port tuned for  $^1\text{H}$  observation.

One port simultaneously tuned for both  $^{31}\text{P}$  and  $^{13}\text{C}$  observation.

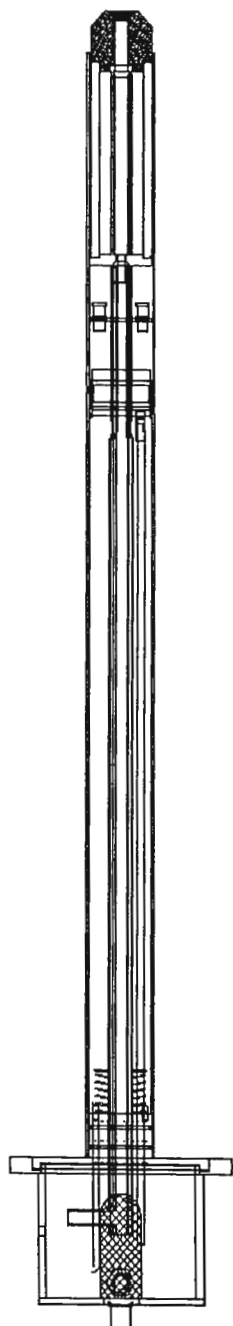
Allows the QE console to observe  $^1\text{H}$ ,  $^{31}\text{P}$  and  $^{13}\text{C}$  spectra without tuning or switching the probe in any way.

Ideal for the "hands on" analytical laboratory.

Very convenient for sample changer operations.

Fourth nucleus option available.

Similar probes available for all NMR consoles.  
Bruker - Varian - GE - Nicolet





*Fremont Magnetic Resonance*  
3315 Seldon Court  
Fremont, CA 94539  
415/623-0722  
FAX 415/623-0851

---

## **Do you have the latest Gossip?**

---

Have you heard that... A cow achieved escape velocity..., The cat has volunteered to wear a bell..., There's a new file transfer method that gives easy and inexpensive transfers from GN and NT spectrometers. But the last statement is no rumor. With our new program, Gossip, you can do serial transfers at 19 kBaud, and you can run the transfer in the background. At 20 kwords (complex)/minute, most transfers will be completed while you are busy with some other operation. (We're still checking on the first two rumors.)

Gossip makes file transfers about as easy as they can be. Just cable together a PC and your 1280 with a standard serial cable, run Gossip on the PC and select 'host' mode. Now you can 'SE' and 'TF' from within CHARM or GEM on the 1280 to send and get files to and from the PC. Since transfers are a background operation, you can immediately go on and do something else.

On older systems running NMC-1280 or NMR-1280 you can still do transfers but may have to run the 'FILTRN' program on the 1280. Consequently these transfers may not be in background.

FMR provides a macro for QE operation that automates aquisition and transfer. Using this macro as a template, you can easily modify your standard macros to include a file transfer after aquisition, after processing, or both.

Files transferred to the PC can be read by PLOT, or translated with our Felix/PC Data Translation software for further processing on your PC using Felix/PC.

Gossip contains a full selection of communications features in addition to the SECS protocol that allow CHARM, GEM or FILTRN file transfers. It supports PC COM ports 1 through 4, many different baud rates and data formats, modem control, and Kermit and Xmodem transfers.

Gossip is available from stock, at a very reasonable price. Why not order it today?

# Mobil Research and Development Corporation

June 18, 1990  
(received 6/19/90)

Dr. Bernard L. Shapiro  
TAMU NMR Newsletter  
966 Elsinore Court,  
Palo Alto, CA 94303

RESEARCH DEPARTMENT  
DALLAS RESEARCH LABORATORY  
P.O. BOX 819047  
DALLAS, TEXAS 75381-9047

13777 MIDWAY ROAD  
DALLAS, TEXAS 75244-4312

M.P. RAMAGE  
MANAGER

Dear Barry:

Large nuclear electric quadrupole coupling constants (several MHz) in solids cause the NMR transition frequencies of a powder to span a range of several MHz. This wide frequency range affects the nuclear spin excitation by a pulse and enables MAS to strongly affect spin-lattice relaxation curves. We have studied these effects using the aluminum NMR of the mineral low albite ( $\text{NaAlSi}_3\text{O}_8$ ) as an example. One of them is reported in this letter.

All of the aluminum in albite has a nuclear electric quadrupole coupling constant of 3.37 MHz and an electrostatic field gradient (e.f.g.) asymmetry parameter of 0.634. The first order quadrupole interaction causes the satellite transitions of a powder to span a range of 2.02 MHz, because of the  $3\cos^2\theta - 1$  dependence on the orientation of the e.f.g. in the magnetic field. The second order quadrupole interaction causes the central transition to span 7.90 kHz (at 6.35 Tesla). As a result of the large first order interaction, the ordinary NMR spectrometer registers signals from only the central transition; signals from the satellite transitions are lost in the noise of the baseline.

As the frequency distribution contained in a square pulse is given by the sinc function, a nominal 5 microsecond pulse contains an effective frequency range of only about 0.24 MHz, far smaller than the 2.02 MHz range of satellite transitions. Consequently, this pulse will excite central transitions for all of the nuclei in  $m = \pm 1/2$  spin states, but it will excite satellite transitions for only those nuclei in  $m = \pm 3/2, 5/2$  spin states that have e.f.g. orientations near the magic angle. Because the pulse flip angle when only the central transitions are excited is  $(1 + 1/2)$  times that when all of the transitions are excited, there is not a unique flip angle for all of the sample. This has consequences in spin-lattice relaxation measurements.

We have made saturating comb spin-lattice relaxation measurements at 11.74 Tesla on powdered albite under both stationary and MAS conditions. The 13.0 microsecond pulses in the comb had ninety degree flip angles if all transitions were excited. The stationary measurement (200 pulses in the comb) gave a  $T_1$  value of 8.8 seconds, but the MAS measurement (96 pulses in the comb) gave 19.4 seconds.

The larger  $T_1$  value with MAS indicates a more complete saturation of the nuclear spin system even though only half as many pulses were used. In the static measurement, many of the spins are not saturated by the comb, for the reason given above. These spins comprise a relaxation reservoir that enables spin diffusion to enhance the relaxation rate. Any given pulse can saturate only those spins that have e.f.g. orientations within a range of about 4 degrees centered near the magic angle. In the MAS measurement, each pulse can saturate a different set of spins because the sample rotation changes the e.f.g. orientations. Because every nucleus passes through the magic angle several times during each rotation, it is highly probable that all of them will be in e.f.g. orientations near the magic angle during at least one pulse in the comb.

Dr. Bernard L. Shapiro

-2-

June 18, 1990

The basic message in all this is that relaxation time measurements of quadrupolar nuclei in solids must be carefully planned.

Sincerely,



D. E. Woessner

DEW/mon

---

### **POSTDOCTORAL FELLOWSHIP**

A 3 year position is available for innovative NMR work in the general area of soil and plant chemistry. The project will involve multinuclear NMR spectroscopy in both liquid and solid phases using a Bruker WH-400 and MSL-300 respectively. The study will also include NMR imaging and localised spectroscopy using a SISCO-200 (4.7T, 30cm bore) imaging spectrometer.

The work is supported by the AFRC, and sets up a link between Queen Mary and Westfield College, London and the AFRC Rothamstead Research Station with its unique collection of plots, each with a documented history of more than 100 years.

Further details can be obtained from the project supervisors who are Dr. David Powlson (Head of Department of Soils and Agronomy at Rothamstead) and Professor Ed Randall at the Dept. of Chemistry, QMW, Mile End Road, London E1 4NS (to whom correspondence should be addressed).



# When faced with a tough analytical problem . . .

## QUESTION

*How do you find all the thiophenol derivatives matching YOUR CARBON SPECTRUM?*

## ANSWER

Sadtler Structure Assignment Library

### STEP:1

Search For  
Thiophenol Derivatives.

Structure Search Version 1.0  
File Draw Search View Print Library Utility  
CAS Registry Search  
Exact Match Search  
Substructure Search  
SHUTDOWN.SHL  
Source Structure  
Number of Hits: 120

Index	MQ1	Lib	Entry	Name
2	1	13C1	73	PHENYL DISULFIDE
3	1	13C1	98	BENZENESULFONYL CHLORIDE
4	1	13C1	287	BENZENESULFONYL FLUORIDE
5	1	13C1	288	BENZENESULFONYL FLUORIDE
6	1	13C1	327	P-TOLUENESULFONIC ACID, METHYL ESTER
7	1	13C1	355	P-TOLYL DISULFIDE
8	1	13C1	732	METHANOL, P-TOLUENESULFONYL-
9	1	13C1	982	BENZENESULFONIC ACID, HYDRATE
10	1	13C1	983	BENZENESULFONIC ACID, SODIUM SALT
11	1	13C1	987	P-TOLUENESULFONIC ACID, BUTYL ESTER
12	1	13C1	988	BENZENESULFONAMIDE
13	1	13C1	919	P-TOLUENESULFONAMIDE, N-BUTYL-
14	1	13C1	974	ACETIC ACID, PHENYLTHIO-
15	1	13C1	997	P-TOLUENESULFONYL CHLORIDE
16	1	13C1	1837	P-TOLUENESULFONAMIDE, N-METHYL-
17	1	13C1	1329	ANILINE, O-METHYLTHIO-
18	1	13C1	1378	SULFIDE, PHENYL 3-PHENYLPROPYL-
19	1	13C1	1296	SULFIDE, P-BROMOPHENYL METHYL-
20	1	13C1	1383	SULFIDE, METHYL N-NITROPHENYL-

### STEP 2:

Match Those Derivatives  
With Your Spectrum.

Sadtler NMR Search 2.10  
File Search View Library Print Utility Import Page

SEARCH  
Searching Hitlist: BEN2SR.IDF  
Total num. of compounds: 151  
0% 20% 40% 60% 80% 100%  
Cancel

Perform a peak search on a saved hit list file

## YOUR SEARCH IS OVER!

NMR Search 2.12  
File Search View Library Print Utility Import Page

LIB PEAK LOCATION  
© 1987, 1988-1990 Bio-Rad, Division. All Rights Reserved.  
Sadtler ID: 8771  
=== First Peak Table ===  
(Total of peaks: 5)  
No. Location Intensity  
1 15.60 4  
2 124.90 5  
3 126.70 9  
4 128.70 9  
5 138.60 1

Source Library: 13C1 - C-13 NMR STANDARDS  
<<Unknown Buffer>>  
File Name: THIDEMO.NDF  
Chem. Name: ODIFEROUS SPECIES  
CAS Registry Number: unknown  
Comment: process shutdown 12/9/89, green  
READY

109.05 ppm  
ad, Sadtler Division. All Rights Reserved.

STRUCTURE  
Print View

3 5 1  
4 2 3 4

... look to SADTLER  
for the knowledge to end your search.

**BIO-RAD**

Sadtler  
Division

3316 Spring Garden Street,  
Philadelphia, Pennsylvania 19104.

Telephone: (215) 382-7800.

Telefax: (215) 662-0585. TWX: 710 670-1186.





UNIVERSITY OF CAMBRIDGE  
DEPARTMENT OF CHEMISTRY  
Lensfield Road  
Cambridge CB2 1EP

Professor Barry Shapiro,  
Editor-in-chief, TAMU NMR,  
966 Elsinore Court,  
Palo Alto,  
CA 94303.

Dear Barry,

18 June 90

(received 6/25/90)

### Overlapping COSY Cross Peaks

One thing the organic chemists often ask is whether it is possible to disentangle overlapping cross peaks in COSY spectra. Of course, one way is to go to higher dimensions to spread out the information, but usually these people are too busy for that kind of complication. We have recently tried out two different 2D methods of separating overlapping cross peaks.

The first uses a line-selective excitation pulse (*spin pinging*<sup>1</sup>) at an  $F_1$  frequency chosen to slice through one cross peak but avoid the other overlapping 2D multiplets. In a certain sense this is the equivalent of a spin tickling experiment. The excitation spreads throughout the chosen multiplet when the first hard  $90^\circ$  pulse of the COSY sequence is applied. Thus we obtain a partial COSY spectrum with only one cross peak from the crowded region. The method lacks the full sensitivity since only one transition is excited, but if we catch two close transitions the sensitivity doubles. Skill is needed to choose a suitable  $F_1$  frequency. Note that this need not be at the extreme edge of the cross peak, it may be at any point that avoids simultaneous excitation of the "unwanted" neighbours. Figure 1 shows the separation of a composite cross peak from a copolymer sample into four separate components.<sup>2</sup> The arrows indicate the selective excitation frequencies. In Figure 1b the four individual components are superimposed again for comparison with the raw data of Figure 1a.

The second approach requires no additional measurements but operates on the existing frequency-domain COSY data. It requires *two* orthogonal traces that catch the desired cross peak but avoid the overlapping neighbours. These two traces are multiplied together to reconstruct the complete 2D multiplet, which is then subtracted from the rest. Where there are several overlapping components they can be taken out one at a time. We call this "deconstruction" by analogy with a concept that has caused some highly productive controversy in the world of literary criticism. Figure 2 shows the 400 MHz proton spectrum of one of the COSY cross peaks of the molecule of tolaasin. Starting with the raw experimental data (Figure 2a), four progressive stages of subtraction take out one primitive cross peak at a time (right-hand column). Figure 2h shows a good example of where the method *cannot* distinguish two cross peaks because all the  $F_1$  frequencies are degenerate. Nevertheless the intensities suggest that these are separate four-line cross peaks, making six overlapping components altogether.<sup>3</sup>

Kindest regards,

Ray

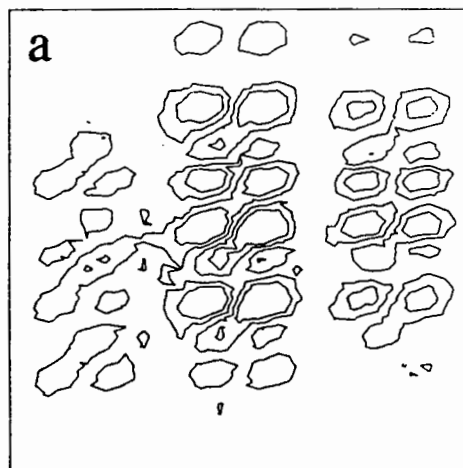
Ray Freeman

<sup>1</sup>X. L. Wu, P. Xu and R. Freeman, *J. Magn. Reson.* **83**, 404 (1989).

<sup>2</sup>P. Xu, X. L. Wu and R. Freeman, *J. Magn. Reson.* to be published.

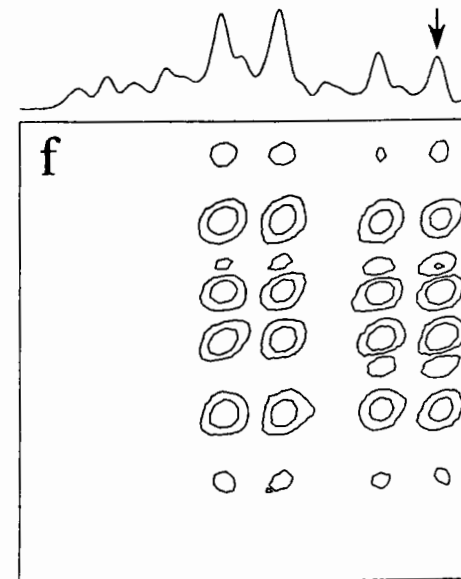
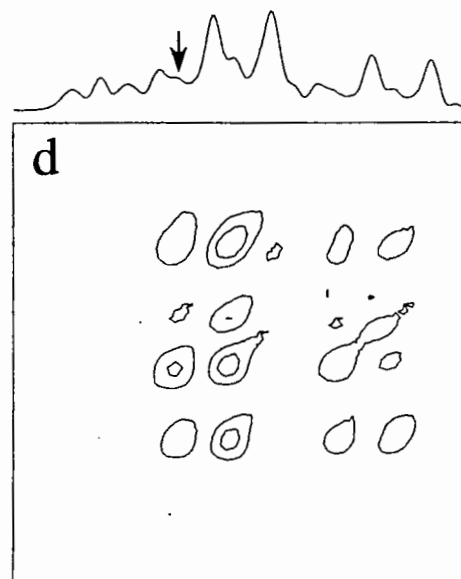
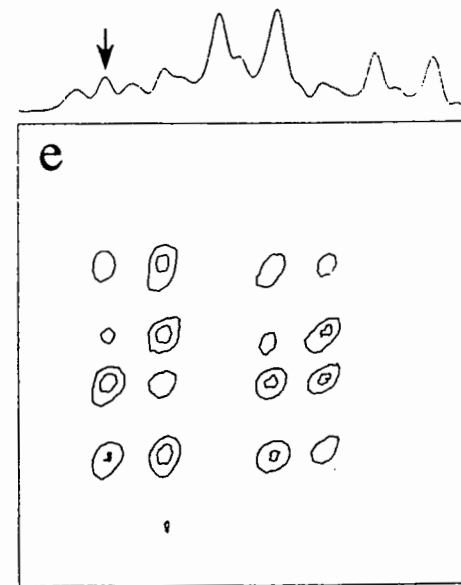
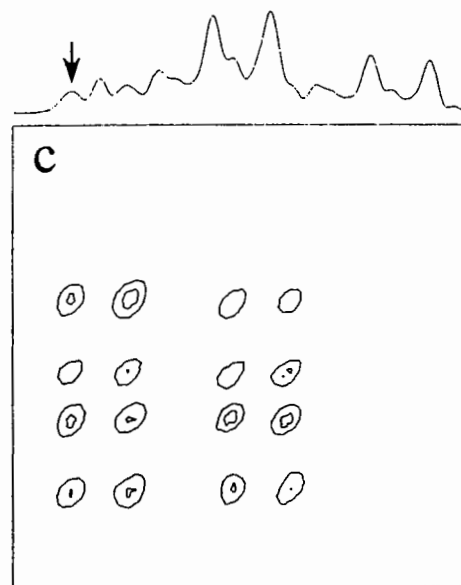
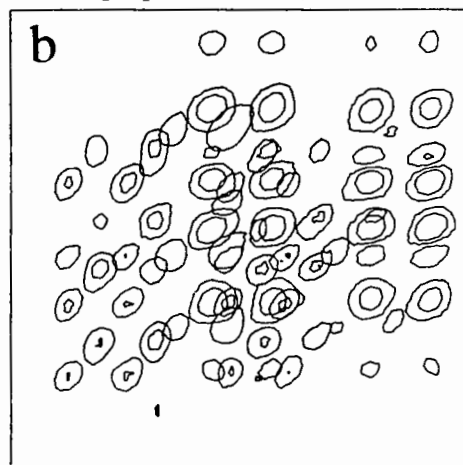
<sup>3</sup>L. McIntyre and R. Freeman, *J. Magn. Reson.* to be published.

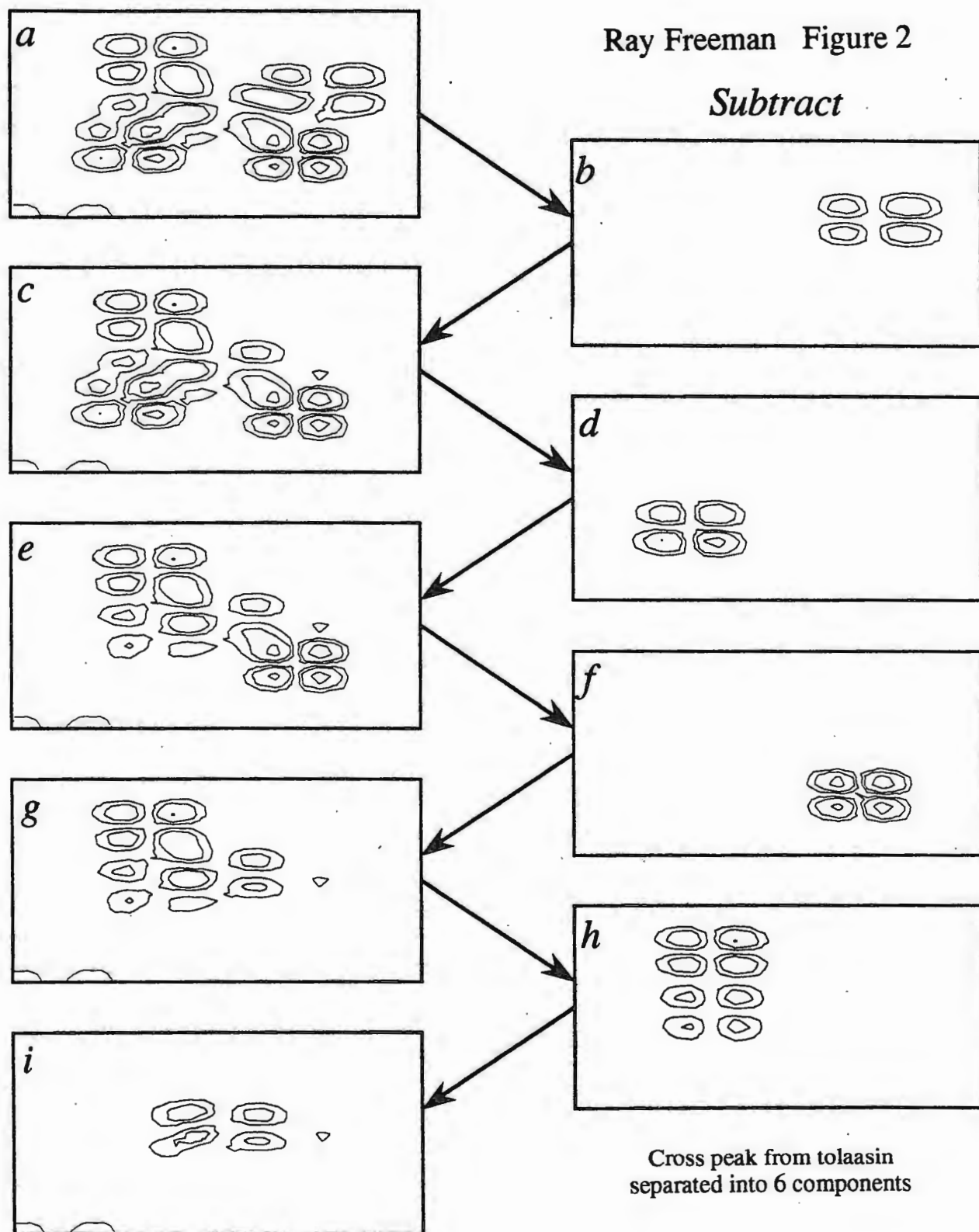
Ray Freeman Figure 1



a Overlapping cross peaks.

b Superposition of c, d e and f.







# VARIAN NMR FLEXIBILITY NOW RESOLVES PROBLEM DIVERSITY



MICROIMAGING

SOLIDS

LIQUIDS

## UNITY LETS YOU SWITCH FROM ONE TO THE OTHER WITH EASE

Combine high performance capabilities with unparalleled flexibility using Varian's new UNITY™ NMR spectrometer. This unique spectrometer is a true, multi-capability instrument that performs high resolution microimaging as easily as it analyzes liquid and solid samples.

UNITY's revolutionary system architecture employs a modular design that addresses all NMR applications with a single instrument.

Analyze liquid samples using a variety of techniques over a wide range of nuclei. Perform CP/MAS, wideline and multipulse for solid samples. Examine microimaging samples with ease. Maximum flexibility has been built in to cover future experimental capabilities for every application.

Resolve problem diversity: invest in the most flexible technology of today to better address the research of tomorrow. Invest in a UNITY NMR spectrometer. For additional information, please call the Varian office closest to you.

**Varian is your full-line  
company for analytical  
instrumentation**

NMR  
UV-Visible-NIR  
Atomic Absorption  
Solid Phase Extraction  
Liquid Chromatography  
Gas Chromatography  
GC/MS

**Varian Associates**  
611 Hansen Way D-298  
Palo Alto, CA 94303  
U.S.A.  
Tel: 1-800-356-4437

**Varian AG**  
Steinhauserstrasse  
CH-6300  
Zug, Switzerland  
Tel: (42) 44 88 44

**Varian GmbH**  
Alsfelderstrasse 6  
D-6100 Darmstadt  
West Germany  
Tel: (0 61 51) 70 30

**Varian Instruments Ltd.**  
3rd Matsuda Bldg  
2-2-6 Ohkubo-Shinjuku  
Tokyo, 169, Japan  
Tel: (3) 204-1211

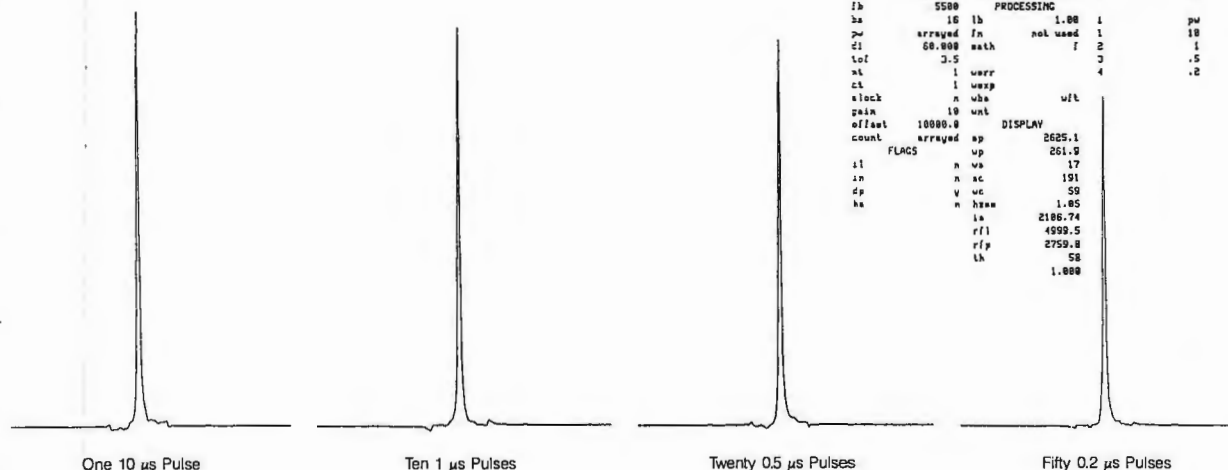
## NMR WITH A FUTURE

**varian** 

# FAST PULSE RISE-TIMES AND HIGH RF REPRODUCIBILITY

Many pulse sequences use a collection of pulses in place of a single pulse. Often the effective flip angle of these pulses is small and the net effect is to produce a specific pattern of excitation, such as no net excitation of water in H<sub>2</sub>O solutions but excitation of other resonances. For minimal offset effects, pulses should be as short as possible consistent with the desired effect. In some experiments, pulses much shorter than 1  $\mu$ sec are required. This time scale is on the order of pulse rise times on some spectrometers. UNITY rf is designed to provide fast pulse rise-times and stable amplitude, even for very short pulses. The DANTE data below show the excellent

performance of UNITY 600 MHz rf in a test of excitation efficiency. Ideal rf performance would show equal signal intensities in all four spectra. The first spectrum is from a single 10  $\mu$ sec pulse. The second used ten 1  $\mu$ sec pulses; the third, twenty 0.5  $\mu$ sec pulses; and, the last used fifty 0.2  $\mu$ sec pulses. The small reduction of amplitude for the last spectrum shows that the rise and fall times of the 200 nanosecond pulses are excellent, confirming the utility of small pulses in modern multi-pulse excitation pulse sequences and decoupling schemes.



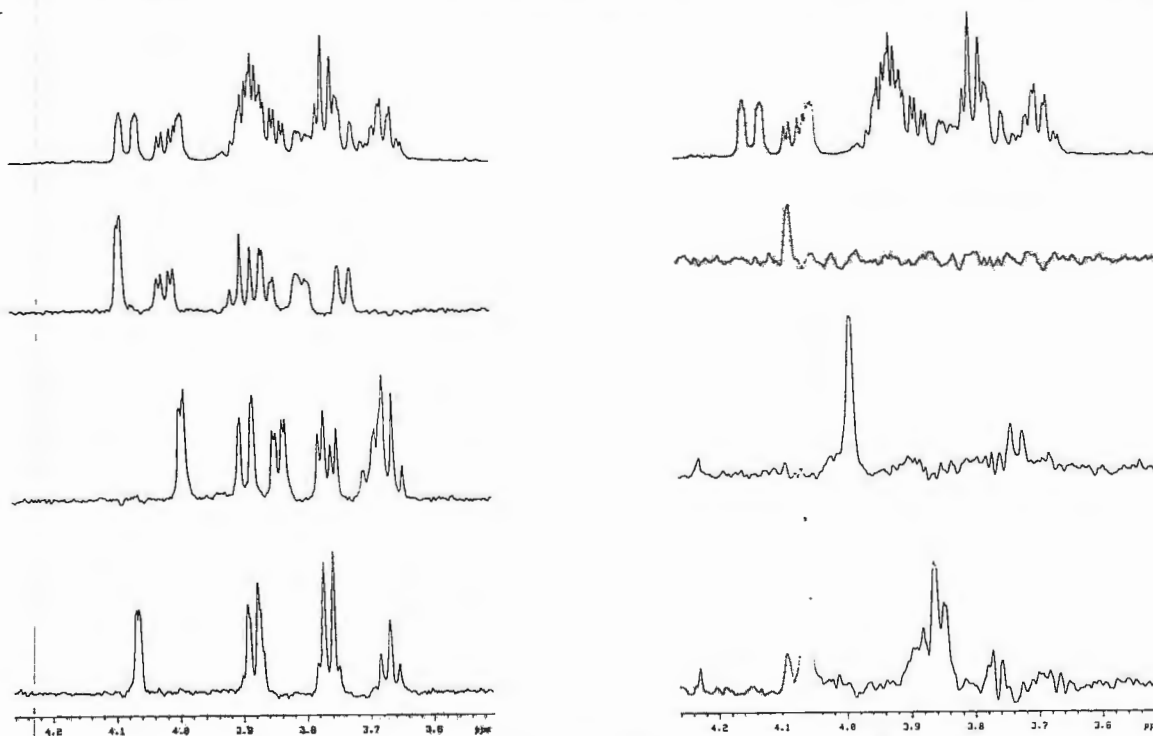
```
d2o danie test
exp4 pulse sequence: danie
SAMPLE      DEC. & UT      ACQUISITION ARRAYS
date Mar 15 89 dn          H1 array (count,pu)
solvent D2O dol            0
file exp de               n arraydia 4
ACQUISITION exp dw
afreq 500.048 dol          200 1 count
tx H1 dhp                20 1
at 1.002 dlp              10 2
xp 20032 hsoo             v 3
sw 10000.0 loop           35.0 4
fb 5500
bs 16 lb 1.00 1 pw
pw arrayed fn not used 1
di 60.000 math f 2
tol 3.5 c 4
nl 1 werr
cl 1 wexp
clock n vba
gain 10 wnt
offset 10000.0
count arrayed ap 2625.1
FLAGS up 261.9
il n va 17
in n ac 191
dp v uc 59
hs n hsm 1.05
io 2186.74
rfl 4559.5
rfp 2759.8
lh 58
1.000
```

MAG 5356/496

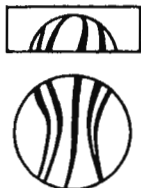
# SEPARATION OF OVERLAPPING SPIN SYSTEMS

1D TOCSY may be used very effectively in cases of overlapped spectra. In the 600 MHz spectra below, a trisaccharide in D<sub>2</sub>O gave overlapped sugar resonances between 3.6 and 4.1 ppm (top spectra). The left are independent 1D TOCSY spectra for the three different anomeric protons (not shown). Clear separation of the spin systems is accomplished, permitting spectral analysis (52 msec selective gaussian pulses using standard hardware).

Another way to gain assignment information is by NOE-difference experiments. The data are presented at the right for the same three anomeric protons. The upper difference spectrum integrates to 0.95% of a proton, showing the excellent stability and cancellation performance required for these demanding low-level NOE's.



MAG 5356/496


**VICTORIAN COLLEGE OF PHARMACY LTD**

Incorporated in Victoria

 381 ROYAL PARADE PARKVILLE VICTORIA AUSTRALIA 3052 TELEPHONE 387 7222  
 FACSIMILE 389 9582

*From the School of Pharmaceutical Chemistry*

June 20, 1990  
 (received 6/30/90)

Professor Bernard L Shapiro, Editor  
 TAMU NMR Newsletter  
 966 Elsinore Court  
 PALO ALTO, CA 94303, USA

Dear Barry

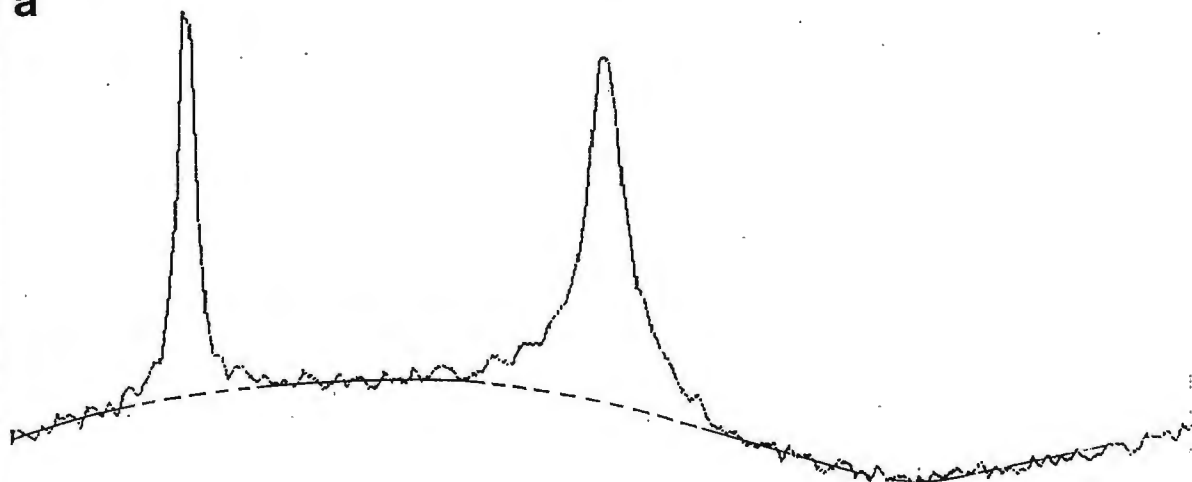
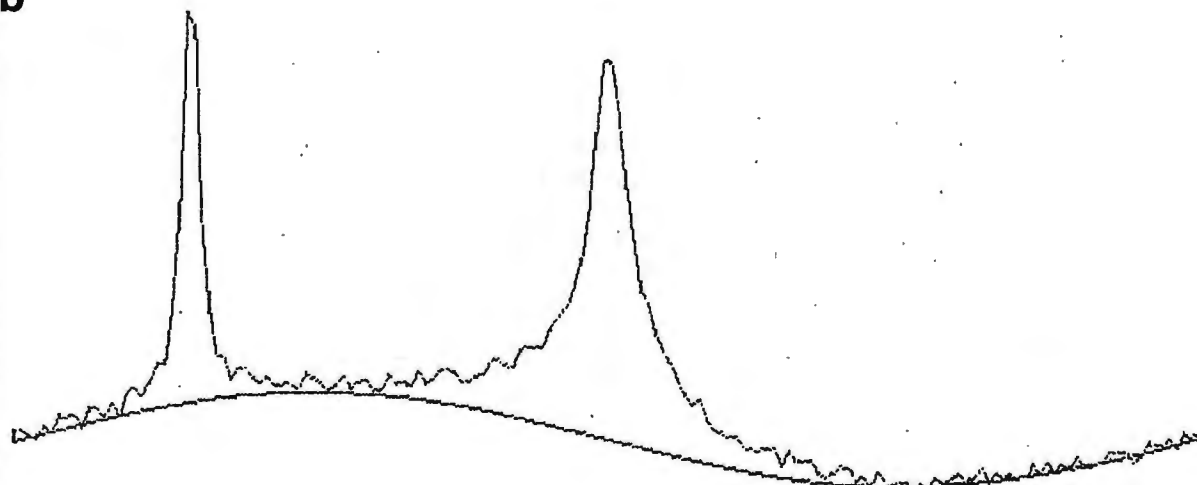
We have been using  $^{39}\text{K}$  NMR to quantitate potassium levels in biological tissue. Previous studies of excised tissue samples have suggested that not all of the potassium present in tissue is 'NMR-visible'. Figures of around 40% detectability have been frequently cited in early studies and rationalized on the basis of the quadrupolar nature of the spin  $3/2$   $^{39}\text{K}$  nucleus. Relaxation is biexponential and it can theoretically be shown that 40% of the signal intensity relaxes with time constant  $T_2^1$  and 60% with time constant  $T_2^{11}$ .

$$\frac{1}{T_2^1} = \frac{1}{20} \left( \frac{e^2 q Q}{\hbar} \right)^2 (1 + \eta^2/3) \tau_c \left[ \frac{1}{1 + \omega_0^2 \tau_c^2} + \frac{1}{1 + 4\omega_0^2 \tau_c^2} \right]$$

$$\frac{1}{T_2^{11}} = \frac{1}{20} \left( \frac{e^2 q Q}{\hbar} \right)^2 (1 + \eta^2/3) \tau_c \left[ 1 + \frac{1}{1 + \omega_0^2 \tau_c^2} \right]$$

For some correlation times, the former signal may be narrow enough to detect, while the latter is significantly broadened, leading to an apparent NMR detectability of only 40% of the total potassium present. Fast exchange between two pools of ions, one immobilized and another 'free', could lead to similar effects.

In recent work we have found, however, that with careful measurement up to 90% of K present in rat thigh muscle may be detected by NMR. Observed lineshapes fit well to two Lorentzian components of around 50 Hz and 400 Hz linewidths. This prompted us to re-examine factors which may lead to reduced visibility. A very significant one is baseline roll, which is often present in the spectra of low-frequency nuclei such as  $^{39}\text{K}$ . To illustrate this we have written a program to simulate tissue spectra with varying degrees of baseline roll and noise. The spectra consist of a tissue peak with 50 Hz and 400 Hz linewidth components (50:50) superimposed (peak to the right in the figure) and a 'reference' peak. In our real spectra this consists of a capillary containing KCl and a dysprosium shift reagent, used as an integration standard.

**a****b**

Part (a) of the figure shows a typical simulated spectrum. If this were a real spectrum, one might be tempted to draw the baseline as indicated by the dotted line and integrate accordingly. The lower trace (b), however, shows the actual baseline used in generating the simulated spectrum. Clearly, in the presence of (i) biexponential peaks, (ii) baseline roll and (iii) moderate noise it is possible to underestimate peak areas substantially. On the lower-field NMR instruments used in the past for such studies, factors (ii) and (iii) may have contributed significantly to reduced visibilities.

Please credit this contribution to Ian Rae's account.

Best wishes

David Craik

Bill Adam

Mark Wellard

Phil Sheehan



# THE WEIZMANN INSTITUTE OF SCIENCE

Department of Isotope Research  
Rehovot 76100  
ISRAEL

Telephone: (972)-02-341979  
(972)-08-342417  
Bitnet: cizax@weizmann

June 15, 1990  
(received 7/20/90)

Dr. Bernard L. Shapiro  
TAMU NMR Newsletter  
966 Elsinore Court  
Palo Alto, CA 94303

## Where's the Hg in $\text{Hg}_{1-x}\text{Cd}_x\text{Te}$ ?

Dear Barry:

For several years now we have been interested in using NMR to explore at the atomic level the structure of some semiconductor alloys of the general form  $\text{Hg}_{1-x}\text{Cd}_x\text{Te}$ . These alloys are useful because, as a function of the cation concentration  $x$ , the band gap can be varied from semimetallic ( $x = 0.0$ ) to just barely semiconducting ( $x = 1.0$ ). In particular, the concentrations  $x = 0.30$  and  $x = 0.20$  have important applications in various detectors; the latter system is found (cooled by liquid  $\text{N}_2$ ) as the detector crystal in most FTIR systems and in infrared-sensing scopes. For NMR enthusiasts,  $\text{Hg}_{1-x}\text{Cd}_x\text{Te}$  is an appealing sample because spin- $\frac{1}{2}$  isotopes of reasonable magnetogyric ratio and natural abundance are available for each of the three constituent atoms. Working in our 200 MHz magnet, and reading off the standard charts of resonance frequencies (which are only very approximate predictors of the actually observed NMR frequencies in these electron-rich atoms) the nuclei, resonance frequencies, and natural abundances are:  $^{199}\text{Hg}$ , 35.655 MHz, 16.8%;  $^{113}\text{Cd}$ , 44.366 MHz, 12.3%;  $^{111}\text{Cd}$ , 42.411 MHz, 12.8%; and  $^{125}\text{Te}$ , 63.194 MHz, 6.99%. Some time ago we measured  $^{125}\text{Te}$  spectra as a function of  $x$  for a large number of samples and made assignments of chemical shifts to local Te environments (i.e. the number of nearest neighbor Hg sites); to our surprise, the average number of Hg sites per Te we derived from those spectra that were deemed most reliable seemed consistently lower than the percent of Hg indicated by the macroscopic formula.

This led us to the investigation of single crystal samples, where the concentrations are "well-known" to the crystal growers and the macroscopic energy gap provides a measure of the concentration. We have looked at a number of samples of  $\text{Hg}_{0.80}\text{Cd}_{0.20}\text{Te}$ , differing in the source of the sample and the quality (meaning the number and nature of the defect sites; "as grown" samples have high numbers of Hg vacancies and are  $p$ -type, while the actual detector crystals undergo substantial annealing in Hg vapor and have a much smaller number of residual Te vacancies. Our experience is that the spectra vary little with the quality of the samples, while  $T_1$  gets very long as the quality improves; therefore we have worked most with the pre-annealed samples where  $T_1$  is measured in seconds (at least, for Hg and Te sites) rather than minutes. One of our questions was whether we could be sure of the assignments we had made based on varying the chemistry, and so we searched for an internally consistent method of making the assignment of Te lines (shown in Fig. 1) to the various microclusters determined by the number of each type of cations in the first coordination sphere (i.e. 0 Hg neighbors, 1 Hg neighbors, 2 Hg neighbors, 3 Hg neighbors, or 4 Hg neighbors). Referenced to CdTe, with positive shifts meaning higher frequency, we have assigned the large peak at c. 500ppm to Hg(3)CdTe and the smaller peak at c. 300 ppm to Hg(4)Te; lower frequencies correspond to species with more Cd neighbors.

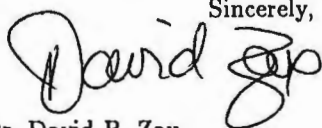
Techniques using magic angle sample spinning seem not to work in these compounds, presumably because the energy gap in the 80-20 crystal is very nearly that of a metal; the eddy currents induced in the sample impede spinning. Furthermore, the dipole-dipole coupling between nearest neighbor pairs of  $^{125}\text{Te}$  and any of the spin- $\frac{1}{2}$  cations is only a few hundred Hz (although the J coupling measured in HgTe is a few kHz). Unfortunately, the  $T_2$  for Hg in these systems, as measured by a two-pulse spin echo experiment, is only a few hundred  $\mu\text{s}$ ; it is only somewhat longer for Te. (This may not be a real  $T_2$  effect so much as the result of rf inhomogeneity.) Thus, simple correlation experiments such as SEDOR (spin-echo double resonance) suffer from very poor signal-to-noise, even neglecting questions of how the natural abundance enters into the question.

Some time ago we discovered that the effective  $T_2$ 's are substantially longer under a Carr-Purcell train ( $> 10$  ms), as long as the inter-pulse spacing was no greater than c. 100  $\mu\text{s}$ . The result of such an experiment, represented in 2-D form, is shown in Fig. 2. Equal linewidths in the  $\omega_1$  dimension reflect comparable  $T_2$ 's at all sites. In a 2-D  $^{125}\text{Te}$ - $^{199}\text{Hg}$  double resonance experiment (at 63.070 MHz and 35.710 MHz) we can explore correlate between dipolar couplings in  $\omega_1$  and the Te chemical shift spectrum in  $\omega_2$ . The widest spectrum in  $\omega_1$  is therefore the Te

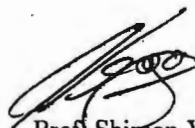


site with the most Hg neighbors, the widths of individual lines should be directly proportional to the number of Hg neighbors, although the natural abundances may make a straightforward interpretation more difficult (as, for example, much less than 1% of the sites with 4 Hg neighbors have 4  $^{199}\text{Hg}$  neighbors; < 2% have 3  $^{199}\text{Hg}$  neighbors, 12% have 2, and 39% have 1). While the Carr-Purcell train averages out all of the dephasing mechanisms at the Te sites, simultaneously applying  $\pi$  pulses to the Hg sites allows us to preserve the heteronuclear couplings. The widths of the dipolar ( $\omega_1$ ) patterns (see Fig. 3) are consistent with our previous assignments of the Te shifts; the display is clearer in Fig. 4 where we show the difference spectrum of the experiments with and without Hg  $\pi$  pulses, and thereby cancel out the large background signal due to Te sites with Hg neighbors none of which are  $^{199}\text{Hg}$ . This leaves us with our initial question: Where is all the Hg? (So far only one line has been observed in the Hg spectrum.)

Sincerely,



Dr. David B. Zax



Prof. Shimon Vega

P.S. Please credit this note to the account of Dr. Rafi Poupko. Also, one of us (DBZ) will be moving to Cornell University this summer. Anyone thinking of selling a high-field widebore magnet? I could be interested. After July 15 or so you can find me at:

David Zax  
Department of Chemistry  
Baker Laboratory  
Cornell University  
Ithaca, NY 14853-1301

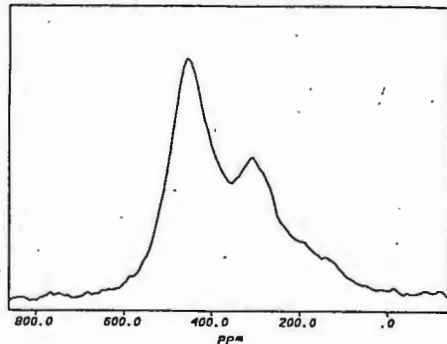


Figure 1

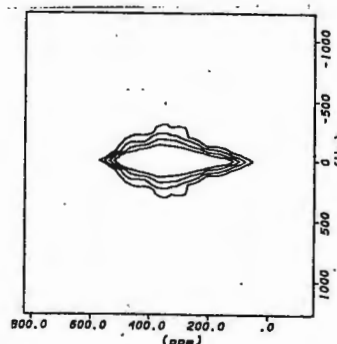


Figure 2

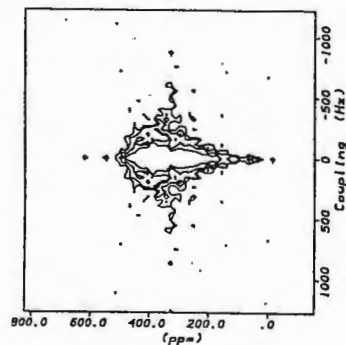


Figure 3

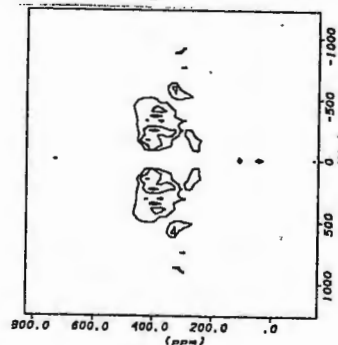


Figure 4

# More people specify Oxford Instruments NMR magnets than any other

## SO WHAT IS THE BIG ATTRACTION?

Oxford Instruments have been the foremost manufacturer of highly homogenous superconducting magnets for high resolution NMR applications since 1968.

A track record which could only have been achieved by a constant search for excellence in every aspect of NMR magnet design. Which is why, in our extensive range of magnets from 200MHz to 600MHz, we painstakingly ensure that every single one is balanced to at least the eighth order on-axis, giving the ultimate in NMR performance.

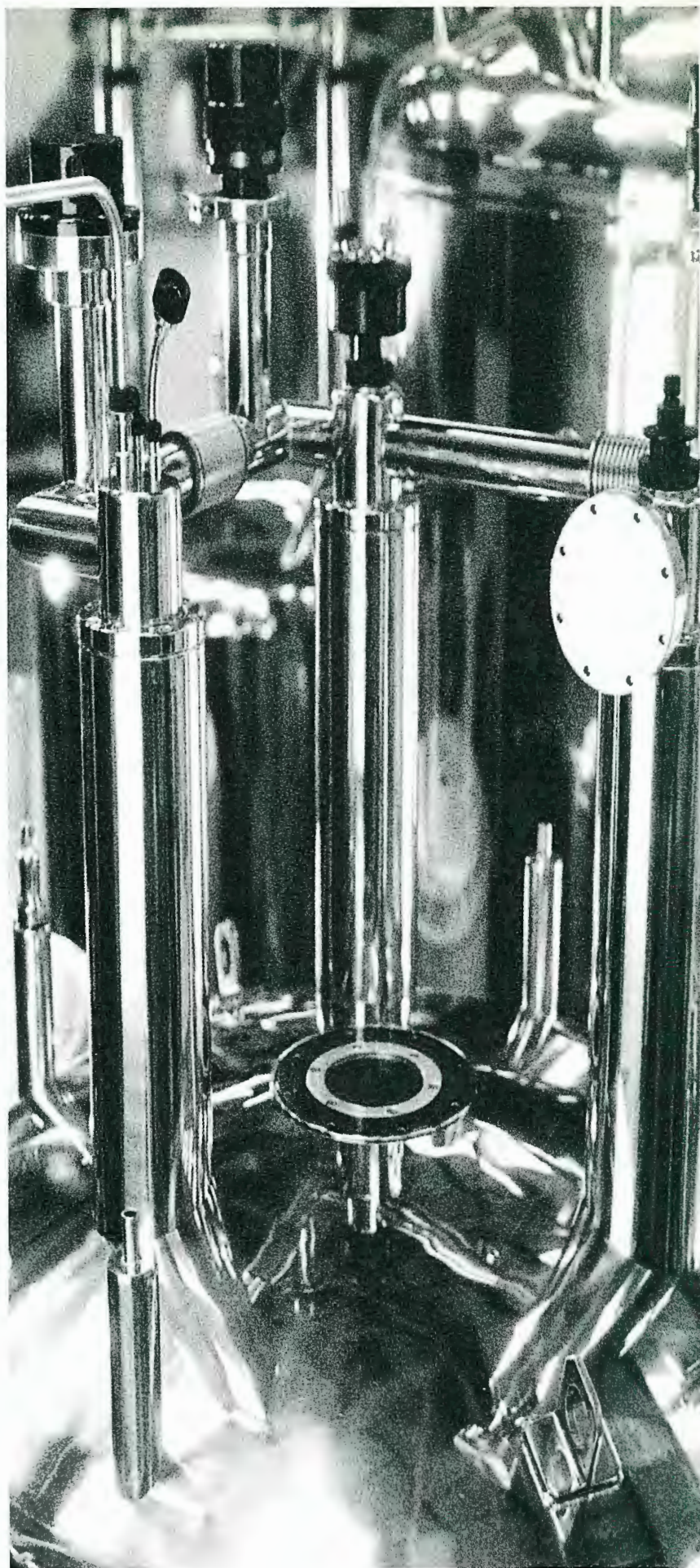
A performance which is also typified by the stability of the fields produced, thanks to our ability to achieve truly superconducting joints – whatever the superconductor. What is more, we design and build the long hold cryostats in which they're installed to the same exacting standards.

But simply producing magnets of such quality isn't all of the story, for we back them with installation and service centres that provide high quality advice and support worldwide.

Innovation, design, quality and service, just some of the reasons why we've remained so attractive for so long.

OXFORD  
NMR Division

*The future demands the best*







ALBERT EINSTEIN COLLEGE OF MEDICINE  
OF YESHIVA UNIVERSITY

1300 MORRIS PARK AVENUE, BRONX, N.Y. 10461: CABLE: EINCOLLMED, N.Y.

DEPARTMENT OF PHYSIOLOGY AND BIOPHYSICS

PHONE: (212) 430-3591

July 1, 1990  
(received 7/14/90)

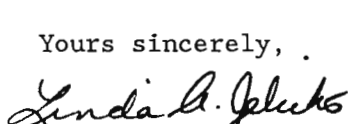
Dr. B. L. Shapiro  
966 Elsinore Court  
Palo Alto, CA 94303

Dear Barry,


<sup>23</sup>Na NMR of Cartilage


The ionic composition of the extracellular matrix of cartilage is related to the extracellular proteoglycan concentration; any change in proteoglycan concentration (such as during compression or swelling) will, thus, affect extracellular ionic composition (1). In order to investigate the feasibility of using <sup>23</sup>Na NMR to study extracellular [Na<sup>+</sup>] in cartilage we undertook a preliminary study of bovine nasal cartilage incubated in Dulbecco's modified Eagle's medium supplemented with 10% bovine serum albumin. The <sup>23</sup>Na resonance of a cartilage sample is comprised of two well-defined components (Fig. 1) which exhibit monoexponential longitudinal relaxation ( $T_1=17.4$  ms).  $T_2$  values of 1 ms and 10 ms were estimated from the linewidths at half height of the broad (300 Hz) and narrow (30 Hz) components. Integration of these two components indicated approx. 37% intensity due to the narrow component and 63% due to the broad component (close to the 40% and 60% intensities expected theoretically for the inner transition ( $-\frac{1}{2} \leftrightarrow +\frac{1}{2}$ ) and outer transitions ( $-\frac{3}{2} \leftrightarrow -\frac{1}{2}$  and  $\frac{1}{2} \leftrightarrow \frac{3}{2}$ ) of spin  $\frac{3}{2}$  nuclei). Double-quantum (DQ) filtered <sup>23</sup>Na NMR spectra of this sample at several values of the DQ preparation time ( $\tau$ ) are shown in Fig. 2. Because cartilage is only approx. 2% cells very little intracellular Na<sup>+</sup> contributes to the resonance intensity, and we believe that the DQ filtered signal represents extracellular matrix associated Na<sup>+</sup>. Unlike our previous studies on blood cells and perfused tissue, which required extensive signal averaging (acquisition of 2048-4096 transients per  $\tau$  value) to achieve mediocre S/N, excellent S/N was achieved with 256 transients (the minimum required for our phase cycling routine) for the cartilage samples. Interestingly, some of the DQ filtered spectra appear to be a superposition of two resonances, each having broad and narrow components (see the spectrum acquired with  $\tau=5$  ms in Fig. 2), presumably arising from Na<sup>+</sup> ions in differing environments.

Yours sincerely,

  
Linda A. Jelicks

  
Pradeep K. Paul\*

  
Elizabeth M. O'Byrne\*

  
Raj K. Gupta

\*CIBA-GEIGY Corporation, Summit, NJ 07901

1. Urban, J.P.G. and Bayliss, M.T. (1989) Biochim. Biophys. Acta 992 59-65.

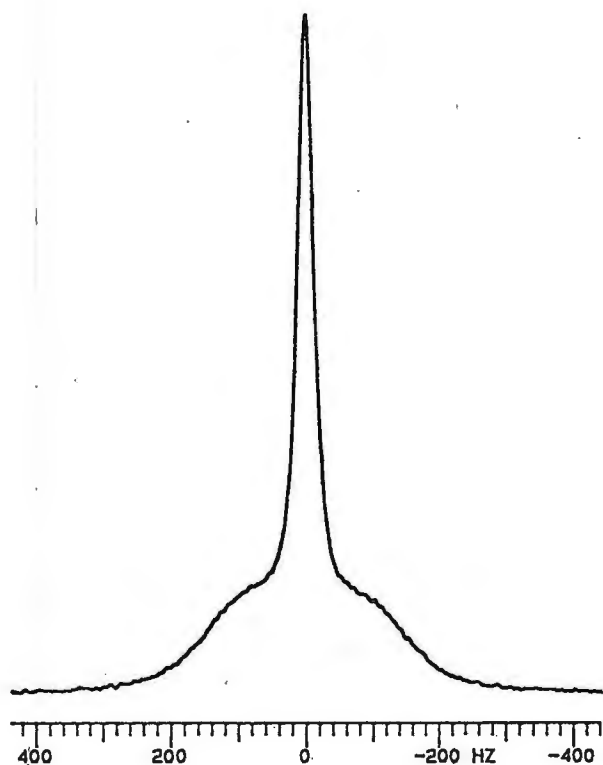


Fig. 1:  $^{23}\text{Na}$  NMR spectrum of a sample of cartilage resulting from signal averaging 256 transients acquired at 53 MHz at room temp. (19°C). No line broadening was applied.

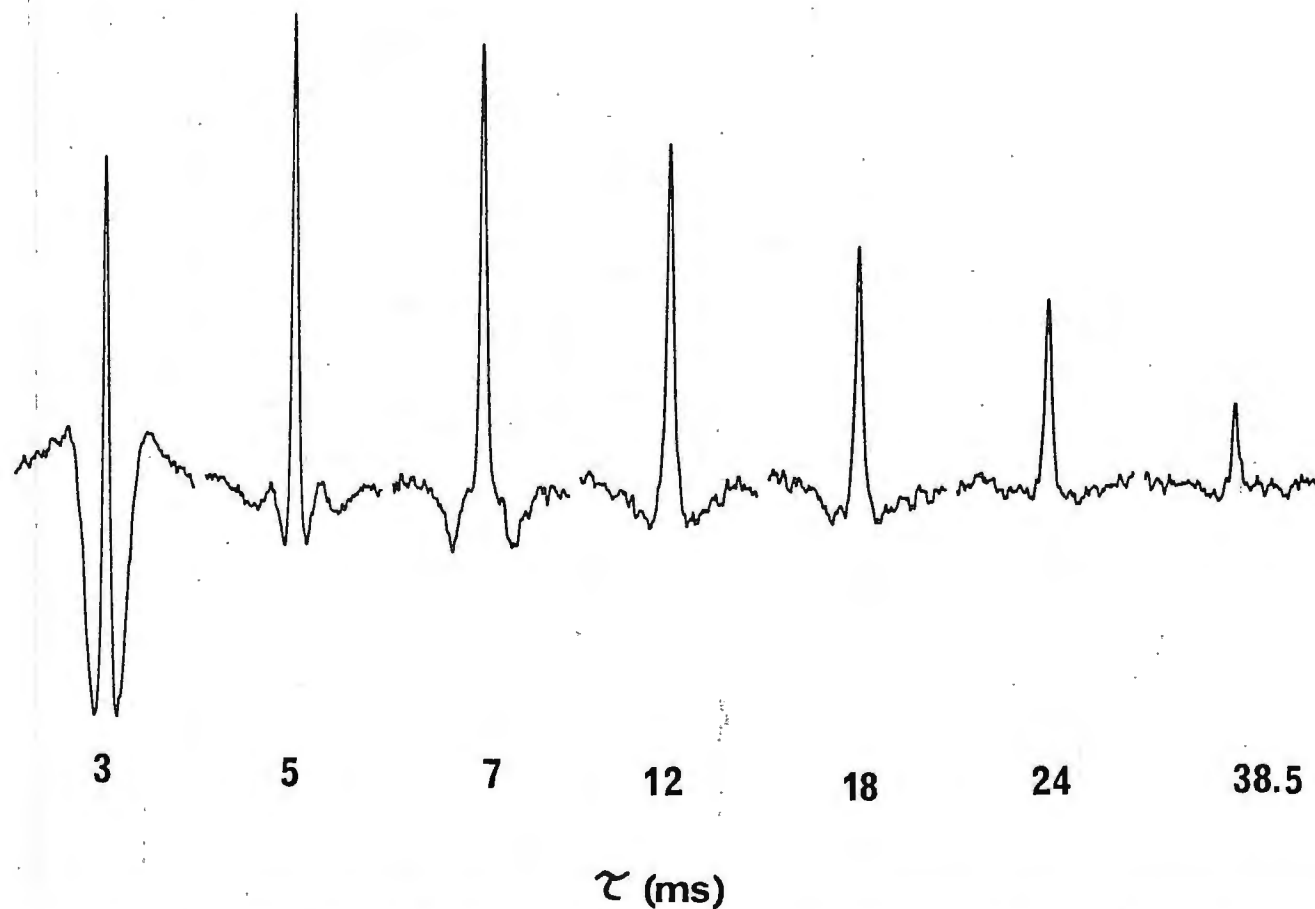


Fig. 2: DQ filtered  $^{23}\text{Na}$  NMR spectra of cartilage acquired with the  $\tau$  values indicated. 256 transients were acquired with a the standard  $90^\circ-\tau/2-180^\circ-\tau/2-90^\circ-\delta-90^\circ$  pulse sequence; 10 Hz line broadening was applied.



## PTS 040

Range: 0.1-40 MHz  
Resolution: 0.1Hz-100KHz (opt)  
Switching: 1-20 $\mu$ s

Output: +3 to +13dBm; 50ohm  
Spurious Outputs: -75dB  
Phase Noise: -75dBc (0.5Hz-15KHz)

Freq. St'd: OCXO, TCXO, Ext.  
Interface: BCD par. or GPIB  
Price: \$4,800.00\*

## PTS 120

Range: 90-120 MHz  
Resolution: 0.1Hz-100KHz (opt)  
Switching: 1-20 $\mu$ s

Output: +3 to +10dBm; 50ohm  
Spurious Outputs: -75dB  
Phase Noise: -75dBc (0.5Hz-15KHz)

Freq. St'd: OCXO, TCXO, Ext.  
Interface: BCD par. or GPIB  
Price \$4,800.00\*

## PTS 160

Range: 0.1-160 MHz  
Resolution: 0.1Hz-100KHz (opt)  
Switching: 1-20 $\mu$ s

Output: +3 to +13dBm; 50ohm  
Spurious Outputs: -75dB  
Phase Noise: -63dBc (0.5Hz-15KHz)

Freq. St'd: OCXO, TCXO, Ext.  
Interface: BCD par. or GPIB  
Price: \$5,850.00\*

## PTS 250

Range: 1-250 MHz  
Resolution: 0.1Hz-100KHz (opt)  
Switching: 1-20 $\mu$ s

Output: +3 to +13dBm; 50ohm  
Spurious Outputs: -70dB  
Phase Noise: -63dBc (0.5Hz-15KHz)

Freq. St'd: OCXO, TCXO, Ext.  
Interface: BCD par. or GPIB  
Price: \$6,700.00\*

## PTS 300

Range: 0.1-300 MHz  
Resolution: 1Hz  
Switching: 1-20 $\mu$ s  
Phase Continuous: 1Hz-100KHz steps

Output: +3 to +13dBm; 50ohm  
Spurious Outputs: Type 1  
-70/65 (typ/spec) Type 2  
-65/60dB  
Phase Noise: -68dBc (0.5Hz-15KHz) -63dBc

Freq. St'd: OCXO, TCXO, Ext.  
Interface: BCD par. or GPIB  
Price: Type 1 Type 2  
\$5,800.00\* \$5,300.00\*

## PTS 500

Range: 1-500 MHz  
Resolution: 0.1Hz-100KHz (opt)  
Switching: 1-20 $\mu$ s

Output: +3 to +13dBm; 50ohm  
Spurious Outputs: -70dB  
Phase Noise: -63dBc (0.5Hz-15KHz)

Freq. St'd: OCXO, TCXO, Ext.  
Interface: BCD par. or GPIB  
Price: \$7,850.00\*

## PTS x10 NEW

Range: 10 MHz band, selected decade 0.1-100 MHz  
Resolution: 1 Hz  
Switching: 1-5 $\mu$ s  
Phase Continuous: 2 MHz band, even or odd steps

Output: +3 to +13dBm; 50ohm  
Spurious Outputs: -65/-60dB (typ/spec)  
Phase Noise: -70dBc (0.5Hz-15KHz)

Freq. St'd: OCXO, TCXO, Ext.  
Interface: BCD par. or GPIB  
Price: \$2,450.00\*

**OTHER OPTIONS:** Programmable Attenuator 0-90dB (or 0-99dB with GPIB)  
n x 10 MHz output (20-140 MHz) or any 10 MHz line

\*Prices are US only, and include manual & remote (BCD) control, 1 Hz resolution, OCXO std.



**PROGRAMMED TEST SOURCES, INC.**

P.O. Box 517, 9 Beaver Brook Rd., Littleton, MA 01460 508-486-3008 FAX Number: 508-486-4495

June 18, 1990

(received 6/25/90)

 Dr. B.L. Shapiro  
 966 Esinore Court  
 Palo Alto, CA 94303  
 USA

### Secondary Isotope effect on F-resonance of $\text{XeF}_2$

Dear Barry,

We would like to report an interesting secondary isotope effect observed in the F-resonance of the compound  $\text{XeF}_2$  (dissolved in  $\text{CD}_3\text{CN}$ ) due to the various isotopes of Xe. The noble gas Xe has the following isotopes with appreciable abundance:

$^{129}\text{Xe}$	26.4%	$^{132}\text{Xe}$	26.9%
$^{130}\text{Xe}$	4.1%	$^{134}\text{Xe}$	40.4%
$^{131}\text{Xe}$	21.2%	$^{136}\text{Xe}$	8.9%

Of these  $^{129}\text{Xe}$  has spin 1/2 so that on the central line of the F-resonance which is shown in the figure the corresponding line is missing.  $^{131}\text{Xe}$  with spin 3/2 is quadrupole relaxed

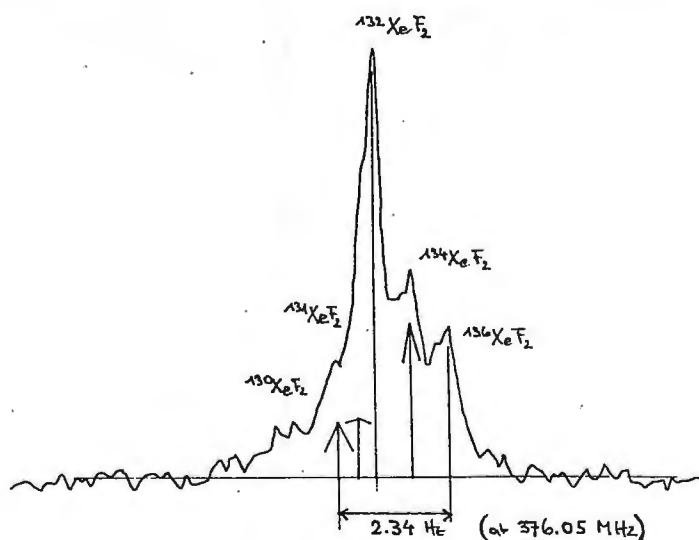


Fig.: Central line of F-resonance of  $\text{XeF}_2$

and the corresponding F-resonance is considerably (5 times) broadened. The remaining isotopes are non magnetic.

A theoretical superposition of the  $^{130}\text{Xe}$ ,  $^{131}\text{Xe}$ ,  $^{132}\text{Xe}$ ,  $^{134}\text{Xe}$  and the  $^{136}\text{Xe}$  isotopes with an upfield shift (per increase of Xe-mass by one unit) of 1.037 ppb. [1 ppb =  $10^{-3}$  ppm] agrees well with the observed spectrum.

Yours sincerely

P. Diehl

J. Jokisaari

*Diehl*

Solids put us on  
THE MAP - - - -

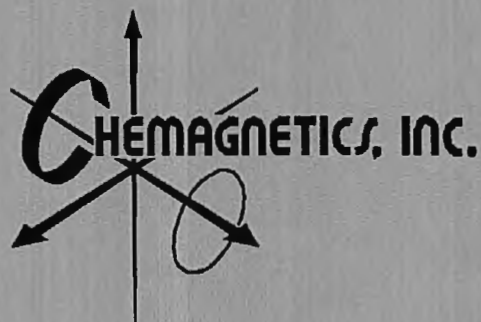


Over 50  
Installed  
Spectrometers.



Dedicated to Design  
Excellence

303 - 484 - 0428



2555 Midpoint Dr., Fort Collins, Colorado 80525  
Fax:(303) 484-0487

WESTERN RESEARCH INSTITUTE  
P.O. Box 3395, University Station  
Laramie, Wyoming 82071-3395  
(307) 721-2011

June 26, 1990  
(received 6/30/90)

Dr. B.L. Shapiro  
TAMU NMR Newsletter  
966 Elsinore Court  
Palo Alto, CA 94303

Dear Barry,

RE: High Resolution (Relatively Speaking) Solid-State Spectra of an Asphaltene and a Coal

I hope that this short report will reinstate our subscription to the TAMU NMR Newsletter. Our solid-state Chemagnetics NMR spectrometer was delivered in early March and we have been running a few fossil fuel samples on it. The configuration of the spectrometer may be unique in that we have a single console and two magnets; 100 MHz for  $^{13}\text{C}$  CP/MAS experiments at 25 MHz and 200 MHz for  $^1\text{H}$  CRAMPS experiment, as well as other nuclei. Because of other commitments, we have only run the  $^{13}\text{C}$  CP/MAS experiments at this time.

Dr. Miknis and I are both pleased with the performance of the spectrometer. Figures 1 and 2 show the  $^{13}\text{C}$  CP/MAS spectrum of a petroleum asphaltene and an Alaskan coal, respectively. The following table shows the solid- and liquid-state carbon aromaticity values for several different types of fractions obtained from the separation of two heavy crudes.

<u>Crude</u>	<u>Base Fraction</u>	<u>Amphoteric Fraction</u>	<u>Asphaltene Fraction</u>
A			
Solid State		0.447	0.475
Liquid State		0.452	0.526
B			
Solid State	0.352	0.381	0.441
Liquid State	0.356	0.357	0.423

The agreement of the  $^{13}\text{C}$  aromaticity values determined in the solid and liquid state are reasonably good and indicates that the experimental conditions used are quite satisfactory.

Sincerely,



Dan Netzels



Fran Miknis



Figure 1. Petroleum Asphaltene

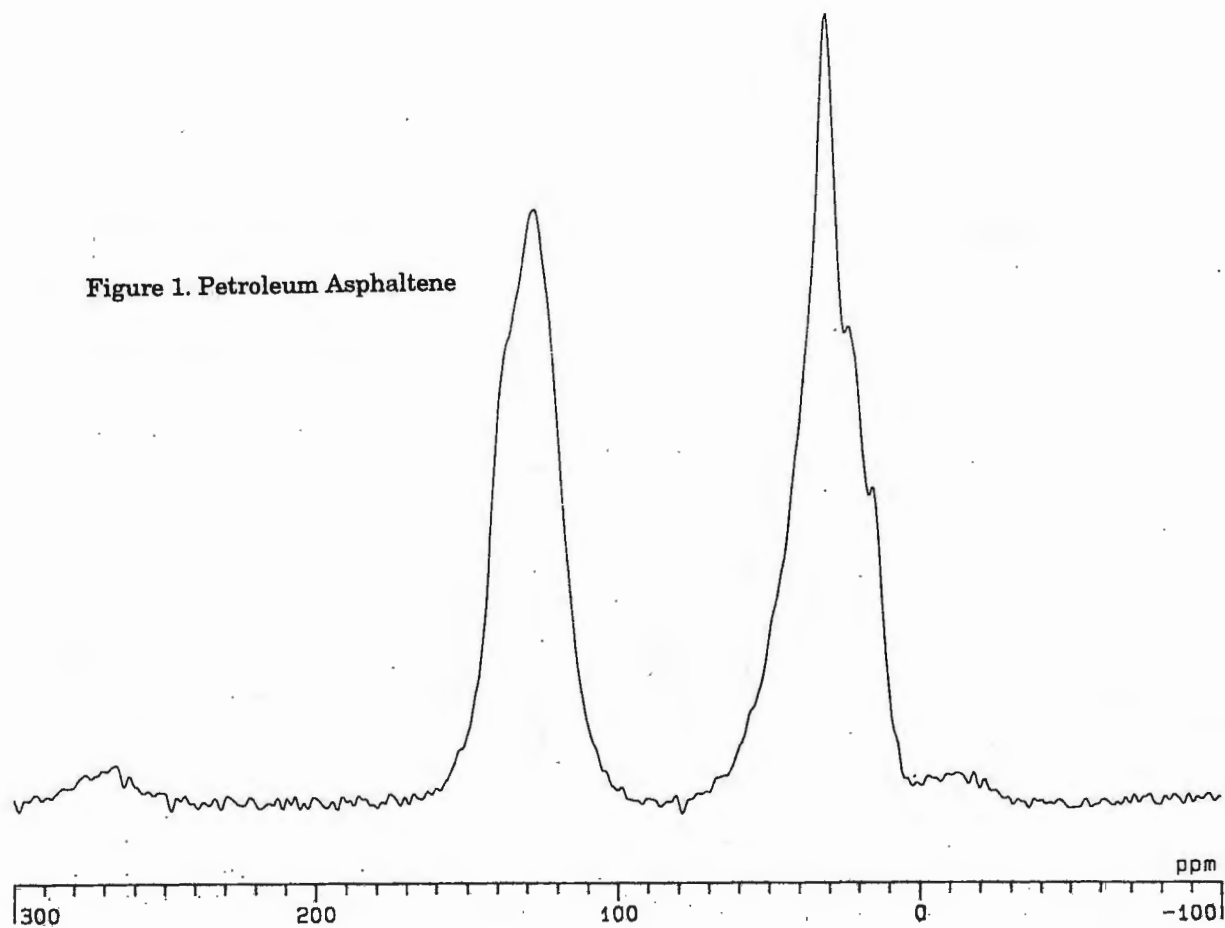
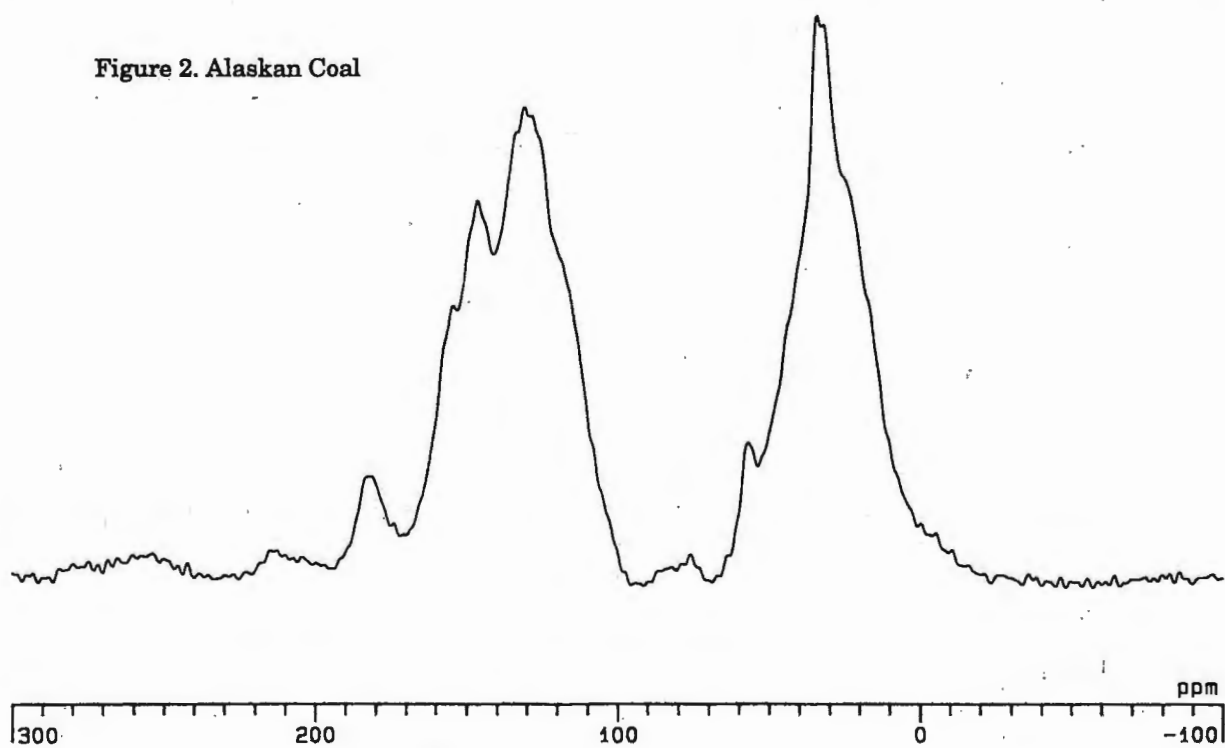


Figure 2. Alaskan Coal



MASSACHUSETTS GENERAL HOSPITAL

HARVARD MEDICAL SCHOOL

## MGH-NMR CENTER

NMR RESEARCH LABORATORIES  
MGH IMAGING CENTER  
MR EDUCATION CENTER



Bldg. 149, 13th Street  
Charlestown, MA 02129  
Phone: (617) 726-  
Fax: (617) 726-5819

Dr. Bernard L. Shapiro  
TAMU NMR Newsletter  
966 Elsinore Court  
Palo Alto, CA 94303

June 19, 1990  
(received 6/20/90)

1. Imaging of Composites
2. Postdoctoral Position in Magnetic Resonance Imaging of Solids

Dear Barry:


Readers of these pages may be familiar with our work in  $^1\text{H}$  NMR imaging of polymeric binders in green ceramics,  $^{11}\text{B}$  and  $^{27}\text{Al}$  imaging in ceramic powders, and  $^1\text{H}$  and  $^{31}\text{P}$  imaging of bone and synthetic calcium phosphates. We also are working extensively with polymeric composites; some of this research is outlined below.

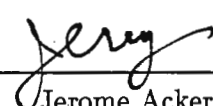
*We have an immediate opening for a postdoctoral fellow to work on some of these projects. Please send your CV or call either of us directly.*

We are continuing with our efforts to extend the use of NMR imaging techniques to the characterization of materials such as organic/inorganic composites. New composite materials with unusual and desirable properties are made possible by the ability to manipulate their microstructure by controlled chemistry. Elastomers reinforced by the *in situ* formation of filler particles are among these new types of materials. We are interested in developing NMR imaging techniques for quantitative evaluation of the chemistry and polymer-filler interactions in such composites.

The figure shows a example of a  $^1\text{H}$  image we have obtained using the two-dimensional FT spin-echo technique. The sample, cylindrical in shape, is polydimethylsiloxane rubber reinforced by  $\text{SiO}_2$  generated in the hydrolysis and co-condensation of tetraethylorthosilicate (TEOS). The changes in signal intensity across the sample are directly related to the extent of the chemical reaction and the degree of silica precipitation, and have been confirmed by independent means. The specimens for this ongoing study are provided by Professor James Mark of the University of Cincinnati. The image demonstrates immediately and nondestructively that there are major spatial variations in the ultimate physicochemical properties of the cured specimen, most likely resulting from the limitations imposed by diffusion of reactants and products into and out of the material.

Specific parameters of this image are: TE = 2.8 ms, TR = 3 s, resolution  $128x$  by  $128y$  ( $180$  by  $200\ \mu\text{m}$  respectively), imaging time 26 min, slice thickness  $500\ \mu\text{m}$ .

  
Leoncio Garrido  
617-726-5820

  
Jerome Ackerman  
617-726-3083



# NMR

## NEWSLETTER

### Table of Contents, cont'd.

<sup>39</sup> K NMR for Quantitation of Potassium in Biological Tissues	Craik, D., Adam, B., Wellard, M., and Shehan, P.	53
Where's the Hg in Hg <sub>1-x</sub> Cd <sub>x</sub> Te?; Equipment Wanted	Zax, D. B., and Vega, S.	55
<sup>23</sup> Na NMR of Cartilage	Jelicks, L. A., Paul, P. K., O'Byrne, E. M., and Gupta, R. K.	59
Secondary Isotope Effect on the <sup>19</sup> F Resonance in XeF <sub>2</sub>	Diehl, P., and Jokisaari, J.	62
High Resolution Solid-State Spectra of an Asphaltene and a Coal	Netzel, D. A., and Miknis, F.	65
Imaging of Composites; Position Available	Garrido, L., and Ackerman, J. L.	67
TAMU NMR Newsletter: Sundry Notices	Shapiro, B. L.	68

\* \* \* \* \*

### Mailing Label Adornment: Is Your Dot Green?

If the mailing label on your envelope of this issue is adorned with a large green dot: this decoration means that payment for your 1990-91 subscription has not been received as of 17 August 1990. Unpaid subscriptions will be suspended before the November issues are mailed. If you are green dotted, please arrange to have your payment executed without delay, or at least contact me to arrange for uninterrupted Newsletter flow. This notice applies to all Subscribers, but not to Sponsors or Advertisers.

### Another (?) Mailing Label Adornment: Is Your Dot Red?

If the mailing label on your envelope of this issue is adorned with a large red dot or circle: this decoration means that you will not be mailed any more issues until a technical contribution has been received by me.

### Page Length Request

Attention overseas subscribers: If you must use paper which is longer than 11", please take care that nothing appears below 10" (25.5 cm) on your pages. It is costly to make reductions. Thank you.

\* \* \* \* \*



# CSI 2T Applications

## Shielded Gradients: Theory and Design

NMR imaging and localized spectroscopy depend on the use of pulsed magnetic field gradients. As these techniques have grown more complex, it has become apparent that eddy currents created in the magnet cryostat and other structures by pulsed gradients have become the chief limitation to many sophisticated applications.

Figure 1a illustrates the design problem for unshielded gradients. Figure 1b illustrates the shielded gradient arrangement. Figures 2 and 3 show the contours of constant flux for an unshielded and shielded Z gradient coil, respectively. This demonstrates that, for the shielded gradients, most of the flux has been kept away from the magnet bore.

The dramatic reduction of eddy currents which can be made over the conventional, unshielded gradients is shown in Figures 4a, b. These graphs show frequency as a function of time following the application of a long, constant amplitude gradient pulse which is suddenly cut off. Soon after cut off, a 90° pulse is applied and the complex FID recorded. The instantaneous frequency is then obtained from the FID and normalized by dividing by the frequency offset at the sample during the gradient pulse.

Figure 4a shows a typical decay of extra magnetic fields in a CSI 2T instrument caused by eddy currents in the conventional, unshielded gradient set with compression.

Figure 4b shows the decay of the uncompensated shielded Z gradient and Figure 4c shows the Z gradient decay with compensation. Note that the time scale for 4b and 4c is five times shorter than that for the unshielded gradients.

Fig. 1a.

### CONVENTIONAL GRADIENT COIL

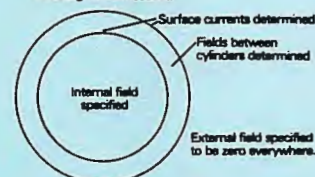
- Currents are constrained to flow on a single cylinder.
- There is only one degree of freedom.



Fig. 1b.

### SHIELDED GRADIENT COILS

- Currents on two cylinders.
- Two degrees of freedom.



**Fig. 1a**—Design problem for unshielded gradients. The field inside the winding is specified to be a linear gradient and the current pattern on the cylinder is determined. **Fig. 1b**—Design arrangement for shielded gradients. The field inside the inner cylinder is specified to be a linear gradient and the field beyond the outer cylinder is specified to be close to zero. The current patterns on both inner and outer cylinders are then determined.

Fig. 2.

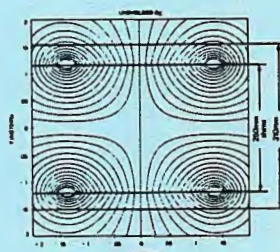
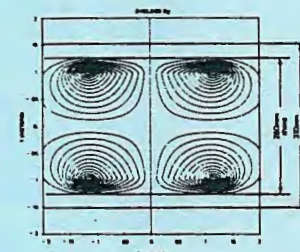


Fig. 3.



Lines of constant flux for Z-gradient. **Fig. 2**—Unshielded gradient. Note that flux lines extend well beyond the cryostat bore. **Fig. 3**—Shielded gradient. Flux lines are kept within the outer gradient cylinder.

Fig. 4a.

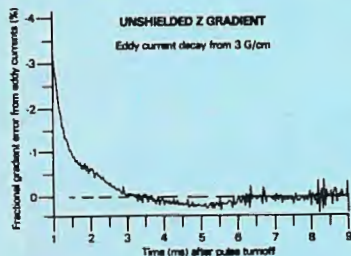


Fig. 4b.

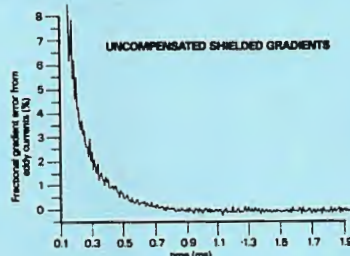


Fig. 4c.

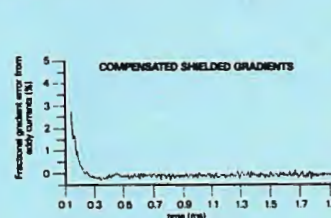


Figure 4b

Decay of field following application of square gradient pulse. **Fig. 4a**—Unshielded gradients. **Fig. 4b**—Shielded S150 gradient with no waveform compensation. **Fig. 4c**—Shielded S150 gradient with waveform compensation.



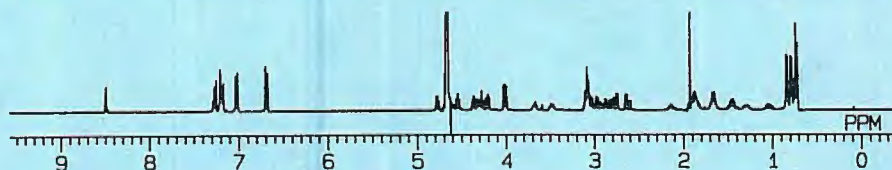
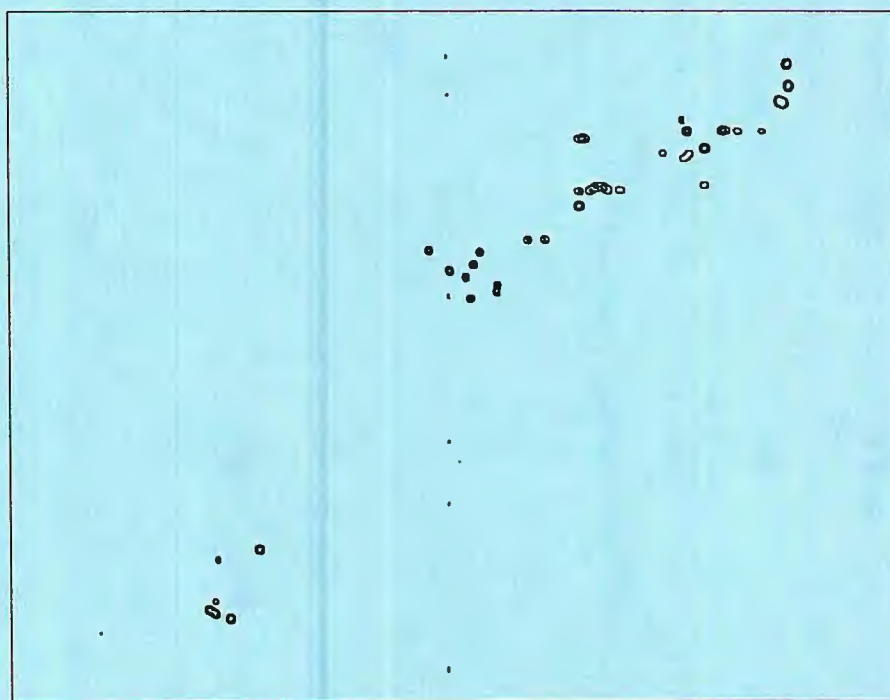
**GE NMR Instruments**



# AFTER THE WORK IS FINISHED...

## THE OTHER CPF COMES OUT TO PLAY

When all of the day's production samples have been run and the piles of spectra plowed through, JEOL's CPF can quickly switch operation modes. This same highly automated machine which is used for all of the production work can produce very high quality research data for those non-routine problems that always seem to appear. In many cases all that is necessary to make the change is to log into the research account. This changes the CPF from an automated, limited instrument into a wide-open research-grade spectrometer. With the addition of the appropriate accessories the low cost CPF is capable of running the most sophisticated research type experiments including CP MAS solids. Now that the CPF is available at a field strength of 400 MHz in addition to the very popular 270 MHz, the high field research spectrometer has become very affordable. The above 400-CPF data is a reverse detection  $^{13}\text{C}$  experiment run on Angiotensin-II. The instrument used for this experiment is a standard CPF with the addition of the optionally available reverse detection Broad Band probe. This data clearly shows that the routine need never be the only thing you can do.



For more information please contact:

**JEOL**

11 Dearborn Road, Peabody, MA 01960 (508) 535-5900 (Phone) (508) 535-7741 (FAX)